STRENGTH, STIFFNESS AND FAILURE MECHANISM OF DOUBLE SHEAR WELDED CONNECTIONS BETWEEN COLD-FORMED AND HOT-ROLLED STEEL

MD. ASRAFUL HOQUE

M.Sc. ENGINEERING THESIS

DEPARTMENT OF CIVIL ENGINEERING
MILITARY INSTITUTE OF SCIENCE AND TECHNOLOGY
DHAKA, BANGLADESH

MARCH 2024

STRENGTH, STIFFNESS AND FAILURE MECHANISM OF DOUBLE SHEAR WELDED CONNECTIONS BETWEEN COLD-FORMED AND HOT-ROLLED STEEL

MD. ASRAFUL HOQUE (SN. 0418110014)

A Thesis Submitted in Partial Fulfillment of the Requirement of the Degree of Master of science in civil engineering

DEPARTMENT OF CIVIL ENGINEERING
MILITARY INSTITUTE OF SCIENCE AND TECHNOLOGY
DHAKA, BANGLADESH

MARCH 2024

STRENGTH, STIFFNESS AND FAILURE MECHANISM OF DOUBLE SHEAR WELDED CONNECTIONS BETWEEN COLD-FORMED AND HOT-ROLLED STEEL

M.Sc Engineering Thesis

By

MD. ASRAFUL HOQUE (SN. 0418110014)

Approved as to style and content by the Board of Examination on 25 March 2024:

Lt Col Khondaker Sakil Ahmed, Ph.D, PEng, CEng Associate Professor Department of Civil Engineering, Military Institute of Science and Technology, Dhaka-1216	Chairman (Supervisor) Board of Examination
Dr. Khan Mahmud Amanat Professor Department of Civil Engineering, BUET, Dhaka-1000	Member (External) Board of Examination
Dr. Tanvir Mustafy,EIT,SEng Associate Professor Department of Civil Engineering, Military Institute of Science and Technology, Dhaka-1216	Member Examination
Brig Gen Md Kamal Uddin Komol,psc Head Department of Civil Engineering, Military Institute of Science and Technology, Dhaka-1216	Head of the Department Member (Ex-Officio)

Department of Civil Engineering, MIST

STRENGTH, STIFFNESS AND FAILURE MECHANISM OF DOUBLE SHEAR WELDED CONNECTIONS BETWEEN COLD-FORMED AND HOT-ROLLED STEEL

DECLARATION

I hereby declared that the study reported in this thesis titled as above is my own original work and has not been submitted before anywhere for any degree or other purposes. Further I certify that the intellectual content of this thesis is the product of my own work and that all the assistance received in preparing this thesis and sources have been acknowledged and /or cited in the reference section.

Md. Asraful Hoque
Student No: 0418110014

Department of Civil Engineering, MIST

STRENGTH, STIFFNESS AND FAILURE MECHANISM OF DOUBLE SHEAR WELDED CONNECTIONS BETWEEN COLD-FORMED AND HOT-ROLLED STEEL

A Thesis

By

Md. Asraful Hoque

Dedicated
To
My Parents and My Family

ACKNOWLEDGEMENTS

First, I would like to express my deepest gratitude to Allah for allowing me to bring this effort to fruition. You have made my all-works lot easier and made my life beautiful.

I would like to express my gratitude to my supervisor Associate Professor. Lt Col Khondaker Sakil Ahmed, Ph.D. for the useful comments, remarks and engagement through the learning process of this master thesis. It was a privilege for me to pursue my MS under his esteemed supervision. He mentored me throughout the last two years and without his profound support, this journey would have been much more difficult.

I would like to thank Prof Dr. Khan Mahmud Amanat and Dr. Tanvir Mustafy, for their thoughtful questions and valuable suggestions. I would like to express my appreciation to the Military Institute of Science and Technology (MIST) for the financial support of my experimental work. I wish to express my gratitude to Dr. Aziz Ahmed, lecturer, school of civil, mining, and environmental engineering, University of Wollongong, Australia for his valuable guidance during this research endeavor. I would like to convey my heartiest thanks to the Department of Civil Engineering, MIST for allowing me to use their structural mechanics lab to conduct the experimental program. I would like to thank to all laboratory members of the structural mechanics lab, MIST for their advice and technical support throughout the experimental program. I would like to thank to the McDonald steel building Product Limited for supplying the cold rolled steel for my research.

I am indebted to my family for the endless support, encouragement, and love they have given me throughout my life. Because of their continuous support in every aspect of my life, I was able to come this long.

ABSTRACT

Strength, Stiffness and Failure Mechanism of Double Shear Welded Connections Between Cold-Formed and Hot-Rolled Steel

Cold-formed steel is widely used for routine structural steel design including portal frames composed of open and/or closed sections. Nowadays, cold rolled steel channel and Z sections are now used in structure as a structural member with the hot rolled steel by welding connection. The connection between hot rolled and cold rolled steel is very important in the structure. Structural behavior of steel structures generally depends on the rigidity of the connections and their force transfer mechanism.

In the present study, an experimental investigation has been conducted on double shear welded connections made of ASTM A653 Gr.50 and ASTM A36 grades of cold-formed steel. Primarily a set of coupons extracted from the cold form steel of different thicknesses and steel grades are tested under uniaxial tension to understand their actual strength and modulus of elasticity. In addition, a total of 4 numbers of weld coupons are fabricated to determine different weld specifications used in this study. Finally, 24 test specimens of double shear welded connections are formed by overlapping two cold-formed steel plates of similar thickness with the two hot rolled steel plates and forming a double shear welded connection at the joint. The influence of weld strength, plate strength, and plate thickness on joint behavior is evaluated meticulously by employing standard data acquisition system. These weld connections are tested on tensile loading until failure.

The response of the double shear welded connections for varying material properties is examined in terms of load-elongation plot, connection strength, failure mode, stiffness, and ductility. It is observed, that with the increase of plate thickness failure mode changes from net-section fracture to weld throat failure. Usually increasing weld strength, steel grade, and plate thickness shows a rise in joint capacity and stiffness. Current American design provisions are evaluated for these ASTM A653 Gr.50 and ASTM A36 grade samples. Research into the Heat Affected Zone (HAZ) strength resulting from joint welding reveals a reduction in joint capacity of 6 to 19% due to the Heat Affected Zone (HAZ) effect.

সারসংক্ষেপ

Strength, Stiffness and Failure Mechanism of Double Shear Welded Connections Between Cold-Formed and Hot-Rolled Steel

Cold formed steel এর খোলা এবং বন্ধ বিভাগগুলির সমন্বয়ে গঠিত পোর্টাল ফ্রেম সহ স্ট্রাকচারাল স্টিল ডিজাইনের জন্য ব্যাপকভাবে ব্যবহৃত হয়। বর্তমান সময়ে Cold formed steel চ্যানেল এবং জেড বিভাগগুলি ওয়েল্ডিং সংযোগের মাধ্যমে Hot-Rolled Steel এর সাথে কাঠামোগত সদস্য হিসাবে ব্যবহৃত হচ্ছে। Hot-Rolled এবং Cold formed স্টিলের মধ্যে সংযোগ কাঠামোতে খুব গুরুত্বপূর্ণ। ইস্পাত কাঠামোর কাঠামোগত আচরণ সাধারণত সংযোগগুলির অনমনীয়তা এবং তাদের বল স্থানান্তর প্রক্রিয়ার উপর নির্ভর করে।

বর্তমান গবেষণায়, ASTM A653 Gr.50 এবং ASTM A36 গ্রেডের Cold formed steel দ্বারা তৈরি Double shear welded connection এর উপর একটি পরীক্ষামূলক তদন্ত করা হয়েছে। প্রাথমিকভাবে তাদের প্রকৃত শক্তি এবং স্থিতিস্থাপকতা বোঝার জন্য বিভিন্ন পুরুত্ব এবং স্টিল গ্রেডের Cold formed steel থেকে বের করা কুপনগুলির একটি সেট পরীক্ষা করা হয়েছে। এছাড়াও, এই গবেষণায় ব্যবহৃত বিভিন্ন ওয়েল্ড স্পেসিফিকেশন নির্ধারণ করতে মোট চারটি ওয়েল্ড কুপন তৈরি করা হয়েছে। পরিশেষে, দুটি Hot-Rolled Steel প্লেটের সাথে একই পুরুত্বের দুটি Cold formed steel প্লেটকে ওভারল্যাপ করে একটি Double shear welded সংযোগ তৈরি করে Double shear welded সংযোগের চব্বিশটি নমুনা তৈরি করা হয়েছে। সংযোগ আচরণের উপর Weld strength, plate strength, plate thickness এর প্রভাব স্ট্যান্ডার্ড ডেটা অধিগ্রহণ সিস্টেম এর মাধ্যমে সতর্কতার সাথে মূল্যায়ন করা হয়েছে। এই ওয়েল্ড সংযোগ ব্যর্থ হওয়া পর্যন্ত Tensile লোডিং এ পরীক্ষা করা হয়েছে।

বিভিন্ন উপাদানের বৈশিষ্ট্যের জন্য Double shear welded সংযোগের প্রতিক্রিয়া লোড-ইলংগেশন প্লট, সংযোগের শক্তি, ব্যর্থতার মোড, কঠোরতা এবং নমনীয়তার পরিপ্রেক্ষিতে পরীক্ষা করা হয়েছে। এতে দেখা যায়, plate বেধ বৃদ্ধির সাথে ব্যর্থতার মোড Net section failure থেকে weld throat failure এ পরিবর্তিত হয়। সাধারণত Weld strength, plate strength, plate thickness বৃদ্ধির সাথে সংযোগ ক্ষমতা এবং দৃঢ়তা বৃদ্ধি দেখায়। বর্তমান আমেরিকান ডিজাইনের নিয়মগুলি ASTM A653, Gr.50 এবং ASTM A36 গ্রেড নমুনার জন্য মূল্যায়ন করা হয়েছে। জয়েন্ট ওয়েল্ডিংয়ের ফলে তাপ প্রভাবিত অঞ্চল (HAZ) এর শক্তির উপর গবেষণায় তাপ প্রভাবিত অঞ্চল (HAZ) প্রভাবের কারণে সংযোগ শক্তি 6 থেকে 19% হ্রাস পেয়েছে।

LIST OF NOTATION AND ABBREVIATION

AISI	American Iron and Steel Institute
ASTM	American Society for Testing and Materials
AS	Australian Standard
d_{y}	Displacement corresponding to yield point
d_{u}	Displacement corresponding to ultimate point
d_{f}	Displacement corresponding to failure point
FCAW	Flux cored arc welding
$F_{y\mathrm{h}}$	Yield strength of hot rolled steel
F_y	Yield strength of cold formed steel
F_u	Ultimate strength of cold formed steel
F_{xx}	Tensile strength of Electrode
F_{u1}	Tensile strength of connected parts corresponding to thicknesses t_1
F_{u2}	Tensile strength of connected parts corresponding to thicknesses t_2
F_{HAZ}	HAZ Strength
FESEM	Field Emission Scanning Electron Microscopy
HAZ	Heat Affected Zone
k	Stiffness
K_1	Hot rolled steel stiffness
K_2	Weld connection stiffness
K_{eqe}	Equivalent stiffness
L	Length of fillet weld
LVDT	Linear Variable Differential Transformer.
MIST	Military Institute of Science and Technology

MIG	Metal inert gas welding
P_{n1}	Nominal strength corresponding to connected thickness t_1
P_{n2}	Nominal strength corresponding to connected thickness t_2.
P_{AISI}	Weld connection strength as per AISI S100-16
$P_{\max}$	Weld connection strength
r_{i}	Initial ductility
r_{f}	Final ductility
SMAW	Shielded metal arc welding
TPM	Tearing of plate at middle
TPAW	Tearing of plate adjacent to the weld
t	Nominal thickness of hot rolled steel
t_w	Effective throat (0.707 w_1 or 0.707 w_2, whichever is smaller)
t_1	Thickness of connected part
t_2	Thickness of connected part
t_n	Nominal thickness of cold rolled steel sheet
UTM	Universal testing machine
w_1	Horizontal Weld leg size
w_1	Vertical Weld leg size
WTF	Weld throat failure

LIST OF TABLES

LIST OF FIGURES

TABLE OF CONTENTS

CHAPTER 1
INTRODUCTION

1.1 General

Structural steel sections play a pivotal role in various construction applications. Structural steel sections may be categorized into two prominent types: hot-rolled and cold-formed. The technology used in their formation and manufacturing distinguishes these two types of steel. Hot-rolled steel sections are produced at elevated temperatures, reaching up to 1400°C, utilizing either blast furnaces or electric arc furnaces. Due to the high-temperature manufacturing process, hot-rolled steel tends to have different material qualities compared to cold-formed steel. It may have lower strength and hardness but is more ductile and flexible. In contrast, cold-formed steel, also known as light gauge steel, is manufactured at room temperature using steel plate, sheet, or strip material. The cold-rolling or brake-pressing technique as shown in Figure 1.1 is generally used in the manufacturing process of cold-formed steel to increase its mechanical properties such as strength and hardness (Hancock and Rogers, 1998). This process also produces accurate sheet thickness.

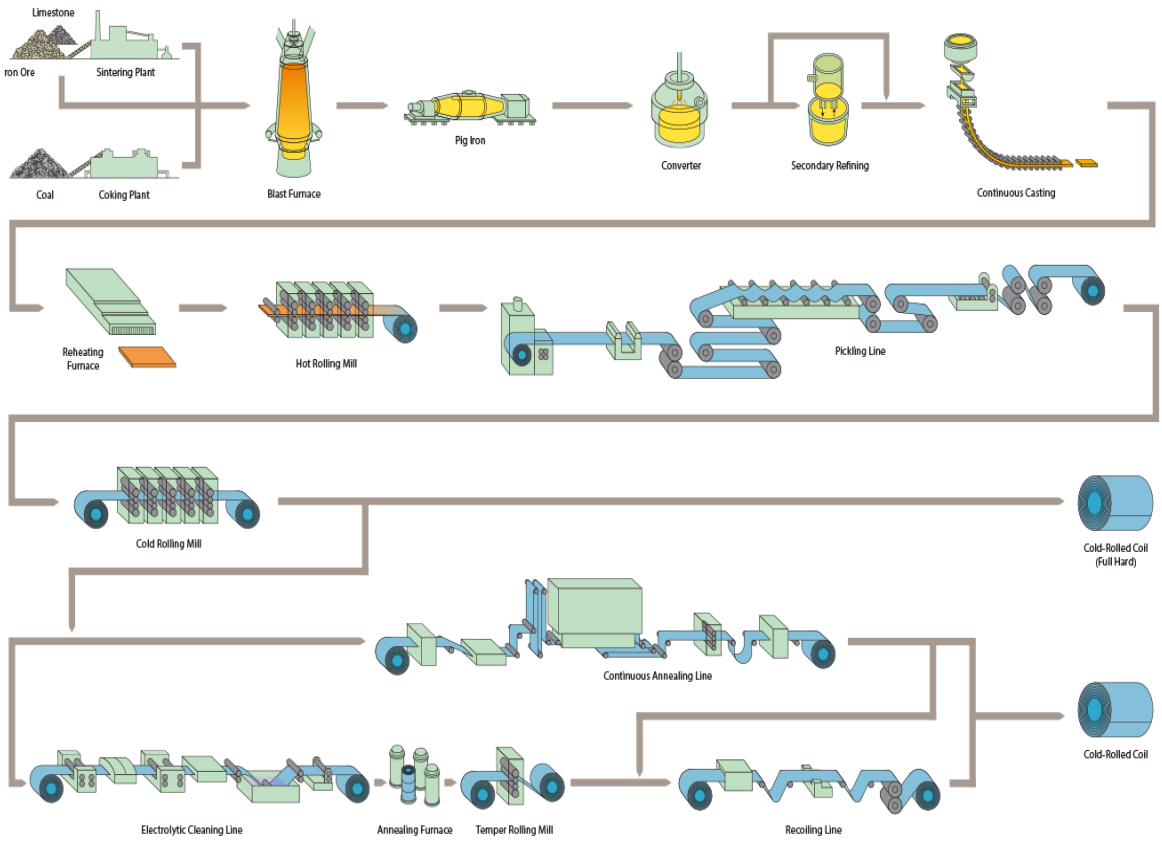

Figure 1.1: Cold rolled steel manufacturing process (Nippon Steel,2007)

Cold-formed steel is known for its structural integrity and precision. Cold-formed steel sheets typically come in a range of thicknesses, varying from 0.378 mm to 6.35 mm (Yu et al., 2019). This range allows for versatility in structural design and application.
Cold-formed steel sections have indeed gained popularity as an alternative to traditional hot-rolled steel components in various construction applications. A few examples of cold formed steel section are presented in Figure 1.2. Cold-formed steel sections are produced by shaping thin sheets of steel through a cold-working process, which increases their strength without significantly increasing weight. This high strength-to-weight ratio makes them suitable for various structural applications, particularly in projects where minimizing dead load is essential. Cold-formed steel sections are typically lighter and more compact than their hot-rolled counterparts. This ease of transportation and handling can lead to cost savings in terms of logistics and on-site assembly (Lee et al., 2014) . Cold-formed steel is commonly used in light steel frame construction, which has become a popular choice for residential and low to medium-rise commercial buildings. The lightweight and efficient nature of cold-formed sections makes them ideal for these applications. Cold-formed steel construction can be more sustainable due to reduced material waste, improved energy efficiency, and recyclability. Additionally, the reduced weight can lead to cost savings in foundation and transportation, which can contribute to overall sustainability in a project.

Light-steel frame building (LSFB) is indeed a modern construction method that has been in use for several decades, particularly in regions like Australia, the United States, and Europe. This method was initially limited to single and double-stored residential buildings are illustrate in Figures 1.3 and figure 1.4 but this approach has now extended its applicability in a wide range of building types due to its numerous advantages. LSFB is known for its rapid construction. The prefabricated steel frames and components can be quickly assembled on-site, reducing construction time. LSFB has evolved from its origins in residential construction to become a versatile and cost-effective building method for a wide range of structures, including multi-storied commercial and industrial buildings. Its lightweight nature, speed of construction, and energy efficiency make it an appealing option for modern construction projects.

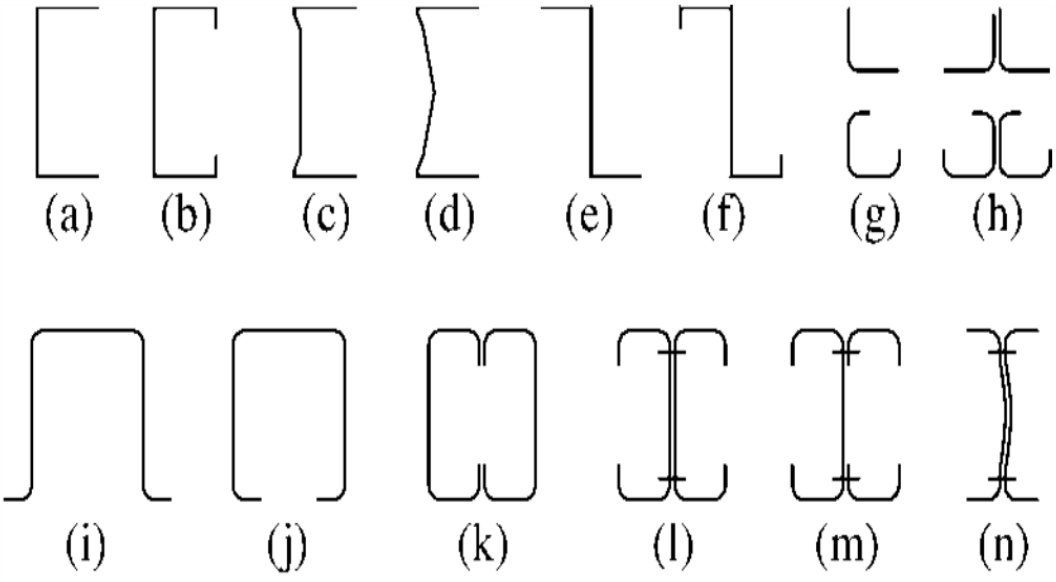

(a) Cold-formed steel sections used for structural framing

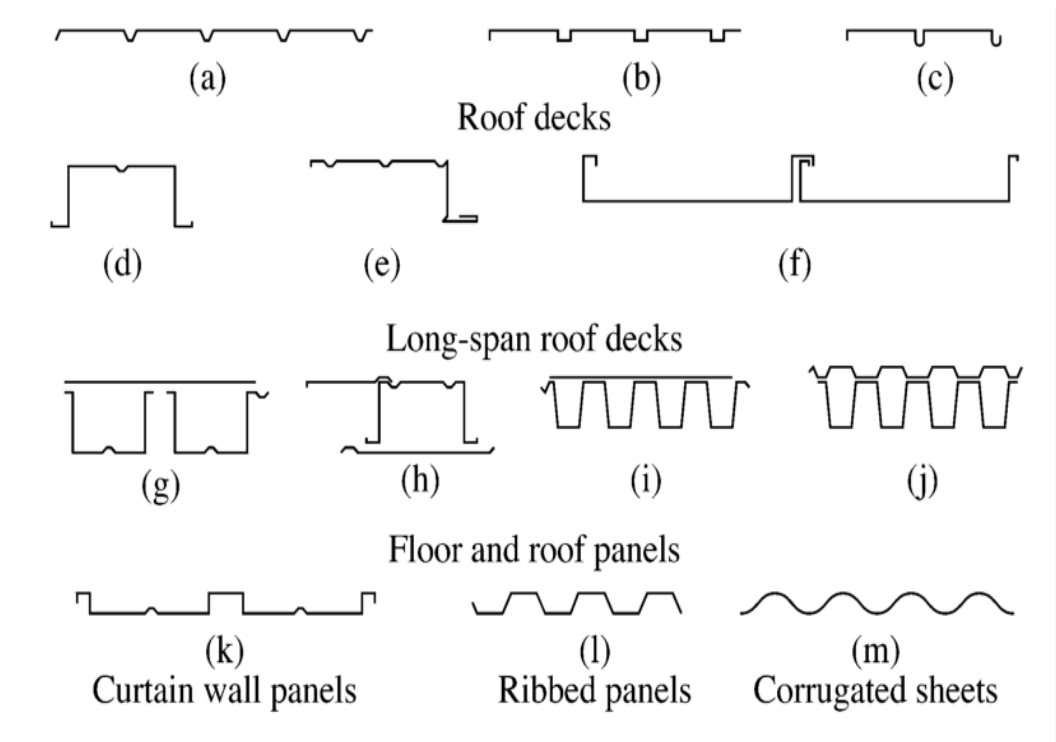

(b) Decks, panels, and corrugated sheets

Figure 1.2: Cold formed steel section for framing and Decking (Yu and LaBoube, 2010).

Figure 1.3: Cold form steel in the frames of houses (Barnard, 2011)

Figure 1.4: Cold-formed steel in walling (Allen, 2022)

LSFB (Light Steel Frame Building) has carved out a position in the renovation industry, particularly in applications involving the extension and/or adaption of existing structures. In the context of renovation, LSFB and other steel section components are mainly used for:

(a) Installing new lightweight walls and partitions with good soundproofing and fire resistance qualities.
(b) Adding extra walls to support new cladding or covering existing facades with light steel sub-frames capable of holding various lightweight cladding materials.
(c) Renovating flat roofs to create more usable living areas.

(d) Using modular units to expand buildings, such as adding toilet or bathroom units, or installing external lifts and stairs.
(e) Building new mezzanine floors in structures with adequate floor-to-ceiling height.

LSFB is used in the following forms for "over-roofing":

(a) Closely or widely spaced trusses spanning between façade walls, with supporting purlins between widely spaced trusses.
(b) Moment-resisting structures, such as portal frames, are supported on the perimeter columns.
(c) A grillage of steel beams supporting a lightweight steel structure.

Joints are an important component of every structural system (Qin1a and Chen, 2016). Structural behavior is generally depended on the connection rigidity and force transfer mechanism. The connection should be strong enough to transfer gravity and lateral load (Maali et al., 2018). It has been noted that for a structure consisting of hot-rolled sections, approximately 30 % of the total costs are directly or indirectly influenced by the connections (Toma and Stark, 1978). There are a variety of joining methods available for such structures. The selection of the correct method is governed by a variety of factors, but the structural behavior of the specific connection will be the most influential. Structural systems transfer their loads through connections. The fabrication of connections is the most labor-intensive aspect of the construction process in cold-formed steel structures, hence a better understanding of the behavior of these connections could reduce fabrication costs, leading to an optimal design. Cold-formed steels (CFS) are thin and therefore connecting mechanics are critical in the construction of such structural parts.

1.2 Statement of Problem

Cold formed steel sections like Z, C, lipped channel or box sections are widely used with hot rolled section in the structure. The connection between hot rolled and cold rolled steel is very important for robust application of cold formed sections in steel structures. Structural behavior generally depends on the connection rigidity and force transfer mechanisms. In the current applications, the connection between hot rolled and cold rolled is used as bolted connection. Bolted connection is semi rigid connection which is not stringent in case of deflection limit state. On the other hand, the welded connection is

inherently rigid connection owning to their superior stiffness. In some cases of long span structures, deflection will be the critical factor for designing the structure. For this case engineer wants rigid and stiffer connection. A stiffer connection can be desirable in certain applications, especially when structural stability or resistance to deformation is a critical factor. Welded connection is the better choice for the engineers in this particular problem. By virtue of superior stiffness, welded connection contributed to the reduction of undesirable deformation and deflection within the structural system.

The welding of cold-rolled steel poses a distinctive challenge within the welding industry, primarily attributed to the details associated with welding thin plates. The thin profile of cold-rolled steel demands a specialized approach and precision in the welding process. The challenges may include issues such as heat distribution, potential distortion, and the need for precise control to avoid compromising the integrity of the thin material. This thesis paper aims to investigate into the feasibility of welding cold-rolled steel with hot-rolled steel, assessing the connection's capacity and its implications for structural performance.

Further investigation is deemed essential to enhance understanding of the welded connection between cold-rolled and hot-rolled steel. The present study aims to conduct an experimental investigation focusing on the double shear welded connection between these two types of steel. Additionally, a comprehensive analysis of the impact of geometric variables on joint behavior will be conducted to clarify the nuanced aspects of the connection. Furthermore, there is a need to assess the applicability and effectiveness of existing guidelines in the context of using welded connections between cold and hot-rolled steel. This evaluation is vital for ensuring that the guidelines align with the details of the specific connection type, providing valuable insights for optimizing structural performance and safety.

1.3 Study Objective

The main objectives of this research are as follows:

a. To determine the connection strength and stiffness of welded connections between cold-formed and hot-rolled steel.

b. To examine the influence of the welding process and electrode types on the strength of weld connections.
c. To investigate the weld failure mechanism of the cold-formed steel connections.

1.4 Scope of Study

This study has covered the experimental study of double shear welded connections between cold-formed and hot-rolled steel subjected to tensile loading. In this test program, two different steel grades ASTM A653 Gr.50 and ASTM A36 cold rolled steel with three different thicknesses are employed in which cold rolled steels are connected with hot rolled thick plates. The coupon test was conducted for each thickness plate to get the mechanical properties of the specific thickness plate. Four electrodes under three welding process are used to prepare the weld coupon. Double shear welded specimens were then prepared, utilizing varying thicknesses of two grades of cold-rolled steel and four types of electrodes. The specimens underwent tension testing. Such experimental study can be used to assess the applicability of current design guidelines for AISI S100-16 (2016) and AWS D1.3 (2008) based on the obtained results and observations.

1.5 Organization of Report

Apart from this chapter, the whole report is divided into four major chapters. Contents of these four chapters are as follows:

Chapter 2 presents some background on cold-formed steel, welded connection, welding process and types of welded connection. Also, current design guidelines for welded connection are discussed. The main part of this chapter is to review past literature which focuses on the tensile test of welded connection. It also provides insight into articles focusing on the microstructure study of cold formed steel due to welding.

Chapter 3 presents the test methodology used in this study. The methodology includes the specimens preparation, test protocol and data acquisition techniques. It also presents the material properties and how they are collected. Details of the testing samples are also provided.

Chapter 4 presents the result of the test program. The results are presented in terms of load-elongation plot, failure mode of joint, connection strength, ductility, and stiffness for connection. Current American design guidelines for cold-formed steel are also evaluated for the test samples.

Chapter 5 is the final chapter of this report which provides the concluding remarks. In the end, some recommendations will be provided for future research purposes.

CHAPTER 2
LITERATURE REVIEW

2.1 Introduction

This chapter provides a comprehensive overview of previous research focused on the utilization of welding in connections for cold-formed steel structures. The content includes a general background on cold-formed steel, explores various applications of welded connections. The review highlights numerous studies that have investigated into the behavior of welded connections, emphasizing key factors influencing their ultimate capacity and failure modes. Notable aspects include welding properties, weld thickness, sheet thickness, and material properties of the steel sheet.

By synthesizing existing knowledge and examining critical aspects of welded connections in cold-formed steel structures, this chapter aims to serve as a valuable resource for researchers, engineers, and practitioners involved in the field of structural engineering. The insights provided herein can contribute to the refinement of design guidelines and enhance the performance and reliability of welded connections in cold-formed steel structures.

2.2 Cold-Formed Steel

Cold-formed steel sections have seen a resurgence in light-gauge construction, becoming primary load-bearing elements in industrial steel structures. Despite challenges like premature buckling, increased use has driven research, leading to more stable and reliable materials. Innovations allow for complex geometries and higher yield stresses. However, successful integration requires ongoing research in design techniques, codes, and calculation models. This review emphasizes the need for continued research to optimize cold-formed steel structural performance.

Davies (2000) extensively examined various recent advancements in this area. Recent trends show increased use of higher quality steels with enhanced yield stress for mass produced items like purlins, sheeting, and decking. Higher strength steels lead to thinner sections, but the need for local stability requires highly stiffened sections with more folds and rolled in stiffeners, making design criteria more challenging.Cold-formed sections are increasingly utilized due to their outstanding corrosion resistance. In cold-formed steel

structural construction, connecting mechanics are crucial due to the material thinness (Davies, 2000) .

2.3 Applications of Cold-Formed Steel

Cold-formed shapes can be used for entire buildings and for complete roof, floor and wall systems. They can also be used as individual framing members such as studs, joists and truss members.

Regular Decks: Permanent metal deck forms are usually galvanized, and are fabricated from lightweight steel in thickness that vary from 0.020 to 0.075 inches (0.50 to 1.9mm) depending on slab thickness and design span. Composite metal deck forms also provide the tension reinforcement for the slab. The embossments provide interlock between the deck and the concrete.

Multi-Function Deck: Some deck systems use cellular cold-formed steel shapes to permit lightweight floors that reduce deadweight. These floor systems can provide electrical power, communications and data cable distribution as well as heating and air conditioning ducts.

Standing Seam Metal Roof: The system consists of factory or job-site roll-formed panels with elevated, field-secured seams and concealed clips that fasten the panels to the structure and permit the panels to accommodate thermal expansion and contraction.

Exterior Walls: A stud wall framing is a wall system with studs connected to the top and bottom tracks and braced with cold-rolled channel linking or diagonal bracing. The stud wall system can be used to carry the floor load to resist the lateral load such as wind or seismic load . Stud wall framing has been widely used in both non-load-bearing and load-bearing construction.

Residential Uses: Another area in construction where cold-formed steel is finding wider application is in residential steel framing systems. Here, steel is used instead of lumber for joists, studs and other structural components of residential construction.

Floor and Roof Trusses: Cold-formed steel trusses offer similar span capabilities and design flexibility as wood trusses but are lighter and more dimensionally stable. They are

typically pre-engineered and prefabricated, allowing for accommodating various roof configurations. This versatility makes cold-formed steel trusses suitable for residential, commercial, institutional, educational, and industrial structures.

Racks: Material handling and storage specialists rely on cold formed steel racks and rack systems to efficiently store the material. New rack systems are so huge that they fill entire buildings and have stacker cranes that rise as high as 100 feet (30m).

Pre-Engineered Buildings: Manufacturers of pre-engineered metal building provide custom designed structures for anything from a small tool shed to a range of sophisticated structures such as schools, churches and other complex manufacturing facilities.

2.4 Advantages of Cold-Formed Steel

Cold-formed steel offers numerous superior advantages compared to other construction materials. Those are listed below.

Lightweight: Cold-formed steel weighs significantly less than wood and masonry materials. A typical stud wall weighs only 10% to 15% of the masonry wall.

High strength and stiffness: As a result of the cold-forming process, cold-formed steel possesses one of the highest strength-to-weight ratios of any building materials. This high strength and stiffness advantage means better design flexibility, wider spans and better material usage.

Fast and easy erection and installation: Building components made of cold-formed steel can be fabricated with high accuracy in a plant and then assembled on job sites, which greatly increases erection efficiency and ensures construction quality.

Dimensionally stable: Cold-formed steel does not expand or contract with moisture content. In addition, it does not split or warp as time goes by and, therefore, is dimensionally stable.

No formwork needed: The use of cold-formed steel decks eliminates the formwork for pouring concrete floor. In addition, composite action between the steel deck and concrete increases floor strength and stiffness.

Durable: Cold-formed steel is durable because it is termite-proof and rot-proof. In addition, galvanized cold-formed steel products can provide long-term resistance to corrosion.

Economy in transportation and handling: The cold-formed members or panels are easy to handle and to transport due to their lightweight.

Non-combustible: Steel does not burn and will not contribute fuel to the spread of a fire, which will result in better fire resistance and lower insurance premiums.

Recyclable: Steel is an environment friendly "green" material. It can be recycled and reused. Steel-framed housing dramatically reduces the number of trees consumed for residential construction, thus conserving one of nature most precious resources.

2.5 Welded Connection

Connections play a vital role in transmitting forces and moments from a structural member to supporting parts. In the hot-rolled constructions, bolted or welded connections stand are the most predominant connectors. Particularly, research investigations have unequivocally demonstrated that welded connections exhibit evidently heightened levels of stiffness (Mallepogu and Madhavan, 2022, Mallepogu and Madhavan, 2023).
In the utilization of cold-formed steel, the choice of connecting technique is influenced by various factors, as outlined by (Lennon et al., 1999).

a) A generic analysis and design method are available.

b) The reliability of the joint and availability of quality control methods.

c) The cost of the connection procedure.

d) The maneuverability of the joining equipment.

2.6 Types of Welded Connection

Several types of arc welds generally used in cold-formed steel construction are:

1. Groove welds

2. Fillet welds

3. Flare groove welds

4. Arc spot welds (puddle welds)

5. Arc seam welds

2.6.1 Fillet Welds

Fillet welds are often used for lap and T-joints. Depending on the arrangement of the welds, they can be classified as either longitudinal or transverse fillet welds. Longitudinal means that the load is applied parallel to the length of the weld and transverse means that the load is applied perpendicular to the length of the weld. As a result, transverse welds are stronger than longitudinal welds of an equal length.

Fillet Welds Subject to Transverse Loading

Fillet welds covered welding of joints in any positions either sheet to sheet, sheet to thicker steel member. The nominal shear resistance of a fillet weld shall be the lesser of P_{n1},P_{n2}.

For transverse loading:

$$P_{n1} = t_1 L F_{u1} \quad \text{..... (2.1)}$$

$$P_{n2} = t_2 L F_{u2} \quad \text{..... (2.2)}$$

Where,

t_1,t_2=Thickness of connected part

F_{u1},F_{u2} =Tensile strength of connected parts corresponding to thicknesses t_1 and t_2

P_{n1},P_{n2} =Nominal strength corresponding to connected thickness t_1 and t_2.

A resistance factor of 0.60 for LRFD is specified for fillet welds subject to transverse loading. For ASD, a factor of safety of 2.5 is used.

In addition, for t > 0.10 in. (2.54 mm), the nominal strength determined in accordance with Eq (2.1) and (2.2) shall not exceed the following value of P_{n3} .

$$P_{n3} = 0.75 t_w L F_{xx} \quad \text{..... (2.3)}$$

t_w=Effective throat (0.707 w_1 or 0.707 w_2, whichever is smaller)

L=Length of fillet weld

According to AISI Specification, in lap joint specimens shown in figure 2.1, the sheet edge leg of a fillet weld is typically equal to the thickness of the sheet, while the other leg is two to three times longer. This results in a fillet weld throat that is generally larger than that of a conventional fillet weld.

In most cases, the primary mode of ultimate failure observed in these fillet weld joints is the tearing of the plate adjacent to the weld. It is found that higher strength weld materials often mitigate the risk of shear failure. However, for plate thicknesses exceeding 2.54mm were tested in the cornell research (McGuire and Peköz, 1980) .The throat dimension may be insufficient, potentially resulting in a tear occurring within the weld itself rather than the plate material.

Research conducted at the University of Sydney, (Zhao and Hancock Gregory, 1995) has further indicated that weld throat failure is not limited to specific thickness ranges. Weld throat failures have been observed in lap joint specimens with plate thickness ranging from 2.54mm to 3.81mm.

Notably, the material strength plays a significant role in the failure modes of these welds. When employing materials with a yield stress of 448MPa or higher, the research at the University of Sydney (Teh and Hancock, 2000) suggests that weld throat failure does not occur in materials less than 2.54mm in thickness.

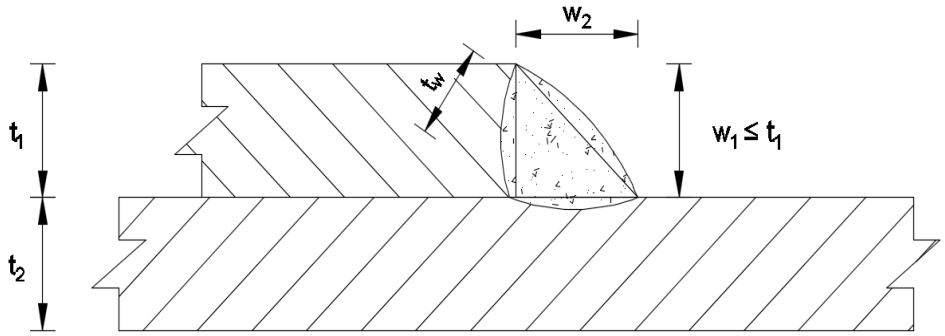

Figure 2.1: Fillet weld lap Joint

Fillet Welds Subject to Longitudinal Loading

A total of 64 longitudinal fillet welds were tested in the Cornell study. An evaluation of the test data indicated that the following equations can predict the ultimate loads of the connected sheets for the failure involving tearing along the weld contour, weld shear, and combinations of the two types of failure:

For L/t <25

$$P_{u1} = (1 - \frac{0.01L}{t})LtF_u \quad \text{..... (2.4)}$$

For L/t≥25

$$P_{u2} = 0.75LtF_u \quad \text{..... (2.5)}$$

Resistance factors of 0.60 and 0.55 are specified for LRFD for Eqs.(2.4) and (2.5), respectively. For ASD, a factor of safety of 2.5 is used.

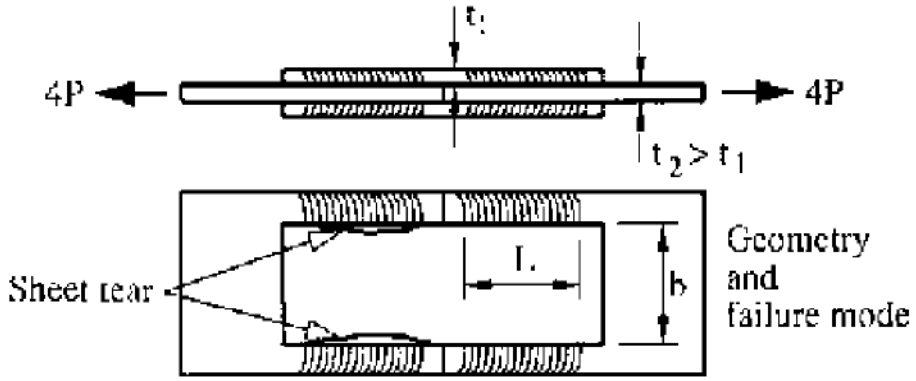

Figure 2.2: Fillet welds subject to longitudinal loading (Hancock et al., 2001).

2.7 Welding Process

Welding can be done in different process. I have used three welding process in this thesis.

2.7.1 Flux Cored Arc Welding (FCAW)

In FCAW (Charles G.Salmon, 2009) process, the Continuously fed filler metal electrode is tubular and contains the flux material within its core is shown in figure 2.3. Gas shielding

is provided by flux core but additional shielding is frequently provided by CO_2 gas. Flux cored arc welding has become a useful procedure for field welding in severe cold weather conditions as well as to speed up high rise construction.

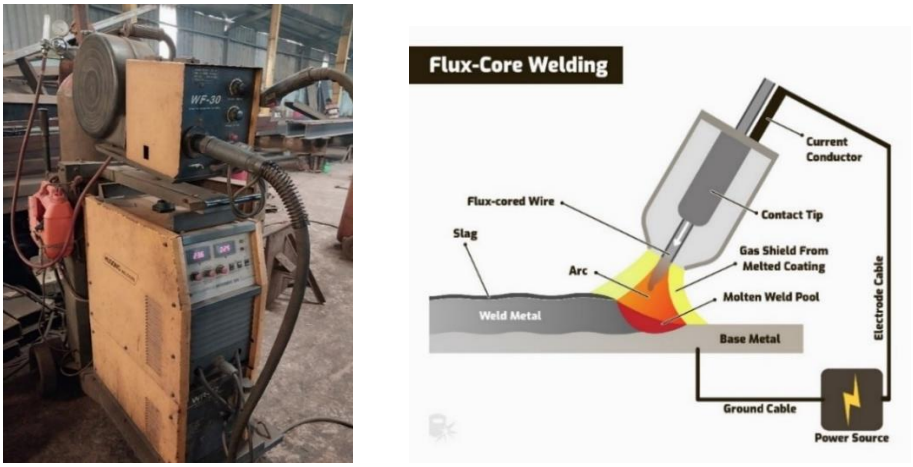

Figure 2.3: Flux cored arc welding (FCAW) (Sild, 2022a)

2.7.2 Metal Inert Gas Welding (MIG)

In the MIG (Charles G.Salmon, 2009) process, a continuous wire electrode is fed from a coil through the electrode holder, as illustrated in Figure 2.4. Shielding gas is essential to safeguard the weld pool from contamination. Optimal performance is achieved with a shielding gas composition of 80% CO_2 and 20% helium.The shielding gas controls the arc and metal transfer characteristics, influences penetration, width of fusion, speed of welding, and helps in controlling undercutting. Notably, the method is distinguished by a high rate of filler material deposition. MIG welding is faster than SMAW and is widely employed in various industries.

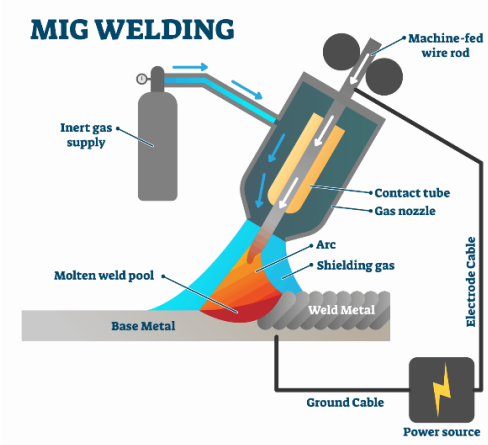

Figure 2.4: Metal inert gas welding (MIG) (Sild, 2022b)

2.7.3 Shielded Metal Arc Welding (SMAW)

Shielded metal arc welding as illustrated in Figure 2.5 ,is one of the oldest, simplest and perhaps most versatile types for welding structural steel (Charles G.Salmon, 2009).The Electrode wire becomes filler material and the coating is converted partly into a shielding gas, partly into slag and some part is absorbed by the weld metal. The Coating is clay like mixture of silicate binders and powder materials such as fluorides, carbonates, oxides, metal alloys and cellulose. The Shielding of the arc prevents atmospheric contamination of the molten metal in the arc stream and in the arc pool. SMAW is used for tag welding in various industries. It is recognized for its portability and versatility in welding applications.

Figure 2.5: Shielded metal arc welding (SMAW) (Sild, 2022c)

2.8 Heat Affected Zone (HAZ) of Welded Connection

The Heat Affected Zone (HAZ) refers to the region situated between the weld metal and the base metal. This region of the base metal undergoes temperatures below its melting point but reaches levels sufficient to modify its microstructure and characteristics as a result of the welding process. The specific microstructural changes within the HAZ are determined by the maximum temperature reached during welding and the duration of exposure within the temperature range of 1500 to 500ºC. Figure 2.6 provides a schematic representation of the iron-iron carbide phase diagram and the heat affected zone of a welded low carbon steel.

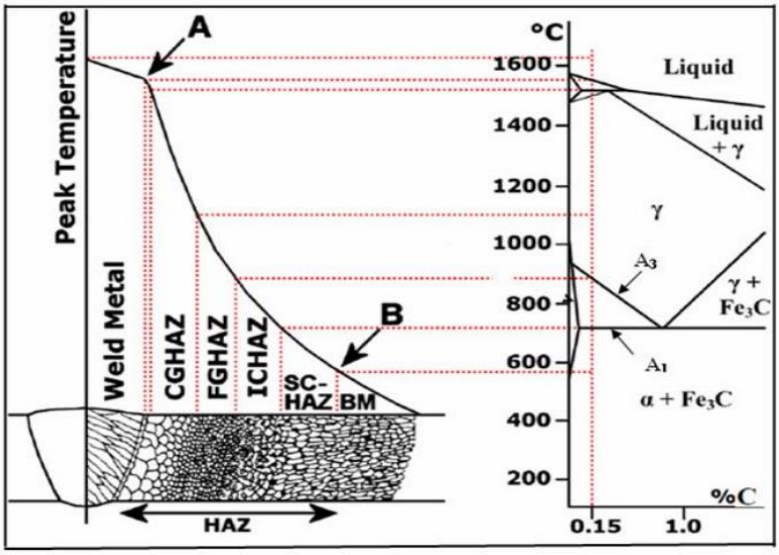

Figure 2.6: Schematic diagram of the heat-affected zone (Amanie, 2011)

The line connecting points A and B in Figure 2.6 illustrates the peak temperatures experienced in the Heat Affected Zone (HAZ), progressively moving away from the fusion line. The iron-iron carbide phase diagram explains how these temperatures correlate with distinct microstructures within the HAZ. In plain carbon steel, as shown in the figure 2.6, the HAZ encompasses four distinct microstructural zones: (i) the coarse grain growth zone ranging from 1500^0 to 1100^0 C, (ii) the fine grained zone spanning from 1100^0 C to A3, (iii) the inter critical zone from A3 to A1, and (iv) the subcritical zone below A1. The peak temperature declines with increasing distance from the fusion zone, consequently leading to a decrease in grain growth. These HAZ regions are identified respectively as coarse-grained (CGHAZ), fine-grained (FGHAZ), inter-critical (ICHAZ), and sub-critical (SCHAZ) zones (Bhadeshia and Honeycombe, 2017).

Zone 1, also known as the coarse-grained Heat Affected Zone (CGHAZ), is situated adjacent to the fusion line. Within this zone, temperatures surpass the upper critical point, promoting the growth of austenite grains. Both the size of the austenite grains and the width of the CGHAZ expand with heightened heat input and reduced cooling rates. Increased heat input correlates with lower cooling rates, resulting in the formation of coarser grains due to prolonged exposure above the A3 temperature threshold.

Zone 2, also termed as the fine-grained Heat Affected Zone (FGHAZ) or recrystallized zone, comprises fine ferrite grains. Within the FGHAZ, the material is subjected to elevated temperatures adequate for austenite formation during welding. However, the peak

temperature reached is insufficient to entirely dissolve the precipitates, such as carbides and nitrides, unlike in Zone 1. Consequently, the formation of fine ferrite grains occurs while the growth of austenite grains is suppressed.

Zone 3, referred to as the inter-critical Heat Affected Zone (ICHAZ), represents a partially austenitic region. Within this zone, ferrite doesn't entirely convert to austenite upon heating. Upon cooling, the transformed grains undergo refinement, while the austenite may undergo transformation into pearlite, martensite, or remain as the martensite-austenite (M-A) microconstituent.

In Zone 4, known as the sub-critical Heat Affected Zone (SCHAZ), where the peak temperature remains below A1, the grain size remains unaffected since no austenite transformation takes place. Consequently, the regulation of austenite grain size within the HAZ is governed by the steel upper critical temperature and the weld encountered thermal cycles.

The mechanical properties of each HAZ zone are different because of the difference in grain size in the zones.Particularly in low carbon and low alloyed steels, emphasis is placed on the CGHAZ due to its exposure to high temperatures, leading to the formation of large austenite grains.

In the field of metallurgical research, it is firmly established that steels, when subjected to various welding processes and different types of electrodes, experience distinct variations in both peak temperature and cooling rate. These variations are influenced by their proximity to the weld fusion line (FL) (Porter, 2015, Guo et al., 2015). These particular parameters are widely acknowledged as essential factors greatly influencing the resultant microstructure and consequential mechanical properties of the welded joint (Amraei et al., 2020, Guo et al., 2017, Ovat et al., 2012) . The paramount region of interest within the context of welded joints is unequivocally the Heat-Affected Zone (HAZ).The macrostructure of the fusion zone,heat affected zone and base metal of welded sample are shown in figure 2.7.

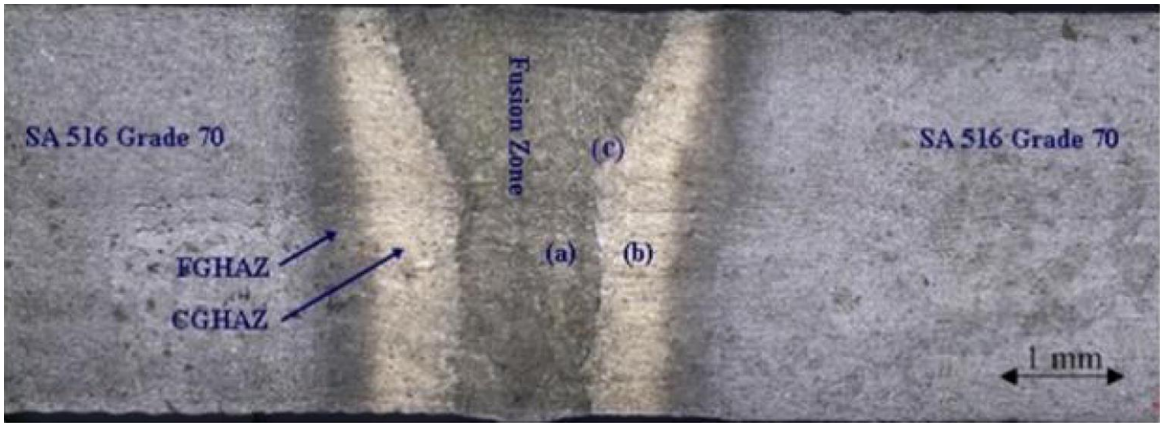

Figure 2.7: Macrostructure of the fusion zone, heat affected zone and base metal of welded sample (Oyyaravelu et al., 2016)

Welding current affects the mechanical properties of welded joint (Owolabi et al., 2016, Ali et al., 2019, Das et al., 2008) . The mechanical properties will be increased with the increase of electrical current up to certain level (Pathak et al., 2020). Beyond this certain current level, both yield strength and tensile strength is found to be decrease with the increase in electrical current (Ogbunnaoffor et al., 2016, Jha and Jha, 2014, Liu et al., 2018, Talabi et al., 2014) . This phenomenon is attributed to the heightened heat input on the heat-affected zone (HAZ), leading to consequential changes in the mechanical properties of the welded samples (Nassar et al., 2021, Amraei et al., 2019, Merchant Samir, 2015). Chen et al.(1999) demonstrate a significant reduction in the tensile strength of the heat-affected zone (HAZ) in sheet steel, indicating a substantial decrease from the initially specified value (García Rentería et al., 2013 , Chen et al., 1999)).

2.9 Failures Modes of Fillet Welded Connection

In the Cornell research by Peköz and McGuire (1979), fillet welds on lap joints had one leg (w_1) equal to the sheet thickness and the other leg (w_2) often two or three times longer. Typically, failure occurred by tearing of the plate near the weld, rather than shear failure of the weld itself (Dhalla and Peköz, 1971). The last provision in the specification's accounts for the possibility of throat dimensions being less than the cover sheet thickness for sections thicker than 0.15 inch (3.81 mm), leading to potential weld failure. The 2001 Specification revision mandates a weld strength check for sheet thickness exceeding 0.10 inch (2.54 mm). Research at the University of Sydney (Zhao and Hancock, 1996) indicated that weld throat failure could even occur between thicknesses of 0.10 inch (2.54 mm) to 0.15 inch (3.81

mm). For high-strength materials with a yield stress of 65 ksi (448 MPa) or higher, (Teh and Hancock, 2002) found that weld throat failure doesn't happen in materials less than 0.10 inch (2.54 mm) thick, supporting the adequacy of AISI Specification provisions for such materials. However, (Kuhlmann et al., 2008) and (Torabian et al., 2018) conducted tests on transverse fillet welds in lapped joints and compared the results with the Eurocode and AISI (2016) specification respectively. The findings indicate that the existing design method might not be sufficiently conservative in thin sheets, leading to discussions on improving strength predictions.The typical failure mode for different weld are shown in figure 2.8.

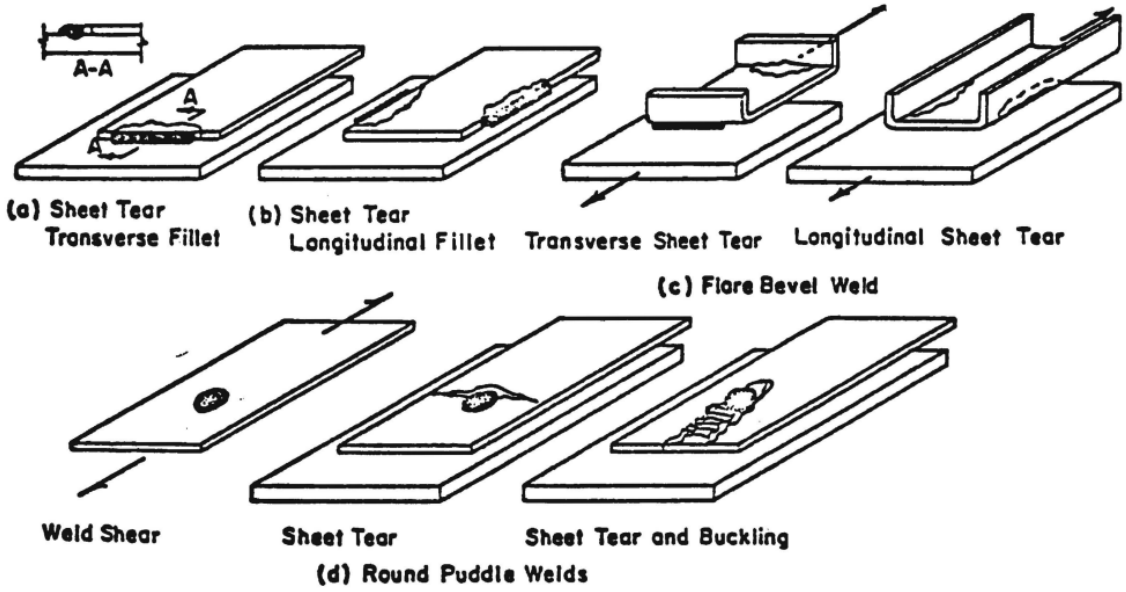

Figure 2.8: Typical failure mode (McGuire and Peköz, 1980)

2.10 Past Studies

This section is dedicated to reviewing previous literature that primarily examines the experimental investigation of welded connection joints. The discussion excludes studies concerning finite element modeling of welded connection joints, as such analyses lie beyond the scope of this research.

2.10.1 Study by Maali et al.(2022)

Maali et al. (2022) investigates into a comprehensive study involving six experimental tests conducted in two groups to explore the rotation capacity of bolted and welded beam-

column connections utilizing cold-formed steel sections under static loading conditions. This research fills gaps in existing standards by studying the rotation capacity of bolted and welded connections. In the bolted group, gusset plates of various thicknesses were welded to the end plate using manual metal arc welding. Additionally, a 2mm thick stiffener was welded to the C Profile. The materials used were designated as S235. Bolts with an M8 diameter and grade 8.8 were used for the connections. The beam, composed of back-to-back light steel channel sections secured by 13 bolts, had a beam-to-column connection area with nine bolts. Load was applied using a hydraulic pump (250kN with 300mm stroke), and beam displacement was measured using three LVDTs (300 mm).

The moment-rotation curves and failure modes are shown in figure 2.9 and figure 2.10 respectively. The failure modes in bolted connections were identified in accordance with Eurocode 3 (1993), while welded connections exhibited specific collapse mechanisms, such as gusset plate yielding in the end-plate area and buckling of the C profile beam. Increasing the thickness of beams and gussets in bolted connections led to improved moment resistance, critical rotation capacity, and energy dissipation, although with a reduced of stiffness. Conversely, welded connections exhibited decreased stiffness, critical rotation capacity, energy dissipation, and joint ductility as beam and gusset thickness increased. The semi-rigid behavior observed in bolted connections compared to welded connections.

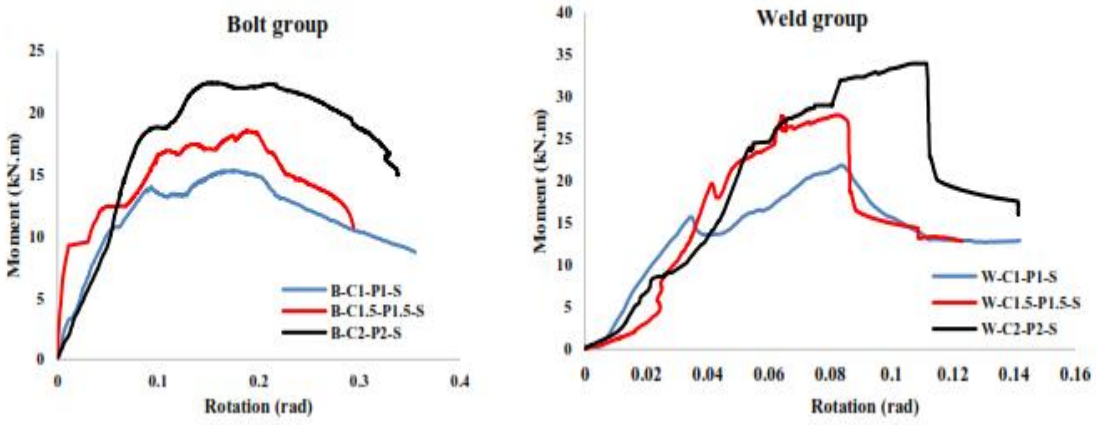

Figure 2.9: Moment-rotation curve of the two group (Maali et al., 2022)

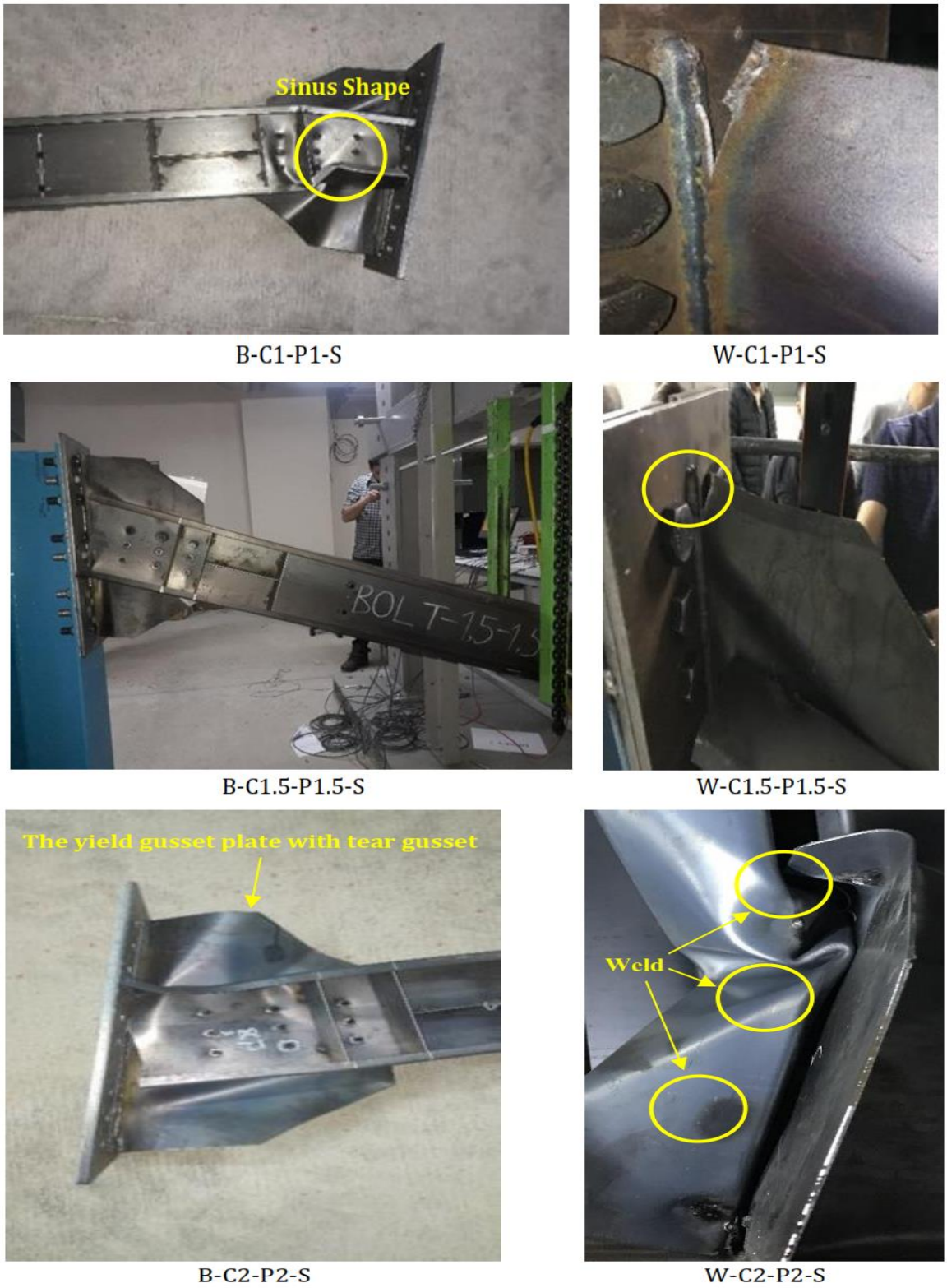

Figure 2.10: Collapse modes of test specimens and comparing collapse mode (Maali et al., 2022)

2.10.2 Study by Mallepogu and Madhavan (2023)

Mallepogu and Madhavan (2023) investigated the shear capacity of the cold-formed steel beam to column welded moment connection using clip-angle and flange-cleat. Total 36 nos sample have been used for the study. The material properties of the cold-formed steel (CFS) clip-angle and CFS flange cleat were determined from the tensile coupon tests .The test specimen consists of an 8 mm thick Hot-Rolled Steel (HRS) beam of 1000 mm length, 2 mm thick lipped C-section CFS columns of 400 mm height, 90^0 bend CFS L-shape connectors (clip-angle) and 90^0 bend CFS L-shape connector (flange-cleat). The web portions of the beam and column were connected by CFS welded clip-angle to form a CFS welded shear connection. Subsequently, it is converted into a welded moment connection by including a flange cleat between the flange portions. In all specimens, one leg of the clip-angle (CA) is fillet welded with 2.5mm thickness to the web of the C-shaped cold-formed steel (CFS) column, while the other leg is connected to the hot-rolled steel (HRS) beam web using M4.6 grade bolts with a diameter of 12mm. For this study, welding was performed using E6013 electrodes. Similarly, one leg of the flange-cleat (FC) is bolted to the flange of the HRS beam with 6mm diameter bolts, while the other leg is fastened to the flange of the CFS column using 5.8mm diameter screws. A four-point bending test was conducted on all the test specimens . An eccentricity of 230 mm was maintained between the center of the loading point and the column face. A 100 mm wide HRS fitting was used to apply the load on the specimens.

This research introduces two shear equations for CFS welded moment connections: (i) a new empirical shear equation and (ii) a new shear equation based on the shear strength of the shear connection. The variability in shear performance is demonstrated through force-displacement plots and clip-angle failure modes, including local buckling and distortional buckling, as depicted in Figure 2.11. The inclusion of flange cleats enhances the shear capacity of welded shear connections by an average of 67%, mitigating issues like load offset from the shear center and free twisting of the beam.

Figure 2.11: Failure modes in WM and WS (a) WM-local buckling; (b) WS-local buckling; (c) WM-distortional buckling; (d) WS-distortional buckling (Mallepogu and Madhavan, 2023)

2.10.3 Study by McGuire and Peköz (1980)

McGuire and Peköz (1980) investigates 342 nos symmetric fillet, flare bevel, arc spot, and arc seam welded connections subjected to static loading. The specimens were derived from 130 connections fabricated in steel shops, 122 under field conditions, and 90 in the Cornell laboratory under simulated field conditions. A standardized configuration was maintained, involving two plates butted together, with one or two cover plate sheets welded to each

side. E6010 electrodes were used for welding. In most cases, the connected plates were 7/16-inch thick hot rolled A36 steel plates. In some cases, the connected plates were sheets having a thickness equal to or greater than the cover plate sheets. Seven different cover plate gages were investigated,made from A446 Grade A or Grade E steel, Tension coupon tests were conducted of all the cover plate steel. The measured ultimate strengths are used in the strength prediction formulas.

Different welding techniques in the conducted tests exhibited varied failure modes. For transverse fillet weld specimens, primary failure mostly involved tearing along the weld contour, with occasional secondary weld shear and out-of-plane plastic deformation. Longitudinal fillet weld specimens showed tensile tearing across connected sheets as the main factor in most tests, with some cases exhibiting weld shear, cracking, or tearing along the weld contour. Transverse flare bevel weld tests predominantly resulted in plate tearing, with limited instances of weld shear failure and notable out-of-plane distortion. Longitudinal flare bevel weld tests primarily experienced tensile tearing across connected sections, with some cases involving weld shear, plate tearing parallel to the weld contour, and out-of-plane deformation. Arc spot weld tests experienced primary failure modes such as simple shear failure, plate tearing from the loaded side. Arc seam welds exhibited similar behavior to arc spot welds, with no observed simple shear failures.

2.10.4 Study by Teh and Hancock (2022)

Teh and Hancock (2022) conducted tests fillet welded connections using G450 cold-reduced steel sheets of two thicknesses, 1.5mm and 3.0mm, with corresponding yield strengths of 450 MPa and 480 MPa. Ten specimens of 0.06-inch sheet steel and nine specimens of 0.12-inch sheet steel were used for double shear welded connections, with the weld length matching the sheet width and the load applied in the rolling direction. The heat-affected zone (HAZ) tensile strength averaged 70.8 ksi (488 MPa) for 0.06-inch sheet steel and 71.8 ksi (495 MPa) for 0.12-inch sheet steel. However, coupon tests showed a notable reduction in HAZ tensile strength, averaging 86.4 ksi (596 MPa) for 0.06-inch G450 sheet steel and 76.7 ksi (529 MPa) for 0.12-inch G450 sheet steel.The study made five specimens each of 0.06-inch and 0.12-inch sheet steel for Double-lap transverse fillet welded connections, adjusting the nominal weld lengths from 1.6 inches (40 mm) to 4.7 inches (120 mm).

The test results showed that the design equation provided in AS/NZS 4600 or AISI Specification is appropriate for G450 sheet steel double-lap fillet welded connections, with a strong agreement between predicted failure loads and actual test loads. Test results also indicated that the design equations specified in AS/NZS 4600 overestimate the failure load of double-lap longitudinal fillet welded connections. The failure modes depends on the sheet thickness. The longitudinal fillet welded connections in the 0.06in sheet steel fail in the HAZs, while those in the 0.12in sheet steel fail mostly in the welds. Ten 0.06in sheet specimens and five 0.12in sheet specimens were fabricated for Single-lap transverse fillet welded connections. Findings suggest that the design underestimates the failure load, particularly for connections with longer welds, and there's inconsistency in the decrease of connection strength per unit weld length as weld length increases. Nine 0.06in sheet specimens and five 0.12in sheet specimens were fabricated for Single-lap longitudinal fillet welded connections. Weld tearing in the 0.12in single-lap connections started from both ends of each weld. This is because both ends of the weld were subjected to cracking action.

2.10.5 Study by M. Amraei et al. (2020)

Amraei et al. (2020) investigates the mechanical properties of ultra-high strength steels (UHSSs) with nominal yield stresses of 960 and 1100 MPa. Seven samples were extracted from S960 and S1100 plates along their rolling direction, with final dimensions measuring 55 x 10 x 5 mm. Utilizing a Gleeble 3800 thermal-mechanical machine, seven simulated weld thermal cycles were implemented, representing the temperature-time history of the joint at different distances from the weld fusion line (FL) in a typical gas metal arc welding (GMAW) process.

The specimens, machined into flat dog-bone shapes, underwent tensile testing to assess mechanical properties, including Vickers surface hardness, uniaxial tensile behavior, and Charpy impact toughness. Additionally, microstructural evaluation using field emission scanning electron microscopy (FESEM) was conducted. The results revealed distinct responses in the two types of steel.

S960, classified as a direct-quenched steel, exhibited a substantial reduction in hardness and tensile strength, with values dropping by up to 29% and 32%. Conversely, S1100, produced through a quenched and tempered process, showed minor softening (up to 4%) at

significant distances from the weld FL. This was accompanied by a modest 2% reduction in tensile strength and localized hardening (up to 13%) close to the FL.

2.10.6 Study by Owolabi et al.(2016)

Owolabi et al. (2016) conducted an experiment the effects of welding current on mechanical properties of welded joints between mild steel and low carbon steel. The experiment utilized an 8mm hot rolled mild steel plate, a 10mm iron rib bar, a E7018 low hydrogen electrode filter rod, and emery paper. Various equipment and tools were employed, including high voltage DC generators, air- and water-cooled electrode holders, a polishing machine, a grinding machine, a Monsanto tensiometer, a spectrometer analyzer, a metallurgical microscope, an impact testing machine, a hardness testing machine, a hack saw, a scrapper, pliers, a table vice, a veneer caliper, and a triangular file. The sample preparation and testing methods copied those outlined in the works of (Talabi et al., 2014).The chemical composition of received low carbon steel and mild steel samples was analyzed.

The primary objective of the study was to determine and compare the mechanical properties of welded joints. The prepared samples experienced cutting, machining, and were subjected to tensile tests, impact toughness tests, and hardness tests to assess their mechanical properties. Particularly, the study revealed that welding current significantly influenced the mechanical properties of welded joints between mild steel and low carbon steel.

With increasing welding current, the hardness of the weld exhibited an initial rise, reaching peaks at 115A for mild steel and 116A for low carbon steel, followed by a subsequent decrease. The ultimate tensile strength decreased overall with an increase in welding current. Both yield strength and impact strength decreased as welding current increased for both mild steel and low carbon steel. Overall, the study highlights the importance of selecting the appropriate welding current to achieve desired mechanical properties in welded joints between mild steel and low carbon steel.

2.10.7 Study by Ali et al. (2019)

Ali et al. (2019) studied on the Effects of welding on the change of microstructure and mechanical properties of low carbon steel.The investigation presented in this study

addresses the critical aspects of Shielded Metal Arc Welding (SMAW) on low carbon steel, focusing on both its mechanical properties and chemical composition.

The welding procedure adopted in this study involved the SMAW method, utilizing the E7010 electrode. A careful notch with a single V shape and a 70° angle was created prior to welding on a 10mm plate. Following the welding process, the specimens were cut in accordance with ASTM E-23 standards.

The study included Charpy impact tests, Rockwell hardness assessments, and micro-macro structure examinations of the welding zone, which included the base metal, Heat Affected Zone (HAZ), and weld metal. Noteworthy findings indicated that the weld metal area exhibited the highest impact toughness at 251 joule/mm², while the HAZ displayed the lowest impact toughness at 119 joule/mm². Hardness values across the welding zones were determined as approximately 87.6 HRB for weld metal, 73.9 HRB for the HAZ zone, and 67.1 HRB for the base metal.

Microscopic examination using an optical microscope revealed the presence of ferrite and pearlite in the microstructures of the weld metal zone, HAZ, and base metal. The consistent identification of these microstructural constituents provides insights into the transformative impact of the welding process on low carbon steel.

The welding induced notable changes in the microstructure and mechanical properties of the welding zone. Specifically, the impact toughness in the weld metal zone surpassed that of the Heat Affected Zone (HAZ). Hardness values varied across the welding zones, with the weld metal exhibiting the highest hardness, followed by the HAZ zone and the base metal.

2.10.8 Study by Nassar et al. (2021)

Nassar et al. (2021) conducted an experimental study of the effect of welding electrode types on tensile properties of low carbon steel. This paper discussed the effect of welding variables on the heat-affected zone (HAZ) by using a tensile test of welded 10 mm thick low carbon steel AISI1010 commercial plate, which is welded using the Shielded Metal Arc Welding (SMAW) method. Ten pieces of carbon steel plates have been prepared and machined to dimensions of (40 mm x450 mm) and (40 mm x 225 mm) to be used in this work. Single V-groove butt joint with 3 mm root face and angle of 75° with 2 mm opening

was prepared to fabricate the welded joints. Different welding electrodes E6013 and E7018 were considered as welding parameters investigated. The welded specimens were tested for tensile test. The results showed that selecting different welding electrodes had a remarkable effect on the mechanical properties such as the ultimate tensile strength, elongation percentage, and yield strength of the welded specimens. The increment in the electrical current for each electrode in the welding processes led to decrease in yield strength and tensile strength. The increased electrical current led to heightened heat input on the heat-affected zone (HAZ), causing observable changes in mechanical properties and potentially creating areas susceptible to defects.

2.10.9 Study by Afkhami et al. (2019)

Two sets of welded joints, one made from S700MC as the base material and the other one made from S1100, were investigated in this study (Afkhami et al., 2019). According to the materials manufacturer, S700MC is a hot-rolled HSS with a minimum yield strength of 700 MPa and S1100 is a hot-rolled UHSS with a minimum yield strength of 1100 MPa which is suitable for cold-forming. Air bending was used to introduce different degrees of pre-strain to the cold-formed base metals. Different degrees of cold-forming (DOC) were matched by using different radius to thickness ratios (r/t) for the bending trials. After that, GMAW, welding process was used to perform the welding procedures. To have a comparison between the cold-formed and virgin materials, each bended plate was welded to its virgin counterpart.

Matching filler materials were used for welding. Böhler alform 700-MC utilized for S700MC and Böhler union X96 for S1100. Uniaxial tensile tests were conducted on flat specimens cut from the welded samples. A Digital Image Correlation (DIC) system recorded displacements during the tensile tests to calculate elongation values.

Microstructure analysis, hardness measurement, tensile test, and Charpy impact test were conducted to assess the weldabilities of the cold-formed base metals. The results showed that the final joints had acceptable characteristics, and the cold-formed base metals demonstrated good weldability. However, it was found that the bending and pre-straining criteria recommended by the manufacturer must be satisfied to achieve an acceptable joint after welding. Beyond these criteria, the fracture elongation and notch toughness of the

welded joints decreased, and some welded samples failed from their cold-formed base metals.

2.10.10 Study by Liu et al. (2018)

Liu et al. (2018) conducted an experiment on mechanical behavior of high strength steel welded sections with various heat input energy. A total of 12 standard tensile tests on cylindrical coupons of welded sections were conducted, and full range deformation characteristics of these coupons were obtained through use of strain gauges and measurements on high resolution digital images. Both welding methods, namely, GMAW and SAW, were employed to prepare full penetration butt-welded sections with various line heat input energy. It was shown that in almost all coupons of the welded sections tested in the study, fracture occurred within the heat affected zones of the welded sections without any failure in neither the weld metal nor the base plates. For welded sections prepared with a line heat input energy equal to 1.0 kJ/mm, there was almost no reduction in the mechanical properties of the welded sections. However, for those welded sections prepared with a line heat input energy equal to 5.0 kJ/mm, only 70% of the yield strength of the base plates was attained. It is evident now that, these welded sections will suffer from a significant reduction in their mechanical properties, i.e. both yield and tensile strengths as well as ductility.

2.10.11 Study by Ovat et al. (2012)

Ovat et al. (2012) investigated the microstructural effect of electrodes types on the mechanical behavior of welded steel joints. Low and medium carbon steels joints were prepared using mild steel electrodes.Standard methods were applied for tensile and compression tests using the extensometer, impact test using the Izod testing machine while hardness was tested on the Rockwell testing machine. Metallic arc welding method was used to produce the joints. Metallography of the joints was conducted using standard techniques. Results obtained from the metallographic tests using Scanning Electron Microscope (SEC) showed that the heat affected zone (HAZ) of the parent material had significant impact on the mechanical behavior of the joint. The result showed maximum tensile strength 435 N/mm2 and 331N/mm2 attained for low and medium carbon steel welded with stainless steel electrodes respectively. Appreciable changes were noticed in

the impact strength for low carbon steel welded with gauge 12 electrode, about twice the impact strength of the low carbon steel. It was therefore recommended that gauge 12 electrode is most suitable for low carbon steel joints for impact strength, while stainless steel electrode is best suited for medium carbon steel joints when hardness property is desired. Stainless steel electrodes were recommended for welded joints when tensile strength is very desirable for low medium carbon steels.

2.10.12 Study by Dhalla and Peköz (1971)

Dhalla and Peköz (1971) conducted a total of 115 specimens on puddle and fillet weld connections under monotonically increasing static load. Basic variables considered in the design were: (a) thickness and the shape of the cover plates, and (b) weld size and its configuration. Three different thicknesses considered for the cover plates were 12 gage (0.108 inch), 18 gage (0.051 inch) galvanized ASTM A446 Grade A steel, and 28 gage (0.018 inch) galvanized ASTM A446 Grade E steel. Two basic weld configurations investigated were: (a) Puddle Welds, and (b) Fillet Welds. Varying the cover plate and weld configurations, 35 different types of connection specimens were fabricated for the present investigation. Most of the specimens had two 7/16 thick hot rolled plates, which were not considered as variables in the design of connection specimens. All connections underwent testing on a Baldwin Southwark hydraulic testing machine, applying a static monotonically increasing load.

Puddle weld connections exhibited notable out-of-plane deformations, particularly when the plate near the weld began yielding. Failure in these specimens typically initiated with plate tearing at the contour of the weld, ultimately resulting in transverse tearing of the plate. Some specimens displayed failure modes resembling shear and bearing failures observed in bolted connections. The average yield and ultimate strength developed by the cover plates were significantly lower than the yield and ultimate strength of the plate.In fillet welded connections, failure typically began near the fusion line of the weld, with only a few instances of primary failure due to shearing of the fillet weld. For longitudinal fillet weld specimens, failure initiated at the ends of the weld, with final failure accompanied by significant out-of-plane deformations and, in some cases, transverse tearing of the plate. In all transverse fillet weld connections, the primary failure mode was plate tearing at the contour of the weld.

2.11 Summary

After reviewing the existing studies on the weld connections of cold formed steel, it is observed that existing literature primarily focuses on welded joints formed using one or two welding processes with a limited number of electrode types. While these studies provide valuable insights, there remains a significant research gap regarding double shear welded joints formed with a broader range of welding processes and electrode types. Additionally, the variation in joint behavior under tensile loading across different plate thicknesses has not been comprehensively explored. Most studies either focus on specific plate thicknesses or overlook the impact of thickness variation altogether. Understanding how different welding processes and electrode types affect joint behavior across various sheet thicknesses is crucial for optimizing welded joint performance in practical applications.

Furthermore, although some research has investigated the impact of the heat-affected zone (HAZ) on higher thickness plates, there is a lack of understanding regarding its effect on lower thickness plates. Lower thickness plates may exhibit different HAZ characteristics and susceptibility to welding-induced distortions compared to thicker plates, highlighting the need for targeted investigation into this aspect. Therefore, the research gap lies in the comprehensive exploration of double shear welded joints, considering a wider range of welding processes and electrode types, and evaluating their effects on joint behavior under tensile loading across different plate thicknesses. Moreover, there is a need to investigate the influence of the HAZ on lower thickness plates to provide a more holistic understanding of welded joint performance across various conditions.

CHAPTER 3
MATERIAL SPECIFICATION AND TEST PROGRAM

3.1 Introduction

This chapter will provide an extensive examination of the material properties in cold-rolled steel plates, including coupon preparation, labelling, experimental setup, and results analysis. In the test program, a total of 24nos samples of double shear welded connection are tested using a universal testing machine (UTM) at the Military Institute of Science and Technology, Dhaka, Bangladesh. Prior to the main test, a series of coupon section having different thicknesses of cold rolled steel will be tested to understand the material specification. In addition, four weld coupon tensile and impact test will be conducted to determine the weld specifications. The chapter will further investigate into discussions on various welding types, procedures for weld coupon preparation, labelling of weld coupons, and a detailed exploration of experimental setups and findings. Additionally, the chapter will offer a demonstration of the specimen preparation, specimen labelling, experimental tensile test setup of the connection.

3.2 Mechanical Properties of Cold Rolled Steel Plate

This study employs two different grade cold-formed steel, namely ASTM A653 Gr.50 (Class-1) (1997) , and locally purchased cold-formed steel, ASTM A36 (2019) , for making the connections. The nominal yield strength of ASTM A653 Gr.50 (Class-1) is 345 MPa, while ASTM A36 has a nominal yield strength of 250 MPa. The plates of ASTM A653 Gr.50 (Class-1) are sourced from a local company and the local company had imported the cold rolled steel from a Chinese manufacturer. On the other hand, ASTM A36 plates are directly purchased from the local market. The plates utilized in this study have a nominal thickness ranging from 1.65 to 3.11 mm. Total six distinct thicknesses of cold-rolled plates has been used to determine their actual mechanical properties. The experimental process involved conducting coupon tests, which included coupon preparation, labelling, setting up the experimental apparatus for the coupon test, and analyzing the experimental results. The subsequent sections will provide detailed descriptions of each stage of the experiment.

3.2.1 Coupon Preparation

Before conducting the connection test, tensile coupon tests were carried out to collect the material properties of the connected cold formed steel plates. Tensile coupons were extracted from the same batch of material as used for the fabrication of the welded connection specimens. The geometric attributes of the coupons are illustrated in Figure 3.1. The dimensioning of the coupon is followed by the American Standard ASTM E8M (2013) guidelines.

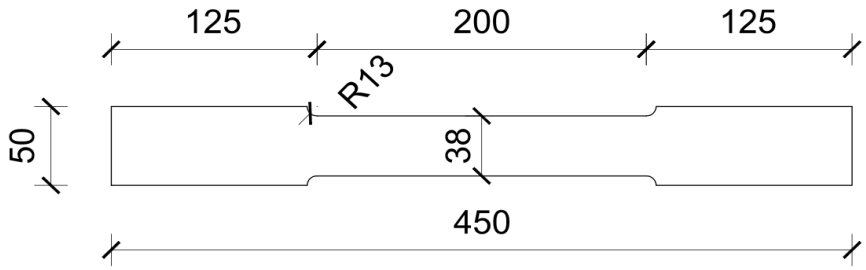

Figure 3.1: Geometric configuration of the coupon

3.2.2 Coupon Labelling

Figure 3.2 provides an explanation of the coupon labelling system, exemplified by a coupon labelled as "C2T1-a.". The initial letter denotes the type of cold-rolled steel, followed by a single digit representing its strength. The first digits of the cold rolled steel strength are used for naming where "3" is associated with 345 MPa cold rolled steel, and "2" is related to 250 MPa cold rolled steel. The letter "T" indicates the cold rolled steel thickness, with "1" representing plate thicknesses of 1.65 and 1.66 mm, "2" representing plate thicknesses of 2.03 and 2.04 mm, and "3" representing plate thicknesses of 3.10 and 3.11 mm. The trailing "a" signifies repetitive samples for the coupon. In this study, a total of 18nos plate coupon were tested, and a detailed list of these coupon is presented in Table 3.1 and 3.2. The coupon pictures for each thickness plate are illustrated in Figure 3.3, showcasing the comprehensive examination of 18nos plate coupons.

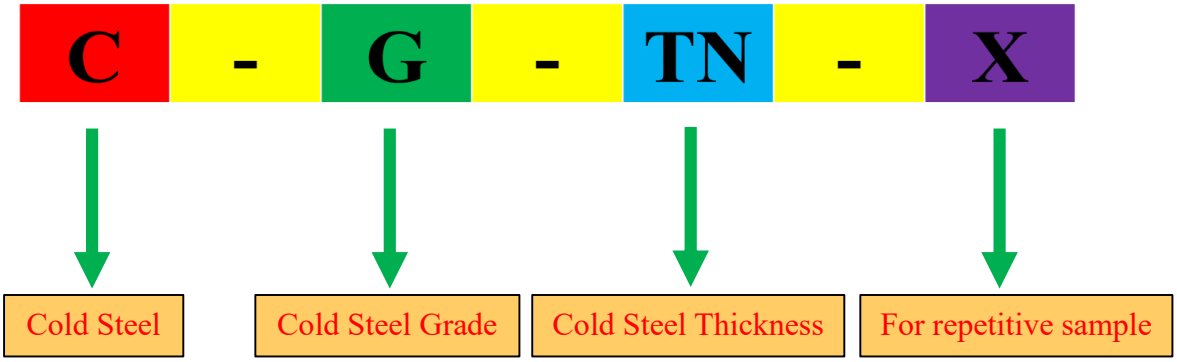

Figure 3.2: Coupon labelling

Table 3.1: Plate coupon test matrix for ASTM A653 Gr.50 (F_y =345 MPa) steel

Cold Steel Coupon, F_y=345ksi			
Sample No	Sample Marking	Cold Rolled Steel Strength, F_y (Mpa)	Cold Rolled Steel Average Thickness, t_n (mm)
1	C3T1-a	345	1.66
	C3T1-b	345	1.66
	C3T1-c	345	1.66
2	C3T2-a	345	2.04
	C3T2-b	345	2.04
	C3T2-c	345	2.04
3	C3T3-a	345	3.11
	C3T3-b	345	3.11
	C3T3-c	345	3.11

Table 3.2: Plate coupon test matrix for ASTM A36 (F_y =250 MPa) steel

Cold Steel Coupon, F_y=250ksi			
Sample No	Sample Marking	Cold Rolled Steel Strength, F_y (Mpa)	Cold Rolled Steel Average Thickness, t_n (mm)
1	C2T1-a	250	1.65
	C2T1-b	250	1.65
	C2T1-c	250	1.65
2	C2T2-a	250	2.03

	C2T2-b	250	2.03
	C2T2-c	250	2.03
3	C2T3-a	250	3.10
	C2T3-b	250	3.10
	C2T3-c	250	3.10

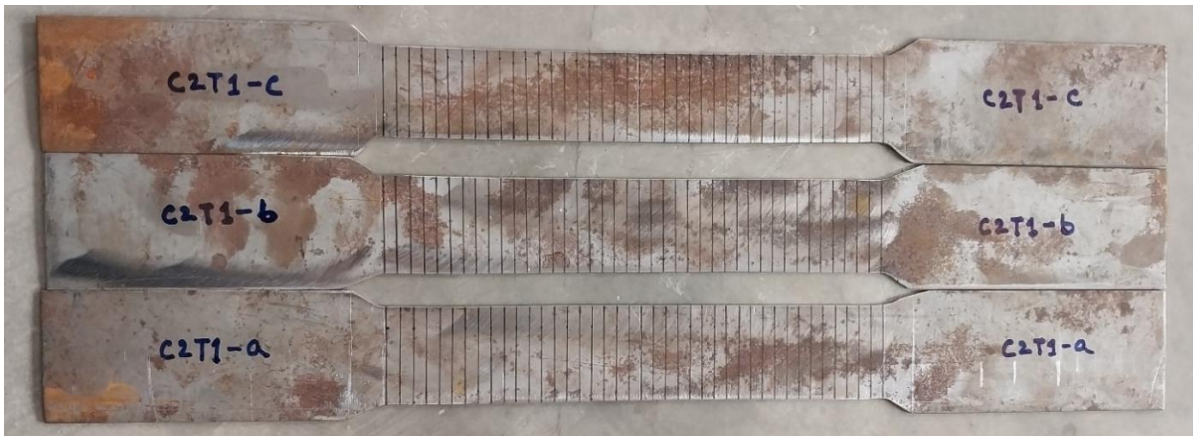

(a)1.65mm

(b)2.03mm

(c)3.10mm

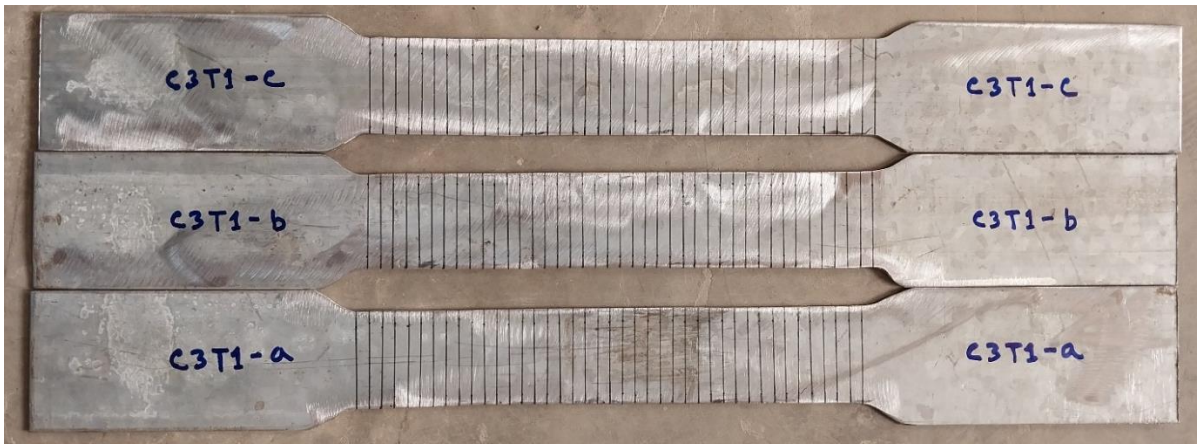

(d)1.66mm

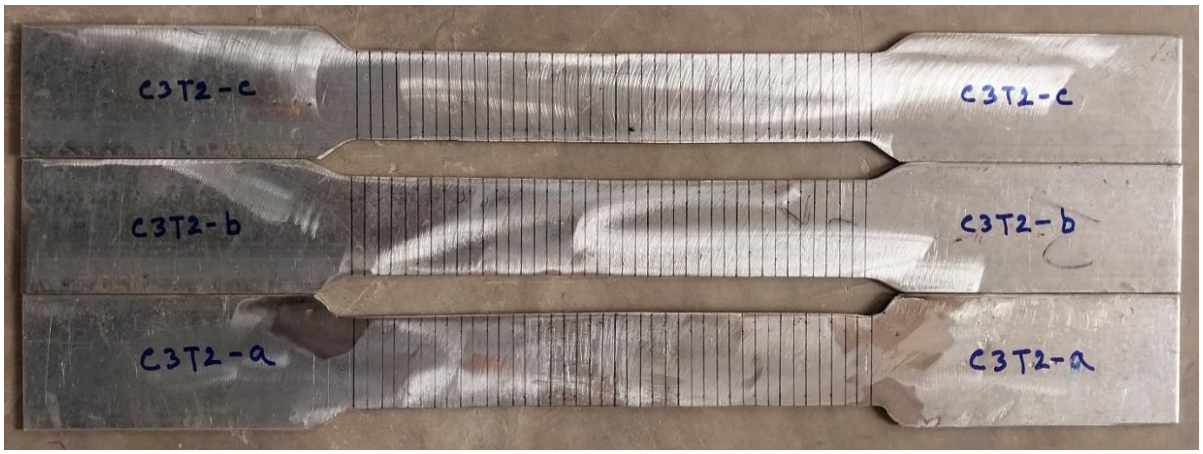

(e)2.04mm

(f)3.11mm

Figure 3.3: Thicknesses of the coupons used in the test program,

(a)1.65mm, (b)2.03mm, (c)3.10mm, (d)1.66mm, (e)2.04mm, (f)3.11mm

3.2.3 Experimental Setup for Coupon Test

The Tensile test of all the coupon was conducted using Instron universal testing machine (UTM). The displacement rate was initially set to 0.2 mm/min up to the elastic point, after which it continued at a speed of 1.0 mm/min. Figure 3.4 represents the setup employed for conducting the tensile test of the coupons. To facilitate the measurement of sample deformation, an extensometer with a gauge length of 100 mm was mounted in the middle of the necked portion. The tensile coupon test took place at the Military Institute of Science and Technology in Dhaka, Bangladesh, utilizing a static universal testing machine with a 1000 kN capacity.

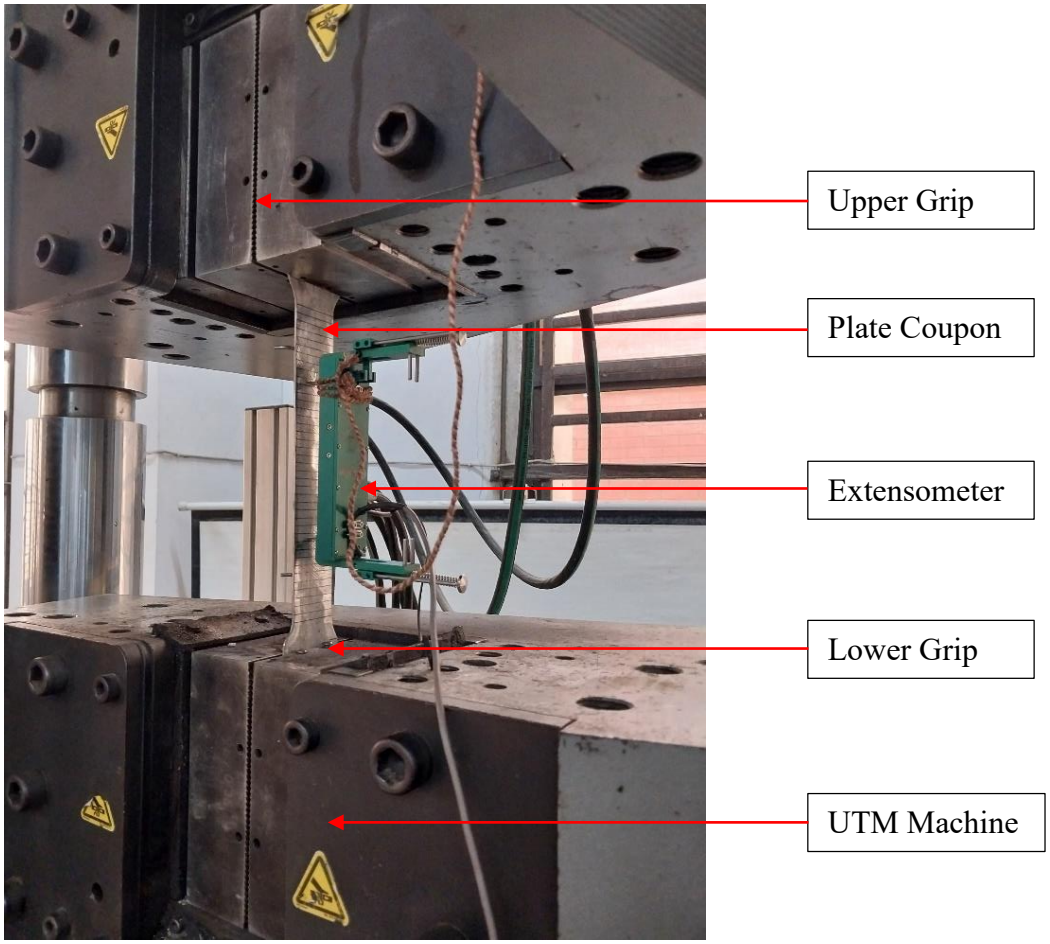

Figure 3.4: Arrangement for tensile coupon test

3.2.4 Coupon Test Result

Figure 3.5 presents the stress–strain curves corresponding to the cold-rolled plate. The tensile test was conducted for each thickness of cold formed steel plate to get the actual mechanical properties. Generally, two types of stress strain curve are seen in cold rolled steel i.c gradual yielding and sharp yielding curve. The measured yield and ultimate strength of cold formed steel shows higher capacity than the nominal properties which is very common. The average value of yield and ultimate strength is taken for each thickness plate which is shown in Table 3.3. For the determination of yield strength ,0.2% offset method has been used. As per the AISI Specification, the ratio of ultimate to yield stress ($F_{u/}F_y$) for steels utilized in structural framing members should not fall below 1.08 to ensure adequate ductility. Experimental findings suggest that this ratio ranges from 13% to 33% which meet the AISI Specification requirement . The necessary ductility for cold formed steel structural members is largely depending upon the specific application and the appropriateness of the material chosen.

Figure 3.6 provides a visual representation of a fractured coupon resulting from the test. The failure mode of cold rolled steel coupon specimen was observed both ductile and shear failure in the tensile test, is coincide with the plate tensile test failure pattern. Ductile and shear failure can occur in plate tensile test due to unique behavior of different materials and the stress conditions they experienced during the test. Shear failure can happen in material with weak interlayer bonding. Shear fracture refers to the breakage and or disintegration of a material due to the application of a strain force on its surface. Shear fractures occur due to concentrations of stress at flawed locations on a materials surface that are already otherwise susceptible to external attack. The occurrence of either ductile or shear failure depends on factors like the materials microstructure, composition and loading conditions. Ductile failure occurs in plate tensile test due to their ability to undergo significant plastic deformation before breaking. Ductile materials have a relatively high amount of toughness and can absorb energy as they deform. The material microstructure has ability to accommodate the movement of atoms without immediate fracture. The cause of ductile failure is the ability of the atoms to roll over each other into new positions without breaking the metallic bond.

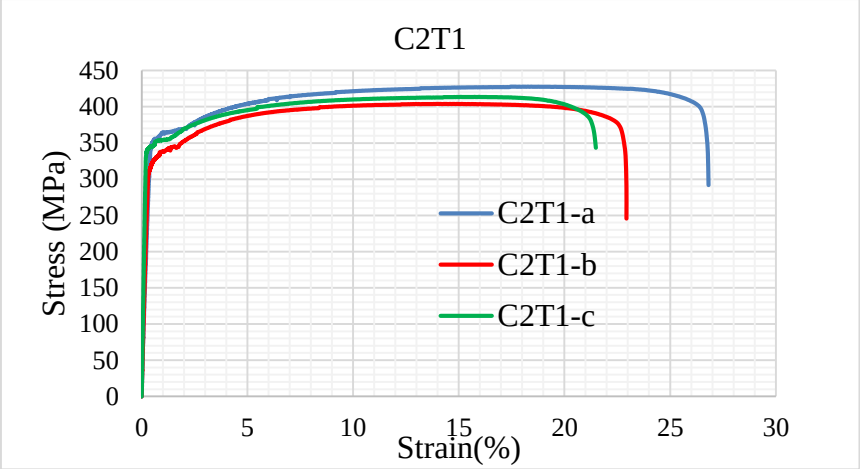

(a)C2T1

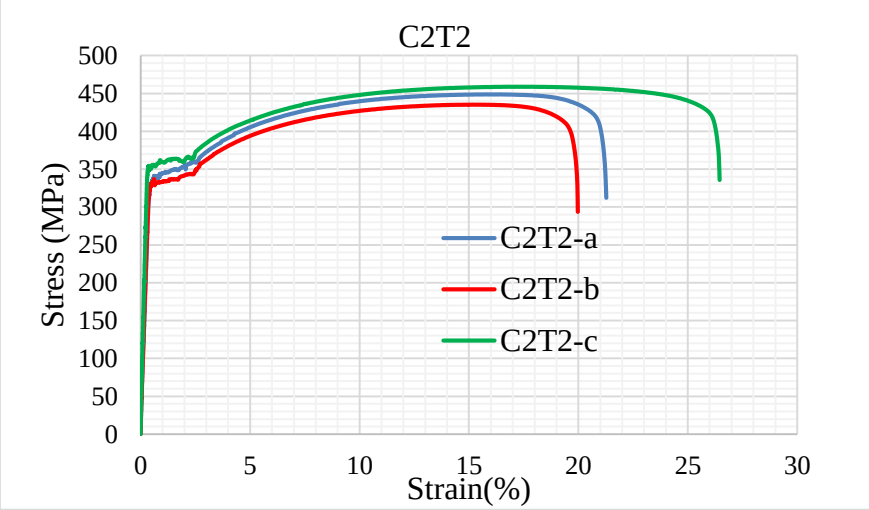

(b)C2T2

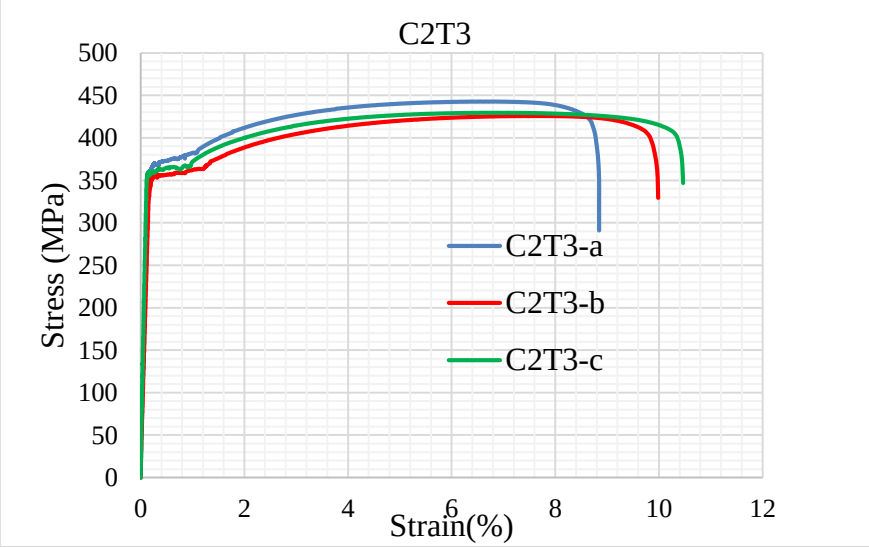

(c)C2T3

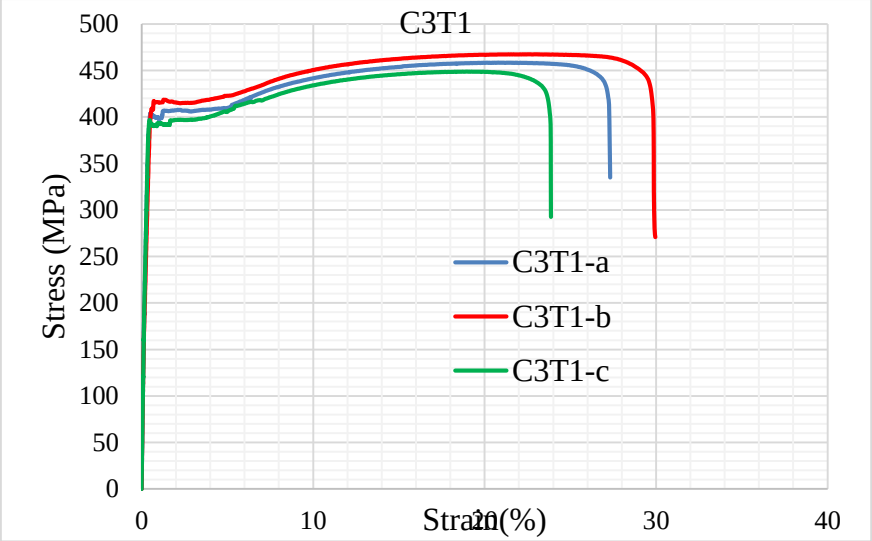

(d)C3T1

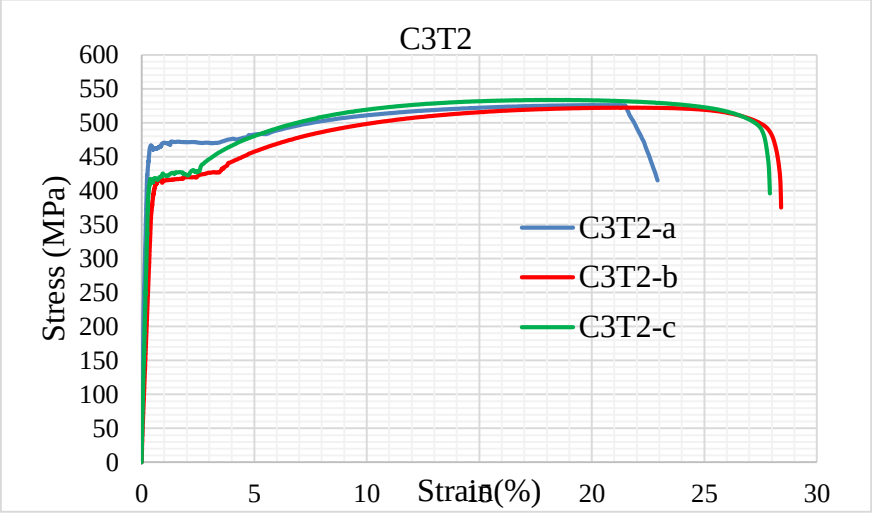

(e)C3T2

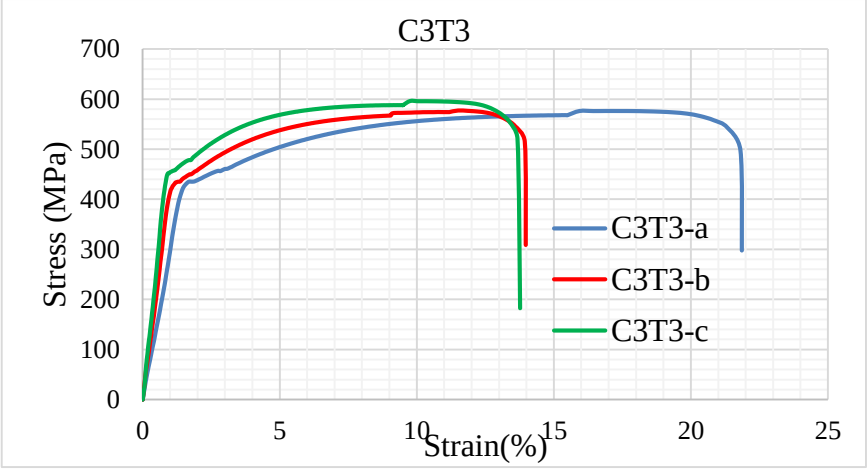

(f)C3T3

Figure 3.5: Stress strain graph for ASTM A653 Gr.50 and ASTM A36 steel

Table 3.3: Machanical properties of ASTM A653 Gr.50 and ASTM A36 steels from coupon test

Cold Steel	Plate Coupon	Average Plate thickness, t_n (mm)	Average Plate Width (mm)	Yield Stress (MPa)	Average Yield Stress, F_y (MPa)	Ultimate Stress (MPa)	Average Ultimate Stress, F_u (MPa)	F_u/F_y
F_y=250 MPa	C2T1-a	1.65	38.52	356	341	428	415	1.217
	C2T1-b		38.22	323		404		
	C2T1-c		35.61	344		414		
	C2T2-a	2.03	39.65	340	343	449	448	1.306
	C2T2-b		40.07	333		435		
	C2T2-c		39.47	355		459		
	C2T3-a	3.10	38.45	372	363	443	433	1.192
	C2T3-b		38.67	356		426		
	C2T3-c		38.62	362		430		
F_y=350 MPa	C3T1-a	1.66	38.57	402	403	459	458	1.136
	C3T1-b		38.26	416		467		
	C3T1-c		38.29	392		449		
	C3T2-a	2.04	36.48	465	432	526	527	1.221
	C3T2-b		38.38	413		522		
	C3T2-c		35.16	417		534		
	C3T3-a	3.11	38.29	431	440	576	583	1.325
	C3T3-b		38.32	434		577		
	C3T3-c		38.25	455		596		

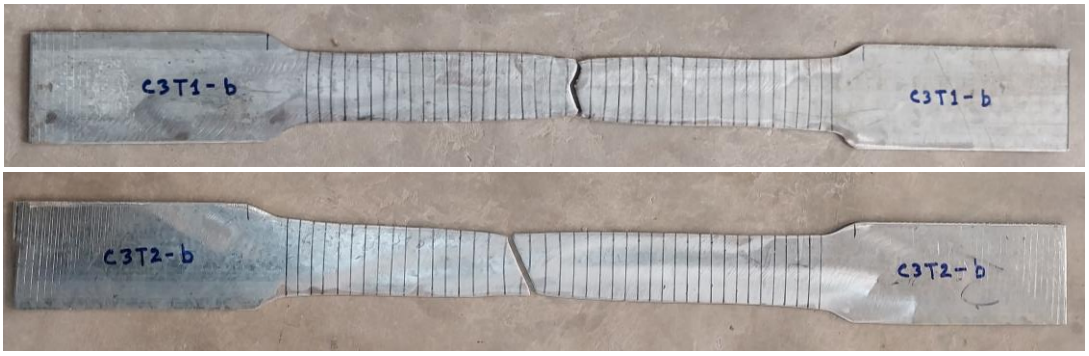

Figure 3.6: Typical failure patterns (Tensile failure mode) of plate coupons.

3.3 Welding Specification

In this study, three distinct welding processes were examined, showcasing the various methods through which welding can be accomplished. The welding process are metal inert gas welding (MIG), Shielded metal arc welding (SMAW), Flux cored arc welding (FCAW). Under this three-welding process, four different electrodes have been employed for making the weld coupon. The subsequent sections will provide detailed descriptions of each stage of the experiment.

3.3.1 Welding Electrode Type

Four electrodes under three welding process are used for making the weld coupon. The electrode is ER50S-G for metal inert gas welding (MIG), E71T-1C for Flux cored arc welding (FCAW) and E6013 and E7018 for Shielded metal arc welding (SMAW). These specific electrode types are represented in Figure 3.7. One weld coupon was made for each type electrode.

(a) Electrode ER50S-G for MIG Welding (MIG)

(b) Electrode E71T-1C for Flux Cored Arc Weld (FCAW)

(c) Electrode E6013 for Shielded Metal Arc Welding (SMAW)

(d) Electrode E7018 for Shielded Metal Arc Welding (SMAW)

Figure 3.7: Different types of electrode of weld processes

3.3.2 Welding Coupon Preparation

The geometric attributes of the weld coupon are illustrated in Figure 3.8. To prepare the weld coupon, two 25mm thick plates are prepared by beveling the edges at a 45-degree angle. This beveling process helps create a V-groove which provides space for the weld metal to penetrate and create a strong bond. The specific type of electrode is used to weld the two beveled plates together. After the welding is completed, a sample is cut from the welded joint. This sample is typically taken from a specific location to assess the quality of the weld and ensure it meets the required standards. The cut weld sample is then used to create a weld coupon. A weld coupon is a standardized test specimen that represents the quality and integrity of the weld. It is used for various tests, such as tensile testing, bend testing, and radiographic examination, to evaluate the weld performance and integrity. The complete fabricating process of weld coupon is shown is Figure 3.9.

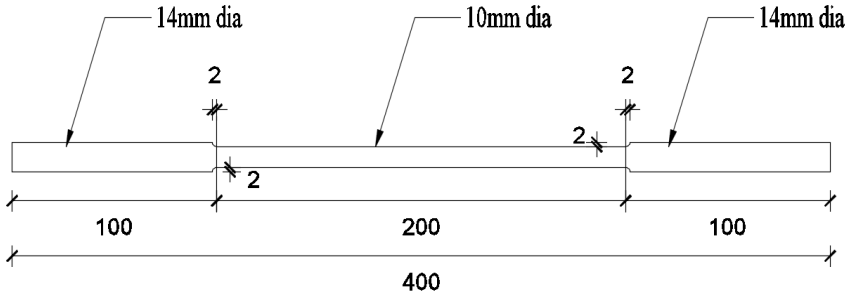

Figure 3.8: Geometric configuration of the weld coupon

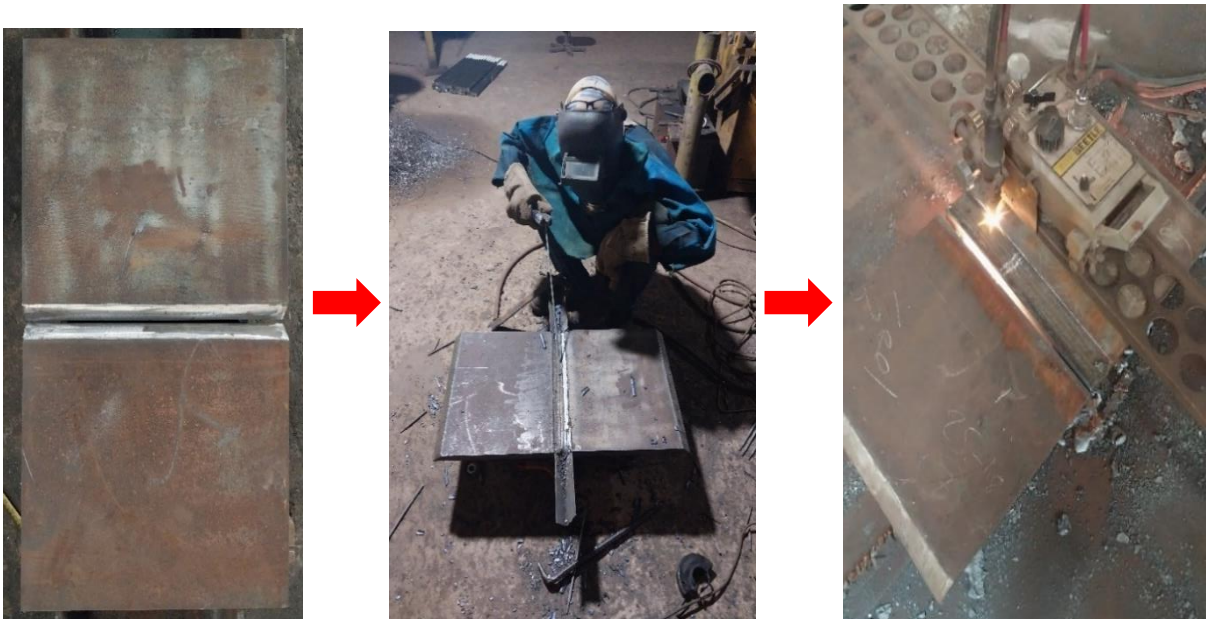

Step-1: Two 25mm thick Plate with 45-degree bevel

Step-2: Welding

Step-3: Sample Cutting

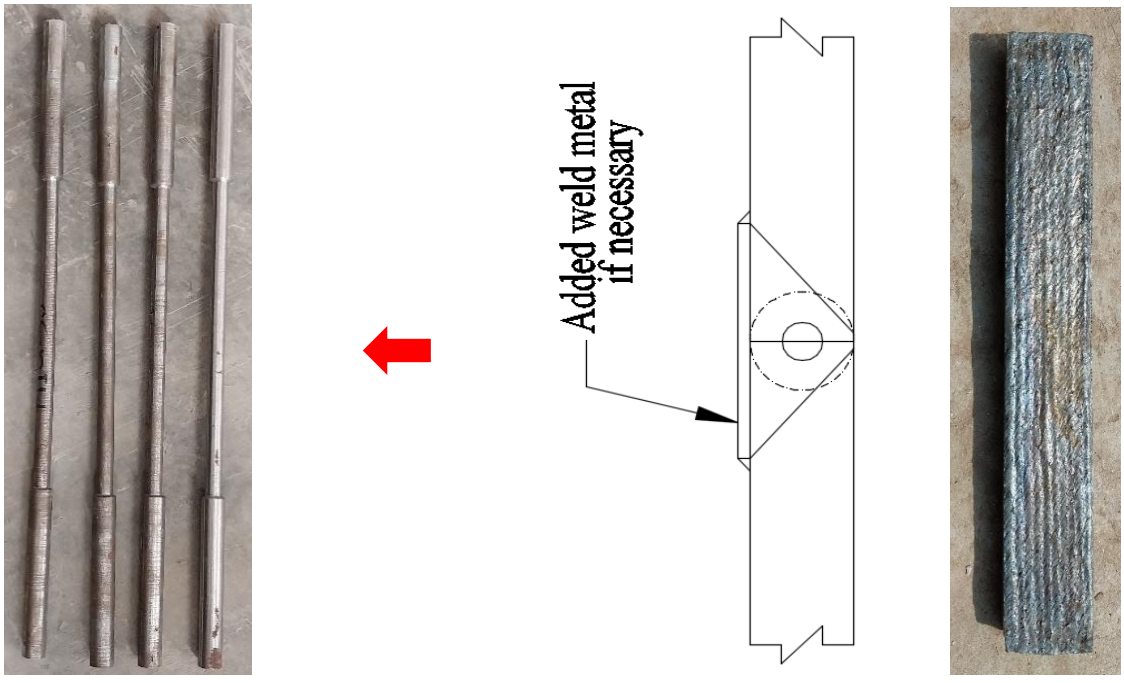

Step-5: Weld Coupon

Step-4: Sample

Figure-3.9: Weld coupon making process

3.3.3 Weld Coupon Labelling

Figure 3.10 provides an explanation of the weld coupon labelling system, exemplified by a coupon labelled as "SMA-48". The initial three letter indicates the welding process, with "SMA" representing Shielded Metal Arc welding (SMAW), "MIG" denoting Metal Inert Gas welding (MIG), and "FCA" indicating Flux Cored Arc welding (FCAW). The subsequent two digits represent the electrode strength. The first two digits of the electrode strength are used for naming: "34" corresponds to the ER50S-G electrode with a strength of 345 MPa, "41" is for the E6013 electrode with a strength of 416 MPa, and "48" is used for both the E7018 and E71T-1C electrodes, each with a strength of 483 MPa.

In this study, a total of 4nos weld coupon were prepared, and a detailed list of these weld coupon is presented in Table 3.4. The weld coupon pictures for each electrode are illustrated in Figure 3.11.

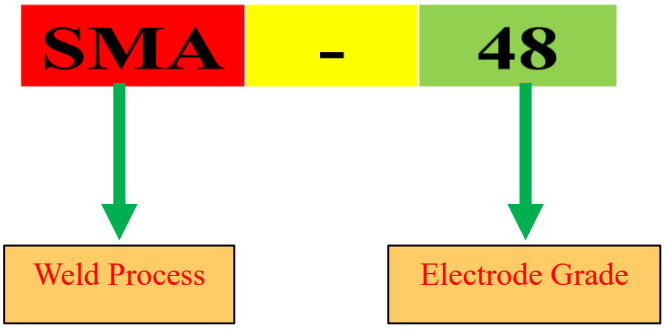

Figure 3.10: Weld coupon labelling

Table 3.4: Weld coupon test matrix

Weld Coupon			
Sample No	Sample Marking	Process	Weld Strength
1	MIG-34	MIG	345
2	SMA-41	SMAW	414
3	SMA-48	SMAW	483
4	FCA-48	FCAW	483

Figure 3.11: Weld coupon sample

3.3.4 Weld Coupon Test

The test specimen is a cylindrical sample with a 10 mm diameter and a gauge length of 200 mm. The geometric attributes of the coupons are illustrated in Figure 3.8. The test setup of weld coupon is shown is Figure 3.12. The specimen is tested in the INSTRON machine according to Australian Standards AS2205.2.2 (Standard, 2003). An extensometer is attached to the gauge length of the specimen. An extensometer is a device used to measure elongation or strain in the material during the test accurately. The test begins with an initial speed of 0.2 mm/min. This slow speed is used in the elastic zone of the material. If the specimen is unloaded in this region, it will spring back to its original length, showing no permanent deformation. The test continues with a speed of 1.0 mm/min in the plastic zone.

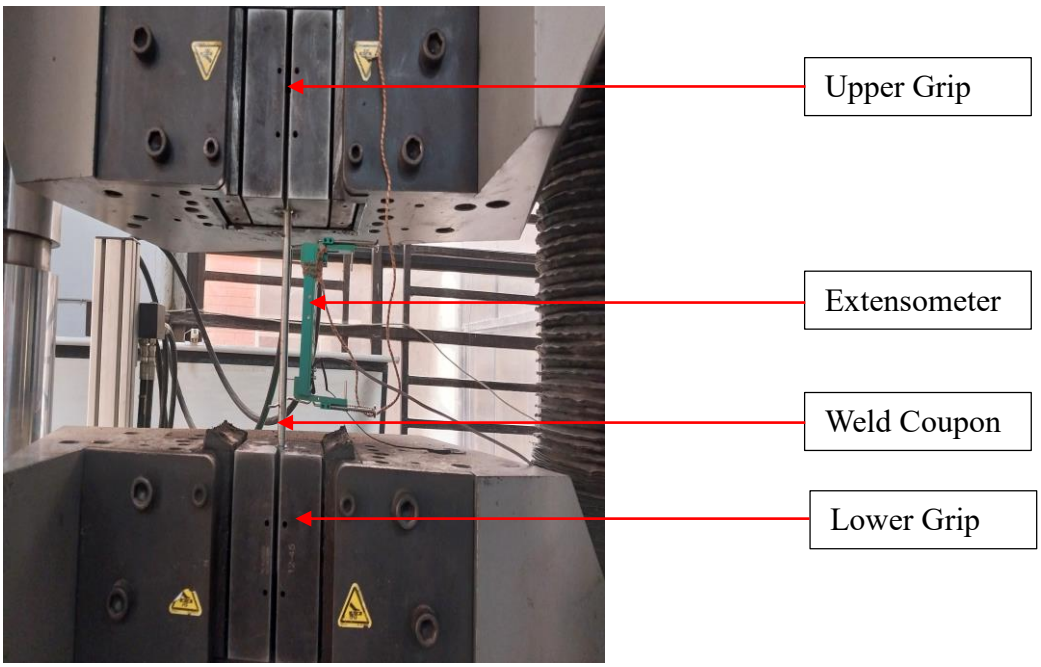

Figure 3.12: Test set-up for weld coupon

3.3.5 Weld Coupon Test Result

The tensile test of the weld coupon specimen revealed a failure mode characterized by both ductile and shear failure, as represented in Figure 3.13. The SMA-41 weld coupon specimen exhibited shear failure, while the remaining three specimens MIG-34, SMA-48, and FCA-48 displayed ductile failure. Shear failures were characterized by a sudden fracture, whereas ductile failures showed a more gradual rupture.

The stress vs strain curves associated with the weld coupon are illustrated in Figure 3.14. From the curve, it is shown that there is a sudden drop in force at the end of the elastic zone, indicating the transition from elastic behavior to plastic deformation. If the specimen were unloaded at this stage, it would exhibit permanent elongation. Following the elastic-plastic transition, there is a stage of constant force with increased elongation. This phenomenon is called the Luders effect, where the material exhibits localized deformation. After a certain amount of strain (Luders strain), the force increases again. Beyond the Luders effect, the force-elongation curve continues with a process known as strain hardening. In this stage, the material becomes stronger as it elongates. This can continue up to the point of maximum force. After reaching the maximum force, the specimen undergoes necking, becoming longer and thinner at a localized section. This necking is a precursor to fracture, and ultimately, the specimen fractures at this point. The stress-strain curve indicates that electrodes with lower strength exhibit greater ductility, while electrodes with higher strength demonstrate lower ductility. The yield and ultimate stress for weld coupon are shown in Table 3.5.

Figure 3.13: Failure patterns of weld coupon.

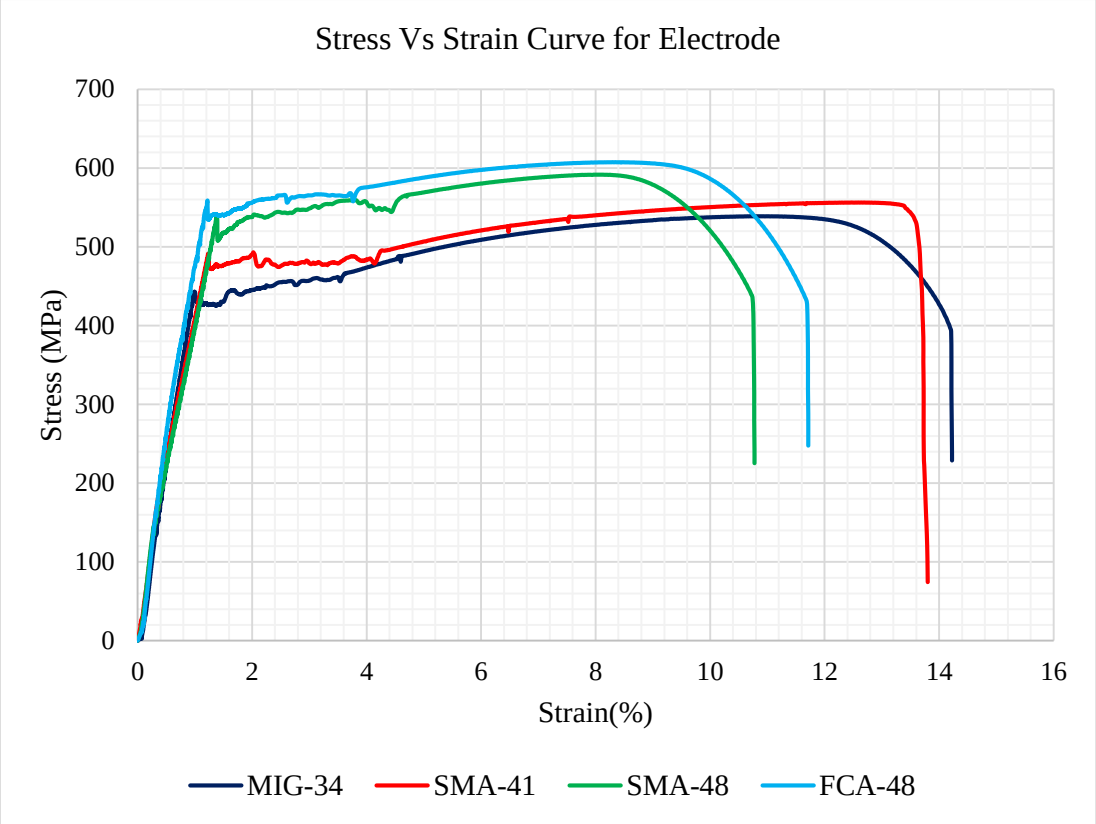

Figure 3.14: Stress Vs Strain curve for weld coupon.

Table 3.5: Machanical properties of weld coupon.

Weld Name	Process	Average Dia	Yield Stress, F_y (MPa)	Ultimate Stress, F_u(MPa)	Ultimate Strain (%)	Strain at Fracture (%)
MIG-34	MIG	10.03	431	539	10.64	13.96
SMA-41	SMAW	10.25	477	556	12.46	13.70
SMA-48	SMAW	10.20	523	591	7.96	10.46
FCA-48	FCAW	10.09	535	608	8.29	11.29

3.4 Charpy Impact Test of Weld Coupon

Notch test or V-notch test is a popular name used for the Charpy Impact Test. It is a highly standardized test which helps to measure the amount of energy absorbed by the specific material when impact load is applied to it. This energy is considered as a pathway to study the ductile-brittle nature of the sample. The Charpy impact test is applied in the industries as it is easy to conduct and offer the accurate and quick results regarding the ductility and

strength of the materials, but the results of the test are sometimes cannot be compared with other results.

3.4.1 Coupon Preparation for Charpy Impact Test

A total of eight Charpy V-notch samples were fabricated for the weld coupons.Two samples were prepared for each weld electrode. The dimensional specifications for the Charpy V-notch follow to the American Standard ASTM E2248-15. The standard specimen size for Charpy impact testing is 10 mm × 10 mm × 55 mm with 2mm depth V notch.The angle of the V notch is 45^0 . The Charpy V-notch samples geometric features are represented in Figure 3.15.

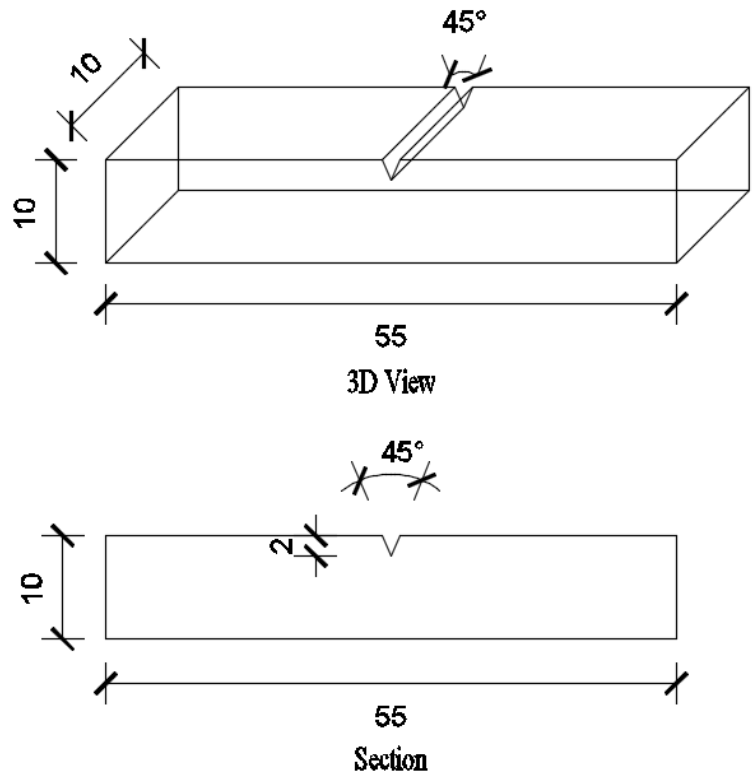

Figure 3.15: Geometric configuration of the Charpy impact test samples

3.4.2 Coupon Labelling for Charpy Impact Test

Figure 3.16 outlines the Charpy V-notch weld coupon labelling system, demonstrated by a sample labelled "MIG-34-a". This system utilizes the initial three letters to signify the welding process. Specifically, "MIG" denotes Metal Inert Gas welding (MIG), "SMA" represents Shielded Metal Arc welding (SMAW), and "FCA" indicates Flux Cored Arc

welding (FCAW). Following the welding process indication, the subsequent two digits in the Charpy V-notch weld coupon labelling system represent the strength of the electrode used. “34" corresponds to the ER50S-G electrode, which boasts a strength of 345 MPa. "41" designates the E6013 electrode, known for its strength of 416 MPa. "48" is utilized for both the E7018 and E71T-1C electrodes, each possessing a strength of 483 MPa. The trailing "a" denotes repetitive samples for the Charpy V-notch weld coupon.

In this study, a total of 8nos Charpy V-notch weld coupon were prepared, and a detailed list of these Charpy V-notch weld coupon is presented in Table 3.6. The Charpy V-notch weld coupon pictures for each electrode are illustrated in Figure 3.17.

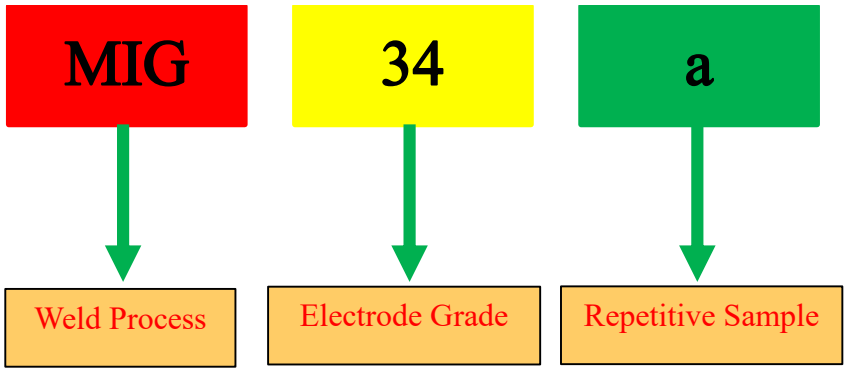

Figure 3.16: Charpy V-notch weld coupon labelling

Table 3.6: Charpy V-notch weld coupon test matrix

Charpy V-notch Weld Coupon			
Sample No	Sample Marking	Process	Weld Strength
1	MIG-34-a	MIG	345
	MIG-34-b	MIG	345
2	SMA-41-a	SMAW	414
	SMA-41-b	SMAW	414
3	SMA-48-a	SMAW	483
	SMA-48-b	SMAW	483
4	FCA-48-a	FCAW	483
	FCA-48-b	FCAW	483

(a).MIG Welding (ER50S-G)

(b).SMA Welding (E6013)

(c). SMA Welding (E7018)

(d).FCA Welding (E71T-1C)

Figure 3.17: Charpy V-notch weld coupon sample

3.4.3 Experimental Setup for Charpy Impact Test

The apparatus consists of a pendulum of mass 21.75kg and length that is dropped from a height 1.456m to impact a notched specimen of material. The energy transferred to the material can be inferred by comparing the difference in the height of the hammer before and after the fracture. The standard Charpy-V notch specimen is 55mm long, 10mm square in section and has a 2mm deep notch with V notch is 45^0 angle. The specimen is supported at its two ends on an anvil and struck on the opposite face to the notch by the pendulum. The amount of energy absorbed in fracturing the test-piece is measured and this gives an indication of the notch toughness of the test material. The test setup of charpy V notch weld coupon is shown is Figure 3.18. The specimen is tested in the charpy impact machine according to ASTM E 2248-15.

Figure 3.18: Charpy V-notch weld coupon test setup

3.4.4 Weld Coupon Impact Test Result and Failure Pattern

Table 3.7 presents the test results for the Charpy impact test conducted on different weld coupons.The Charpy impact test results reveal that SMA-41 specimen exhibits a lower impact value compared to the other three electrode specimens. MIG-34,SMA-48 and FCA-48 sample shows 48%, 81%, 100% higher value then the SMA-41 sample respectively. This lower impact value observed in the SMA-41 specimen might be attributed to the presence of slag during welding, which can introduce impurities and weaken the weld. Conversely, electrodes with higher strength like SMA-48 and FCA-48 demonstrate higher impact values. The superior quality of the material in these higher strength electrodes likely contributes to their increased impact resistance. Although the MIG-34 sample exhibits lower strength,but it shows good impact results.This can be caused to the absence of slag in the MIG-34 electrode. Without the presence of impurities introduced by slag, the weld remains free from weaknesses, leading to higher impact values.The failure pattern of Charvy V notch weld specimen are represented in Figure 3.19.

Table 3.7: Charpy V-notch weld coupon test result

Charpy V-notch Weld Coupon								
SL No	Sample Marking	Average width,a (mm)	Average depth,b (mm)	Notch depth (mm)	Effective depth, d=(b-2) (mm)	Impact Energy, K(Jule)	Average Impact Energy, K_{ave} (Jule)	Impact strength, H=K/(a*d) (Jule/mm2)
1	MIG-34-a	9.98	10.105	2	8.105	105	104	1.30
	MIG-34-b	10	9.895	2	7.895	104		1.32
2	SMA-41-a	10.08	10.015	2	8.015	74	70	0.92
	SMA-41-b	10.06	10.03	2	8.03	66		0.82
3	SMA-48-a	10.135	9.97	2	7.97	136	127	1.68
	SMA-48-b	10.205	10.12	2	8.12	118		1.42
4	FCA-48-a	9.85	10.25	2	8.25	136	140	1.67
	FCA-48-b	9.78	9.83	2	7.83	144		1.88

(a).MIG Welding (ER50S-G)

(b).SMAW Welding (E6013)

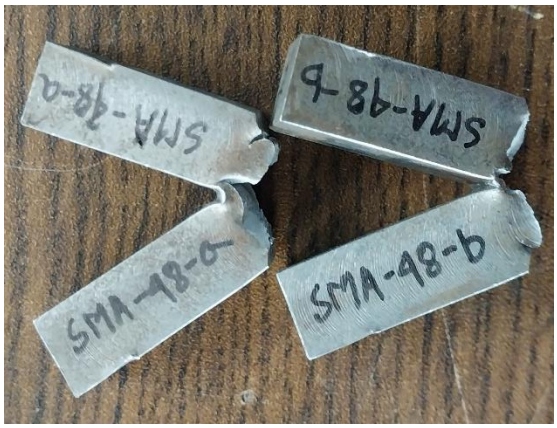

(c).SMAW Welding (E7018)

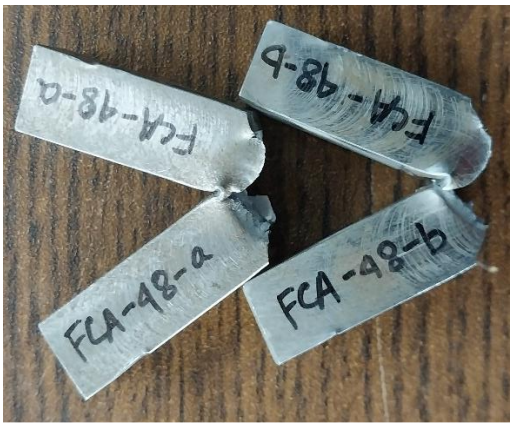

(d).FCAW Welding (E71T-1C)

Figure 3.19: Charpy V-notch weld coupon failure pattern

3.5 Double Shear Welded Specimen Details

The test specimens are constructed by arranging two hot rolled steel plates and two cold rolled steel plates. On the both sides, the two cold rolled steel plates overlap with the two hot rolled steel plates, forming a double shear welded connection at the joint. The dimensions of the hot rolled steel plates are 300X100 mm, and the cold rolled plates measure 150X75 mm. The experimental setup replicates the configuration detailed in Hancock , Wilkinson and Teh study (Hancock et al., 2000). The dimensions of the hot rolled plate are determined based on the UTM machine specifications. Each specimen is clamped at the hot-rolled plates on both ends within the UTM machine, with a distance of approximately 340 mm between the two grips. The dimensions of the cold rolled plate are selected to accommodate the extensometer configuration, ensuring precise positioning within the cold formed steel. Additionally, the weld length is applied along the width of the cold rolled plate, ensuring uniform distribution of tensile stresses across the cover plates. Figure 3.20 visually illustrates the geometric configuration of the samples.

Within the scope of this study, the investigation focuses on four distinct geometric parameters: weld process, weld electrode, Steel Grade, and plate thickness. The objective is to systematically vary these parameters and examine their respective effects on the behavior of the connections.

The specified ranges for the parameters used in this study are as follows:

Weld process: In this research, three welding processes have been employed. These welding processes include Metal Inert Gas Welding (MIG), Shielded Metal Arc Welding (SMAW), and Flux Cored Arc Welding (FCAW).

Weld Electrode: Four electrodes have been utilized in the preparation of the specimens. Specifically, the electrodes chosen for each welding process are as follows:

- For Metal Inert Gas Welding (MIG): ER50S-G
- For Shielded Metal Arc Welding (SMAW): E6013 and E7018
- For Flux Cored Arc Welding (FCAW): E71T-1C

Plates thickness: Six cold rolled steel plates of varying thicknesses are employed in the preparation of the specimens. The plate thicknesses used in the study are 1.65 mm, 1.66 mm, 2.03 mm, 2.04 mm, 3.10 mm, and 3.11 mm.

Steel Grade: This study involves the utilization of two distinct steel grades: ASTM A653 Gr.50 and ASTM A36.

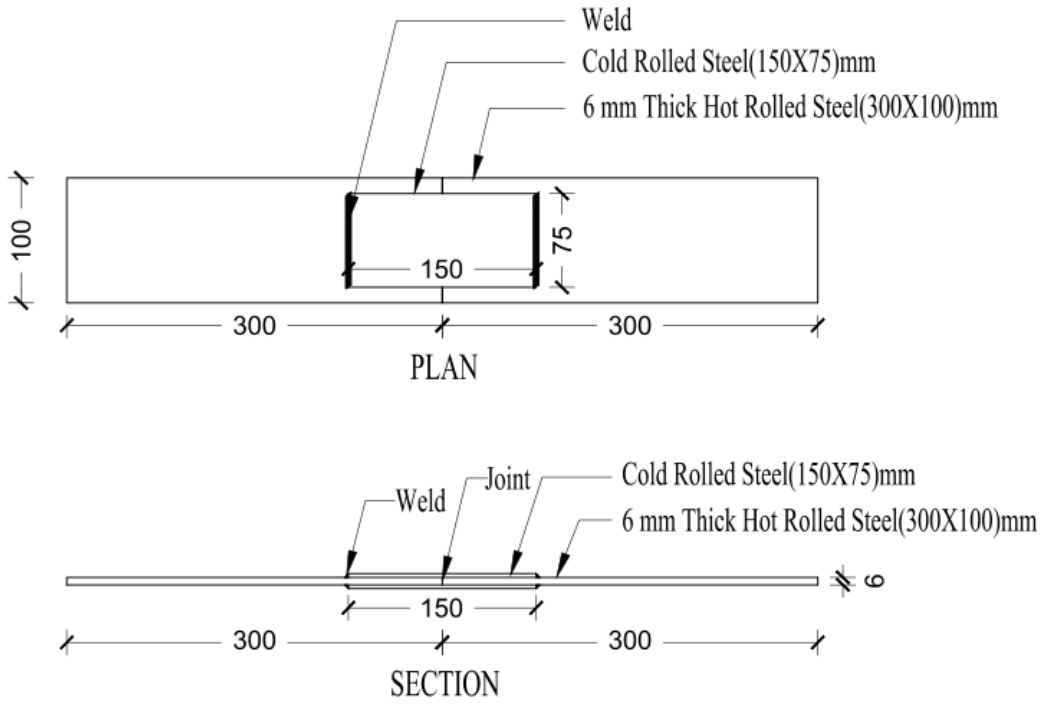

Figure 3.20: Geometric configuration of the samples

3.5.1 Double Shear Welded Specimen Labelling

Figure 3.21 provides an explanation of how specimens with welded connections are named in this study. For instance, a sample denoted as “M34C3D1H2F” follows a specific naming convention:

- The initial letter indicates the welding process, with "M" denoting Metal Inert Gas welding (MIG), "S" representing Shielded Metal Arc welding (SMAW), and "F" indicating Flux Cored Arc welding (FCAW).
- The subsequent two digits represent the electrode strength. The first two digits of the electrode strength are used for naming: "34" corresponds to the ER50S-G electrode with a strength of 345 MPa, "41" is for the E6013 electrode with a strength of 416 MPa, and "48" is used for both the E7018 and E71T-1C electrodes, each with a strength of 483 MPa.
- "C3" denotes the cold steel grade, where "C3" is associated with 345 MPa cold steel, and "C2" is related to 250 MPa cold steel.
- The letter "D" signifies a double shear welded connection.
- "T" stands for cold steel thickness, with "1" representing plate thicknesses of 1.65 and 1.66 mm, "2" representing plate thicknesses of 2.03 and 2.04 mm, and "3" representing plate thicknesses of 3.10 and 3.11 mm.
- "H2" represents the hot rolled steel grade, and "F" represents the fillet weld.

In this study, a total of 24 welded connected joints were utilized, and a detailed list of these samples, along with their geometric and material properties, is presented in Table 3.8 and 3.9. The Specimen ID for each sample is assigned following the instructions provided in Figure 3.21.

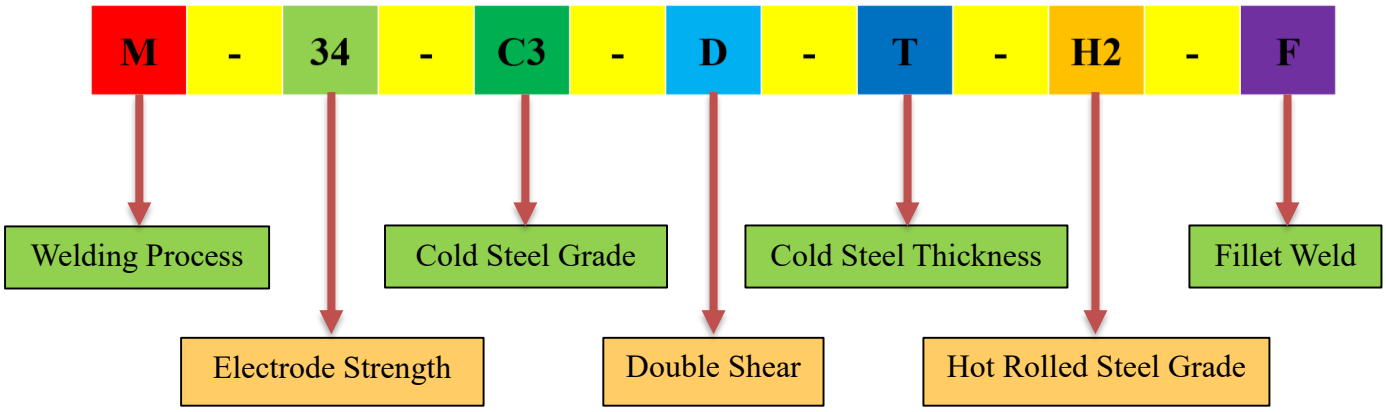

Figure 3.21: Labelling guideline of test specimens

Table 3.8: Test matrix of double shear welded joints for ASTM A653 Gr.50 (F_y =345 MPa) steel.

Cold Rolled Steel ASTM A653 Gr.50 (F_y =345 MPa)									
SL. No	Specimen ID	Weld Process	Weld Strength, F_w(MPa)	Cold Rolled Steel Strength, F_y(MPa)	Cold Rolled Steel Thickness, t(mm)	Connection Type	Hot Rolled Steel Strength, F_{yh}(MPa)	Hot Rolled Steel Thickness, t(mm)	Weld Type
1	M34C3D1H2F	MIG	345	345	1.66	Double Shear	250	6	Fillet
2	M34C3D2H2F	MIG	345	345	2.04	Double Shear	250	6	Fillet
3	M34C3D3H2F	MIG	345	345	3.11	Double Shear	250	6	Fillet
4	S41C3D1H2F	SMAW	414	345	1.66	Double Shear	250	6	Fillet
5	S41C3D2H2F	SMAW	414	345	2.04	Double Shear	250	6	Fillet
6	S41C3D3H2F	SMAW	414	345	3.11	Double Shear	250	6	Fillet
7	S48C3D1H2F	SMAW	483	345	1.66	Double Shear	250	6	Fillet
8	S48C3D2H2F	SMAW	483	345	2.04	Double Shear	250	6	Fillet
9	S48C3D3H2F	SMAW	483	345	3.11	Double Shear	250	6	Fillet
10	F48C3D1H2F	FCAW	483	345	1.66	Double Shear	250	6	Fillet
11	F48C3D2H2F	FCAW	483	345	2.04	Double Shear	250	6	Fillet
12	F48C3D3H2F	FCAW	483	345	3.11	Double Shear	250	6	Fillet

Table 3.9: Test matrix of double shear welded joints for ASTM A36 (F_y =250 MPa) steel.

Cold Rolled Steel ASTM A36 (F_y =250 MPa)									
SL. No	Specimen ID	Weld Process	Weld Strength, F_w(MPa)	Cold Rolled Steel Strength, F_y(MPa)	Cold Rolled Steel Thickness, t(mm)	Connection Type	Hot Rolled Steel Strength, F_{yh}(MPa)	Hot Rolled Steel Thickness, t(mm)	Weld Type
13	M34C2D1H2F	MIG	345	250	1.65	Double Shear	250	6	Fillet
14	M34C2D2H2F	MIG	345	250	2.03	Double Shear	250	6	Fillet
15	M34C2D3H2F	MIG	345	250	3.10	Double Shear	250	6	Fillet
16	S41C2D1H2F	SMAW	414	250	1.65	Double Shear	250	6	Fillet
17	S41C2D2H2F	SMAW	414	250	2.03	Double Shear	250	6	Fillet
18	S41C2D3H2F	SMAW	414	250	3.10	Double Shear	250	6	Fillet
19	S48C2D1H2F	SMAW	483	250	1.65	Double Shear	250	6	Fillet
20	S48C2D2H2F	SMAW	483	250	2.03	Double Shear	250	6	Fillet
21	S48C2D3H2F	SMAW	483	250	3.10	Double Shear	250	6	Fillet
22	F48C2D1H2F	FCAW	483	250	1.65	Double Shear	250	6	Fillet
23	F48C2D2H2F	FCAW	483	250	2.03	Double Shear	250	6	Fillet
24	F48C2D3H2F	FCAW	483	250	3.10	Double Shear	250	6	Fillet

3.6 Experimental Setup for Double Shear Welded Connection

Tensile test of the double shear welded connection was conducted using Instron 1000 kN universal testing machine (UTM). The experimental program was carried out at structural mechanics laboratory of Military Institute of Science and Technology (MIST) in Dhaka, Bangladesh.

The test was displacement controlled and specimens were loaded at speeds from 0.2mm/min to 1.0 mm/min. Some trial test was conducted before the main testing to get some insight into the testing periods. The test samples were mounted onto the Universal Testing Machine (UTM) by inserting them into the top and bottom grip of the machine as illustrated in Figure 3.22. The specimen was loaded until they failed which is indicated by a sudden drop in the load. The elongation was measured using Epsilon axial extensometer having gauge length of 100mm. This extensometer allowed the recording of elongation until the failure of the joint. The extensometer was placed centrally on the specimen. A schematic view of the joint test setup is shown in Figure 3.23. A data logger was used to record the load results from the UTM and the elongation from the extensometer simultaneously shown in Figure 3.24.

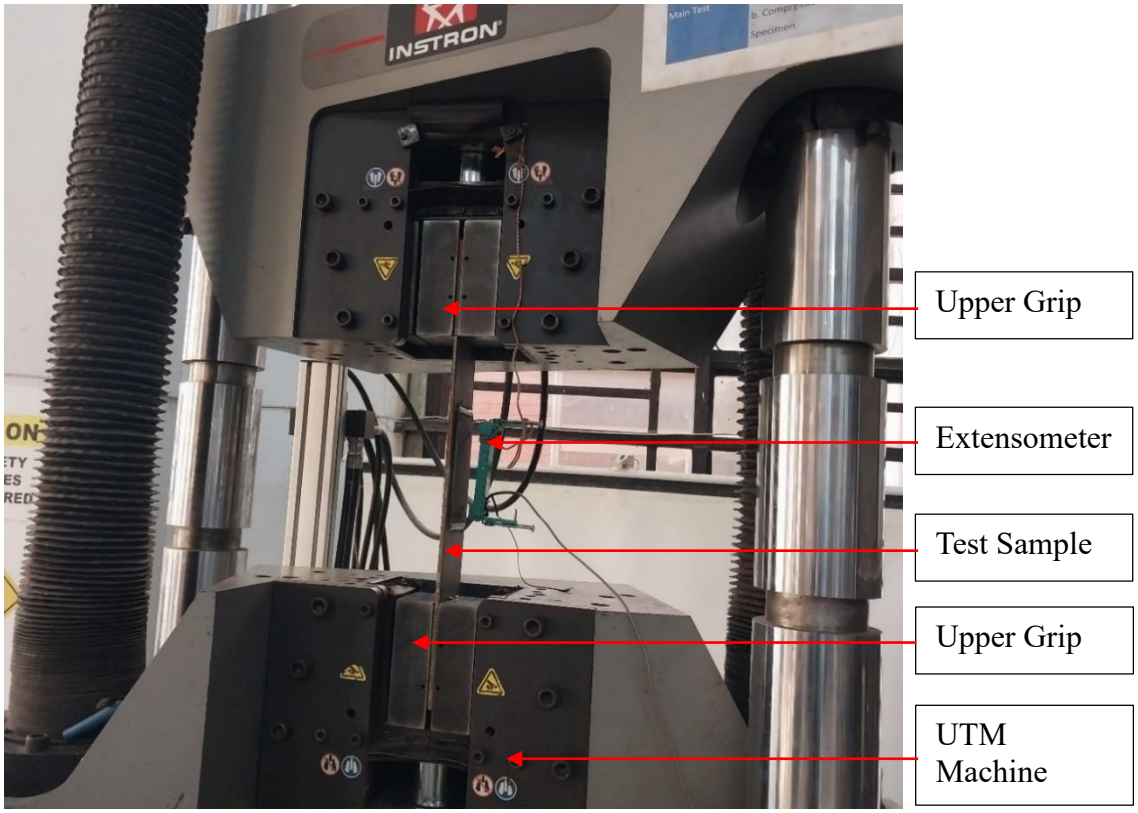

Figure 3.22: Experimental setup for tensile test of double shear welded connection

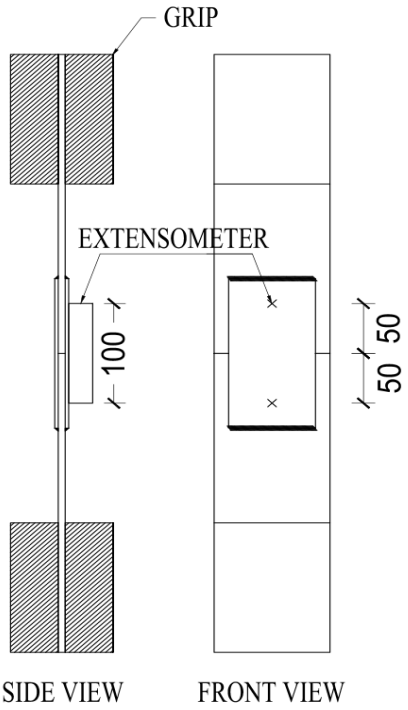

Figure 3.23: Schematic view of the joint test setup

Figure 3.24: Setup for load and elongation data acquisition

3.7 Summary

This research involves the use of two different grades of cold steel with a total of six distinct thicknesses of cold-rolled plates to prepare plate coupons. The plates nominal thickness in this study ranges from 1.65mm to 3.11mm, with three coupons made for each thickness, resulting in a total of 18 nos plate coupons. The 0.2% offset method was employed to determine the yield strength, and the ratio between ultimate and yield stress ranged from 13% to 33%, indicating the material suitability for ductilile structures. Both ductile and shear failures were observed in the tensile tests of the cold-rolled steel coupon specimens.

For the weld coupons, four electrodes were used under three welding processes: Metal Inert Gas Welding (MIG), Shielded Metal Arc Welding (SMAW), and Flux Cored Arc Welding (FCAW). The electrodes used were ER50S-G for MIG, E71T-1C for FCAW, and E6013 and E7018 for SMAW. One weld coupon was created for each electrode, and the failure modes observed in the weld coupon specimens included both ductile and shear failures.

The experimental program aimed to evaluate the behavior of double shear welded connections, investigating how it is influenced by the geometric and material properties of the connection. Double shear welded joints experienced testing until a significant drop in load occurred, marking the point of failure. The failure mode was documented based on the observed behavior at this critical point.

CHAPTER 4
RESULT AND DISCUSSION

4.1 Introduction

This chapter provides the results of tensile tests conducted on double shear welded connections between cold rolled and hot rolled steel. The experimental findings are presented in terms of the load-deformation relationship, failure mode, strength of connection, stiffness, and ductility. Here, Differences in these factors are documented with respect to the strength of the weld, the thickness of the plate, and the grade of the steel plate. The chapter also highlights the most critical factors influencing the behavior of the connections. In the final section, a comparison is drawn between the failure mode dependencies of the connection strength and thereby predicts the connection strength corresponding to the failure modes following AISI S100-16 guideline. Additionally, the chapter also addresses the impact of welding heat on the heat-affected zone.

4.2 Load-Displacement Response

The load-displacement relationship refers to the correlation between the applied load and the resulting elongation (deformation or extension) of a material or structure under stress. This relationship is commonly depicted in a load-displacement curve. In tensile testing, this relationship provides valuable information about the mechanical properties of a material. The curve typically exhibits distinct phases such as elastic deformation, plastic deformation, and ultimately failure. The slope of the initial linear portion of the curve represents the material stiffness or modulus of elasticity, while other features of the curve indicate aspects like yield strength, ultimate strength, and ductility. Understanding the load-displacement relationship is vital in assessing the behavior and performance of materials under various conditions, helping engineers and researchers characterize the mechanical properties and integrity of materials for diverse applications. In this section, load-elongation profiles of the connection are studied for varying plate thickness, and cold rolled steel grade. The load-displacement curves have been generated using extensometer data. The graphs are formed through plotting load in kN along the y-axis and elongation in mm along the x-axis.

4.2.1 Effect of Plate Thickness

Figure 4.1 to 4.8 exhibit the load deformation curves corresponding to plate specimens of varying thicknesses (1.66mm, 2.04mm, 3.11mm, 1.65mm, 2.03mm, and 3.10mm). The 1.65mm to 2.04mm thick plate specimens exhibit more ductility compared to the 3.10 mm and 3.11mm thick plate specimen. It is observed that, “Plate net section failure” occurs in plate specimens with a thickness range of 1.65mm to 2.04mm. For plates below 2.04mm thickness, the throat thickness of the weld will be nearly equal to the thickness of the plate itself. This occurs because one leg of the weld is three to five times longer than the other leg. Consequently, the weld capacity to withstand loads exceeds that of the plate net section capacity. The specimen in this thickness range exhibits good deformability and can withstand significant deformation before failure. Net section failure exhibits good deformability before reaching ultimate failure because the material around the stress concentration points undergoes plastic deformation. This plastic deformation allows the material to redistribute stresses and accommodate the applied load to some extent, leading to visible signs of deformation such as stretching or bending. During this phase of deformation, the material may undergo significant strain hardening, where its resistance to further deformation increases. This can provide the appearance of good deformability as the material can absorb more energy before reaching its ultimate failure point. It indicates that the connection failure will gradually occur over an extended period of time.

The 3.10mm and 3.11mm thick plate specimen has significantly higher connection strength compared to the 1.65mm to 2.04mm thick plate specimens. Joint with higher thickness plate has higher load carrying capacity owing to its material continutity,load distribution and no stress resiers. In a welded joint, the material of the two connected parts is fused together, creating a continuous and seamless connection. This continuity allows for the transfer of loads without interruption, resulting in a higher overall strength of the connection. Welded joints distribute loads more evenly across the connected parts compared to mechanical fasteners like bolts or rivets. This distribution of load helps in minimizing stress concentrations, thereby increasing the overall strength of the connection. Unlike bolted or riveted connections, welded joints do not introduce stress raisers such as holes or clearance gaps, which can weaken the structure. This absence of stress raisers contributes to the higher strength of welded connections. It is observed that, “Weld throat failure” occurs in plate specimens with a thickness of 3.10mm to 3.11mm. Increasing plate

thickness can heighten the likelihood of weld throat failure due to various factors such as increased stress concentration, reduced heat dissipation, and increased residual stress. The larger cross-sectional area of the material being welded leads to elevated stress concentrations at the weld throat, making it more vulnerable to failure. Moreover, welding thicker plates requires more heat input, but these plates dissipate heat slowly, which can result in slower cooling rates. This slower cooling can lead to issues such as slower solidification rates, larger grain size, and increased susceptibility to defects. Additionally, thicker plates may introduce higher levels of residual stresses, inducing distortion and concentrating stresses at the weld throat, further raising the risk of weld throat failure.

The 3.10mm and 3.11 mm thick plate specimen shows less ductility and the connection will fail suddenly without much deformation. This is happened due to the high stiffness and brittle behavior of welded connection. Welded joints tend to be stiffer and exhibit more brittle behavior compared to mechanical connections. This stiffness and brittleness can result in lower deformability and a more sudden failure mode. This implies that the specimen in this thickness range has lower deformability and may undergo rapid fracture without warning.

The observation that the initial slope of the load-deformation curve for each thickness specimen is very stiff suggests that the welded connection has high stiffness. The combination of material continuity, high stiffness of weld metal, limited flexibility, and reduced resilience to deformation contribute to the stiffness of welded connections. A stiffer connection can be desirable in certain applications, especially when structural stability or resistance to deformation is a critical factor. However, it's important to note that while high stiffness can be disadvantageous in some cases, it may also lead to reduced ductility. As a stiffer connection may reach its ultimate load or failure point more abruptly without significant deformation. The load deformation response curve for all specimen has four distinct regions namely, initial linear, yielding, Strain hardening and failure.

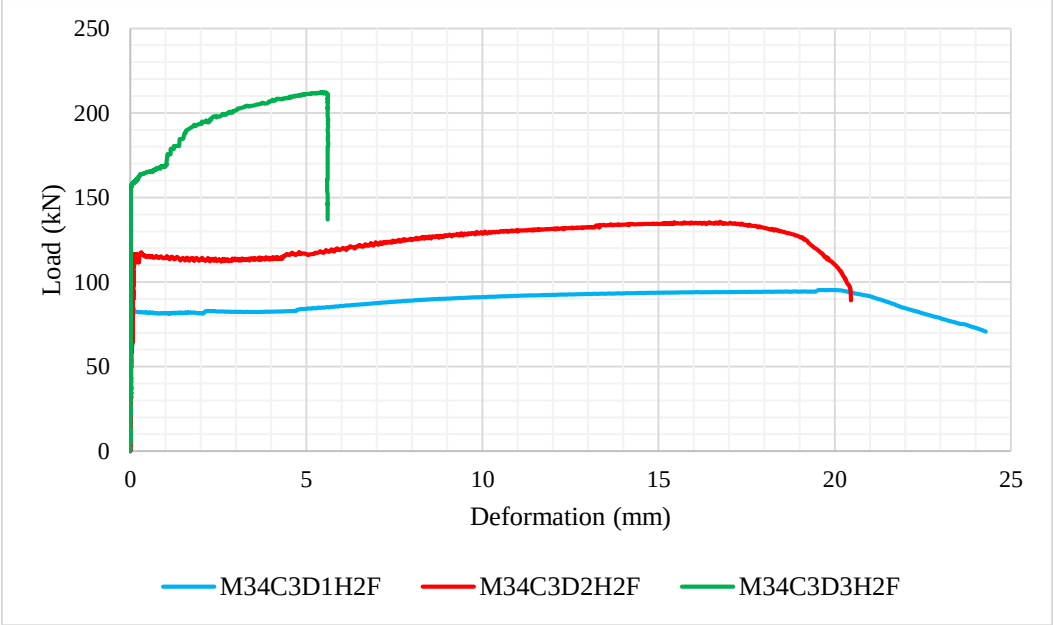

Figure 4.1: Load deformation curve for MIG-34 weld strength with 1.66mm,2.04mm,3.11mm (ASTM A653) plate thickness specimen.

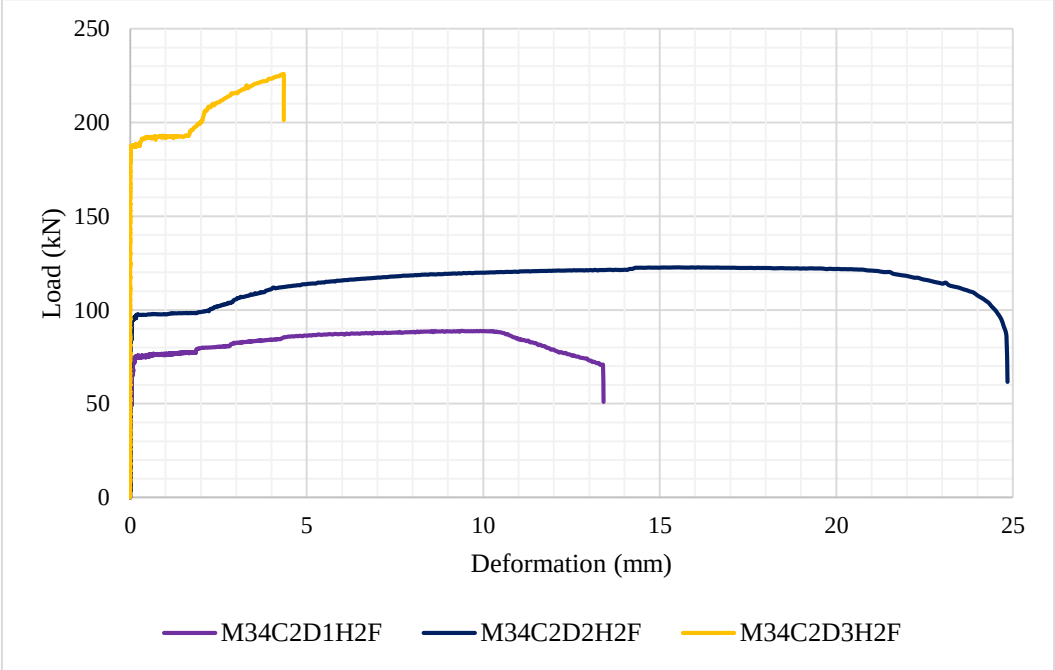

Figure 4.2: Load deformation curve for MIG-34 weld strength with 1.65mm,2.03mm,3.10mm (ASTM A36) plate thickness specimen.

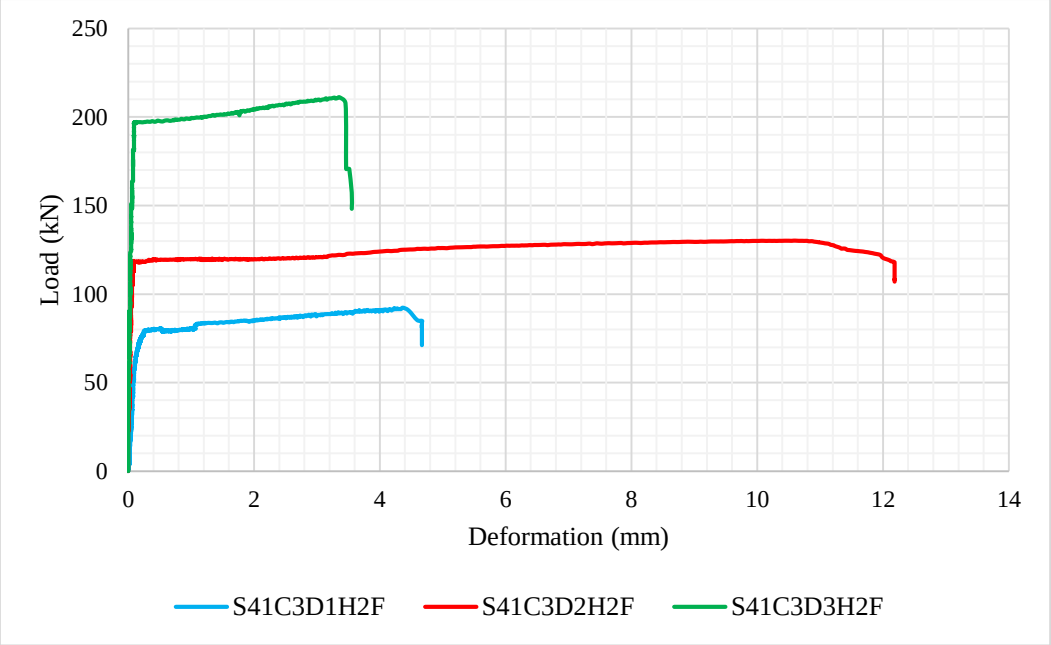

Figure 4.3: Load deformation curve for SMA-41 weld strength with 1.66mm,2.04mm,3.11mm (ASTM A653) plate thickness specimen.

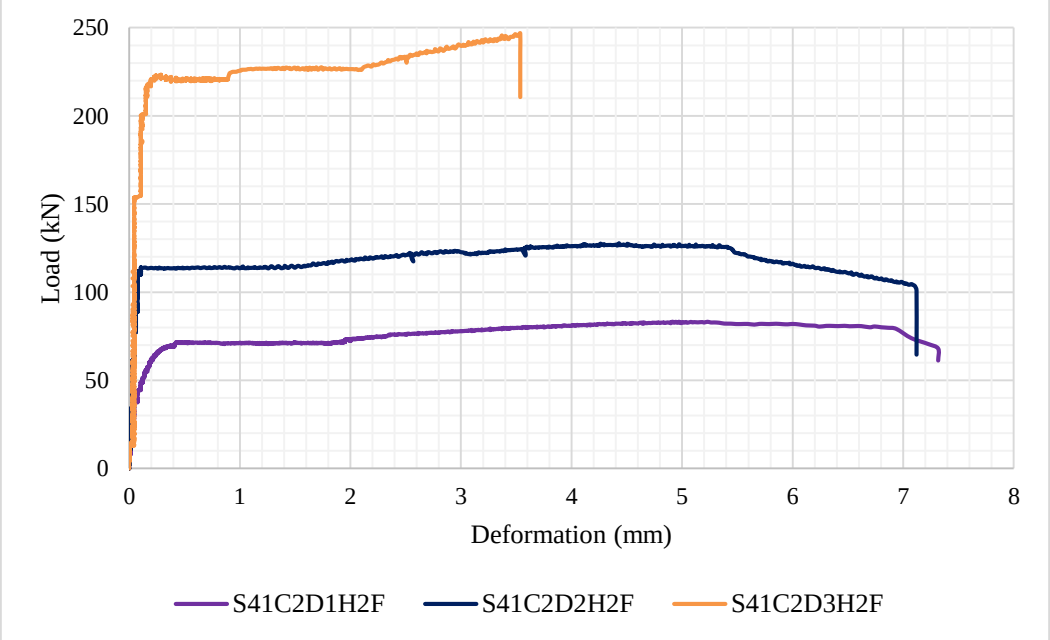

Figure 4.4: Load deformation curve for SMA-41 weld strength with 1.65mm,2.03mm,3.10mm (ASTM A36) plate thickness specimen.

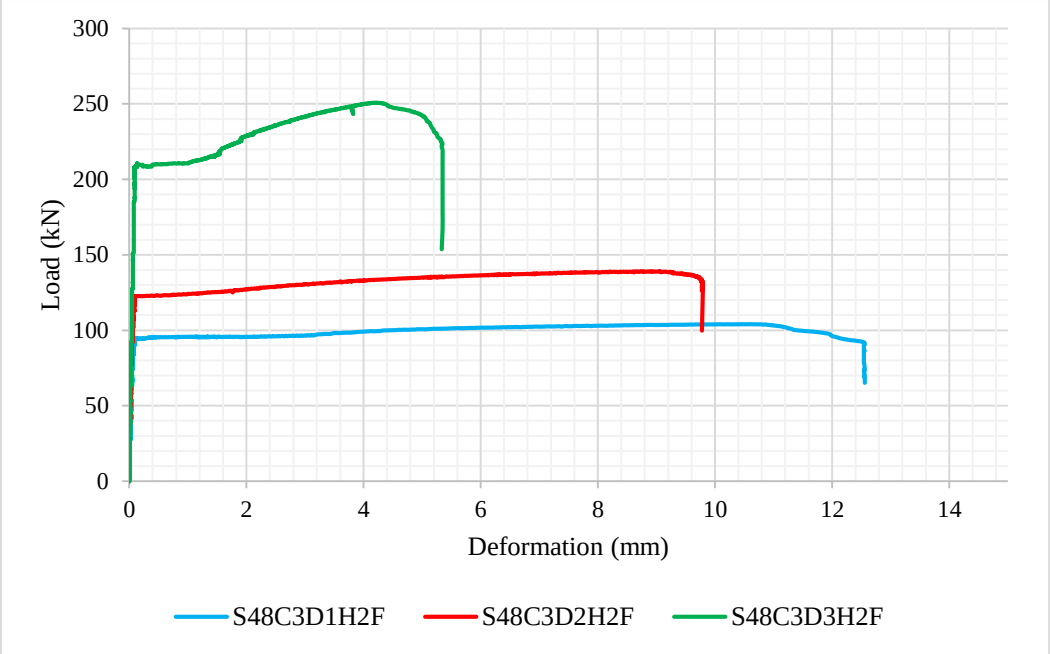

Figure 4.5: Load deformation curve for SMA-48 weld strength with 1.66mm,2.04mm,3.11mm (ASTM A653) plate thickness specimen.

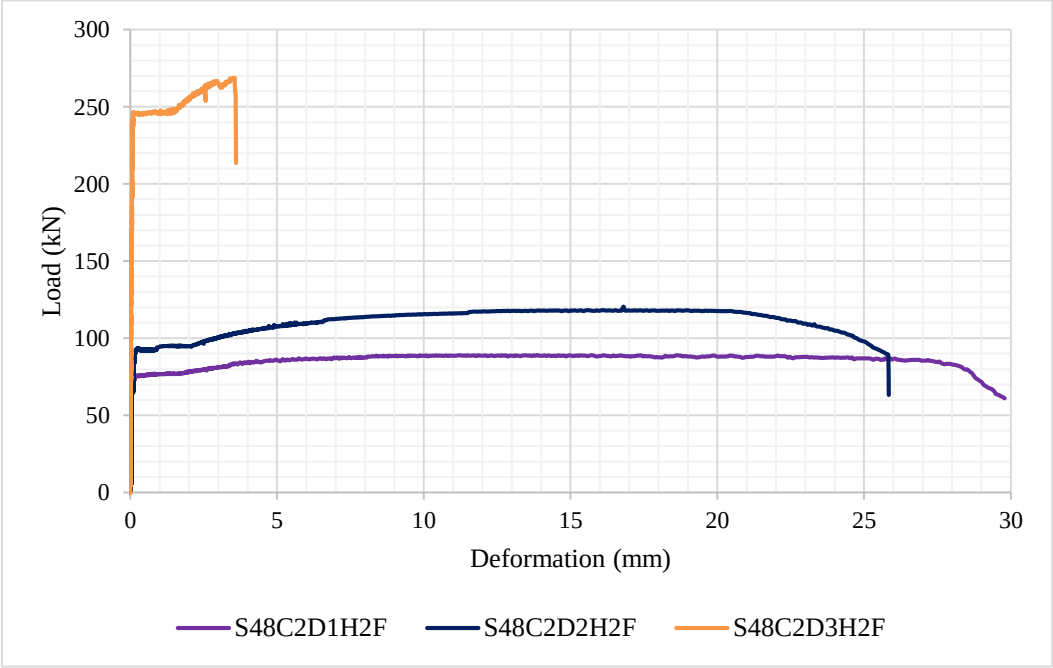

Figure 4.6: Load deformation curve for SMA-48 weld strength with 1.65mm,2.03mm,3.10mm (ASTM A36) plate thickness specimen.

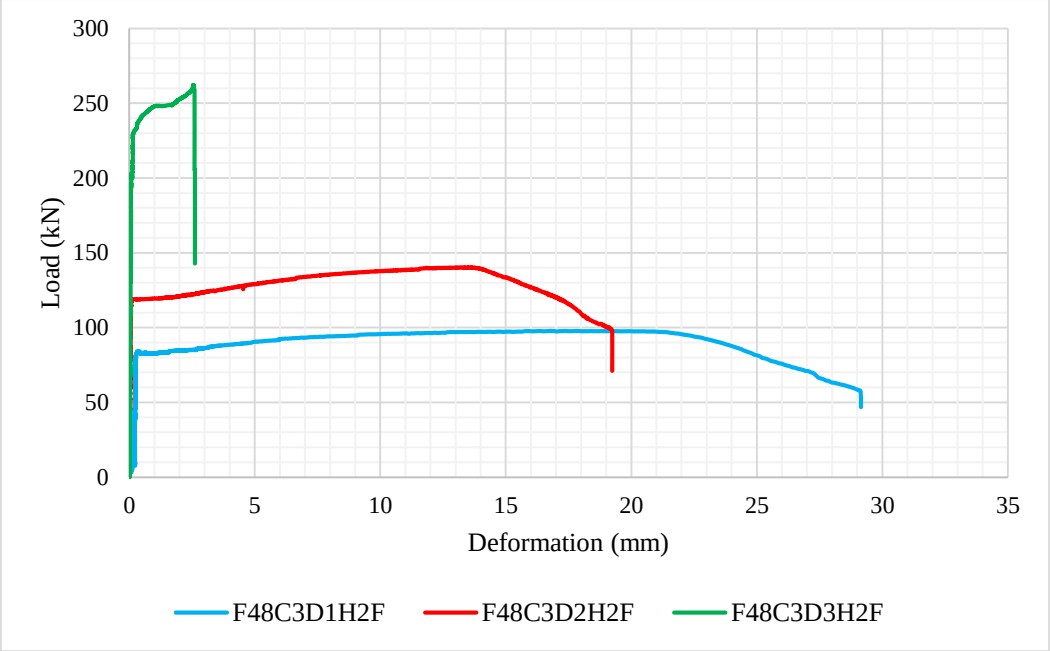

Figure 4.7: Load deformation curve for FCA-48 weld strength with 1.66mm,2.04mm,3.11mm (ASTM A653) plate thickness specimen.

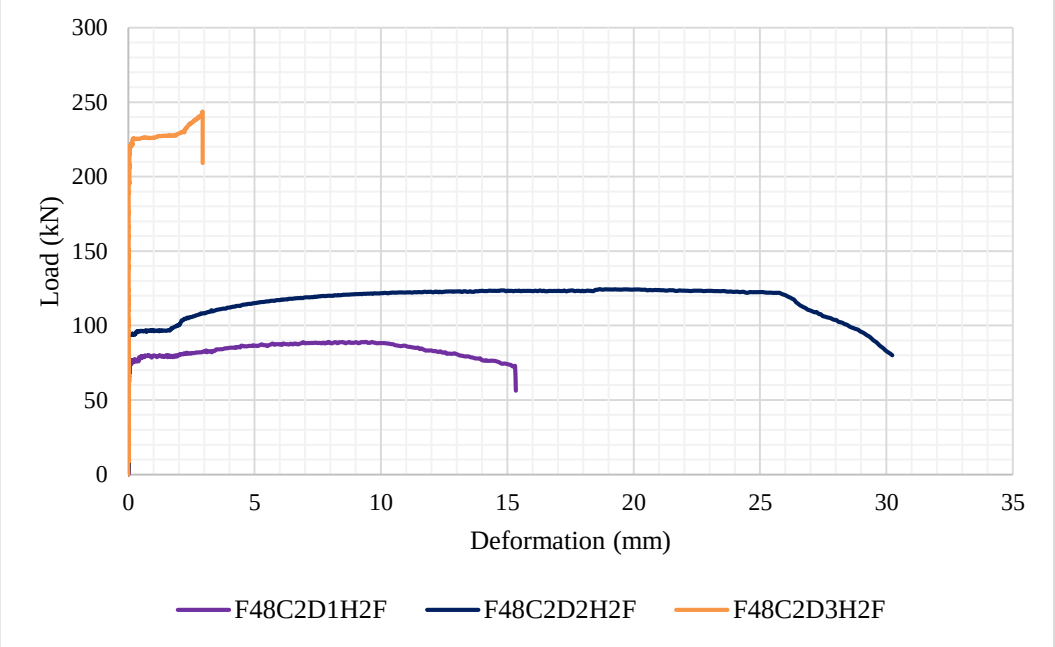

Figure 4.8: Load deformation curve for FCA-48 weld strength with 1.65mm,2.03mm,3.10mm (ASTM A36) plate thickness specimen.

4.2.2 Effect of Steel Grade

Figures 4.9 through Figure 4.11 represent the variations in load-deformation curves across different steel grades for plate specimens of varying thicknesses, including 1.66mm and 1.65mm, 2.04mm and 2.03mm, and 3.11mm and 3.10mm, respectively. Observations from Figures 4.9 and 4.10 reveal that specimens of ASTM A653 grade exhibit greater connection strength compared to those of ASTM A36 grade. Higher-grade steels typically possess superior mechanical properties, including higher ultimate strength. As a result, plates made from ASTM A653 grade steel are capable of withstanding higher loads before reaching their ultimate strength compared to plates made from ASTM A36 grade steel. Since the failure mode is plate net section failure, the connection strength is heavily dependent on the ultimate strength of the plates. When subjected to loading, the plates experience stresses that can lead to failure if the applied loads exceed their ultimate strength. Therefore, higher grade specimens with higher ultimate strength demonstrate greater resistance to failure and consequently exhibit higher connection strength relative to lower-grade specimens. Furthermore, the microstructure and composition of the steel can significantly influence its ultimate strength and deformability. Higher-grade steels typically have finer microstructures and fewer impurities, leading to improved mechanical properties and enhanced resistance to deformation and failure.

Additionally, in both Figure 4.9 and Figure 4.10, it is apparent that the majority of ASTM A36 samples display superior ductility compared to ASTM A653 samples. Lower grade steel often exhibits higher deformability compared to higher grade steel due to differences in their microstructures and mechanical properties. Lower grade steels typically have a microstructure with larger grains and more impurities compared to higher grade steels. These larger grains and impurities help to dislocation movement, making it easier for the material to deform plastically without fracturing. Higher grade steels, on the other hand, have finer microstructures with fewer impurities, which hinder dislocation movement and make them less deformable. Higher grade steels often contain alloying elements like carbon, manganese, and silicon in precise proportions to enhance strength and other mechanical properties. These alloying elements can form stronger bonds within the steel matrix, reducing its deformability. Lower grade steels typically have fewer alloying elements or lower concentrations of these elements, resulting in a softer and more deformable material.

Specifically, in Figure 4.9, specimens S41C2D1H2F and S48C2D1H2F exhibit higher ductility compared to S41C3D1H2F and S48C3D1H2F samples, respectively. Conversely, specimens M34C2D1H2F and F48C2D1H2F display lower ductility compared to M34C3D1H2F and F48C3D1H2F samples, respectively. In Figure 4.10, it is notable that joints with ASTM A36 grade specimens generally show more elongation, with the exception of S41C2D2H2F. Furthermore, Figure 4.11 highlights the low connection ductility across all samples, indicating a brittle nature of the welded connection. This occurs because welded connections are often stiffer and more brittle than mechanical connections. This lack of flexibility in welded joints contributes to their tendency for sudden, brittle failures. This stiffness and brittleness make welded connections less deformable and more likely to fail abruptly. In all cases, immediate failure occurs upon reaching ultimate load, indicating a sudden failure mode for the welded connection.

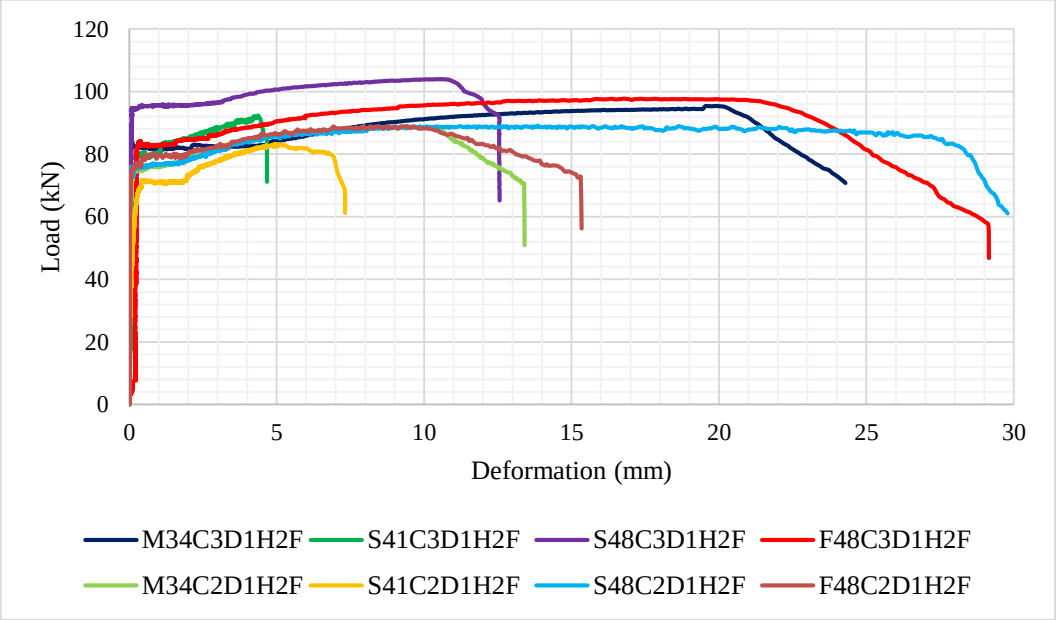

Figure 4.9: Load deformation curve for 1.66mm & 1.65mm plate thickness specimen for ASTM A653 and ASTM A36 steel.

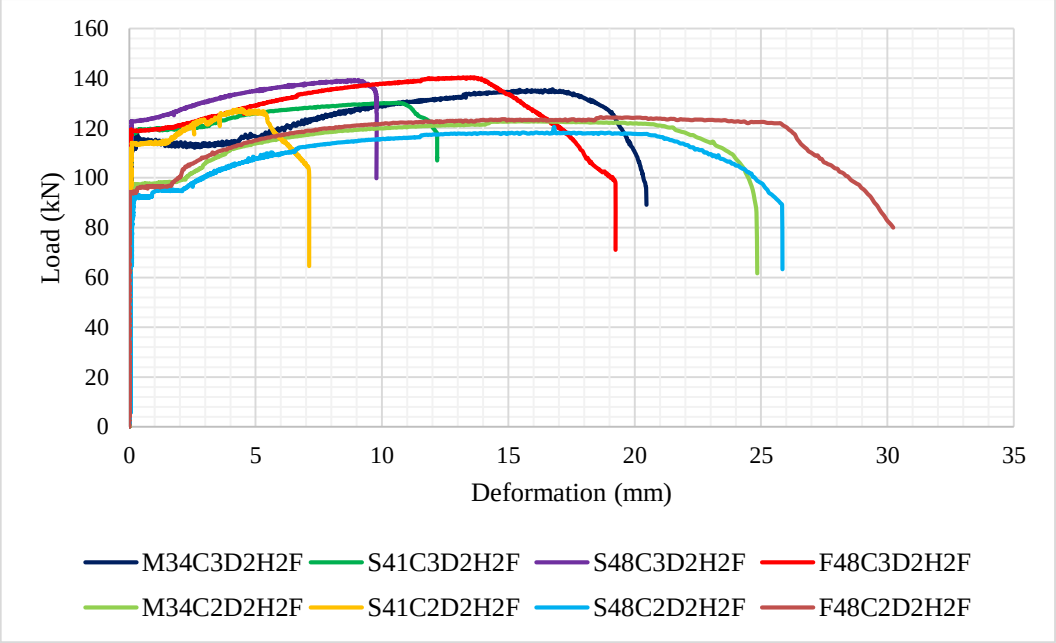

Figure 4.10: Load deformation curve for 2.04mm & 2.03mm plate thickness specimen for ASTM A653 and ASTM A36 steel.

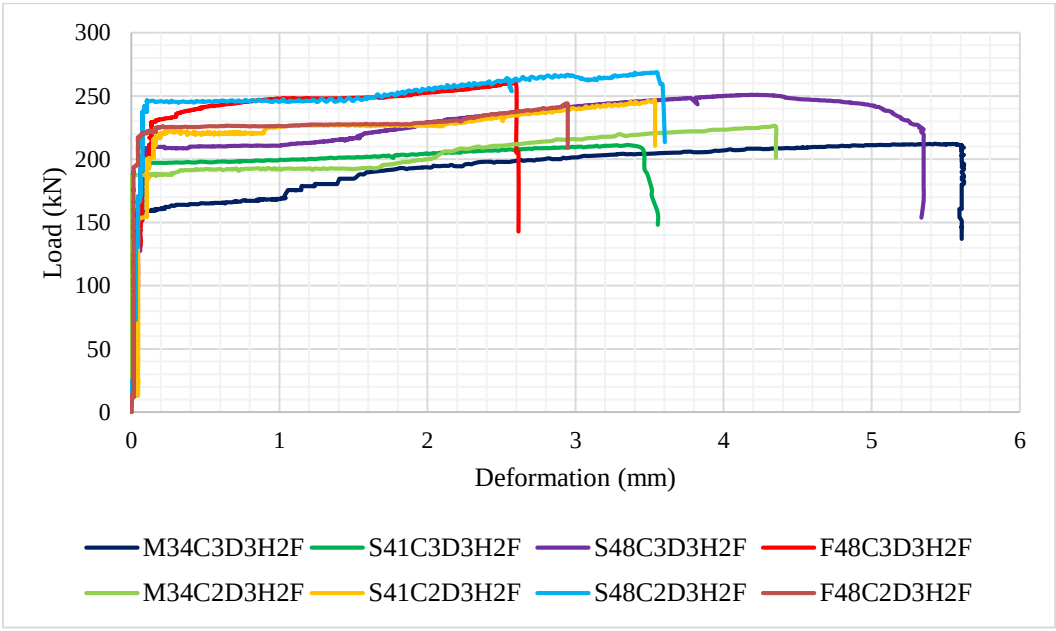

Figure 4.11: Load deformation curve for 3.11mm & 3.10mm plate thickness specimen for ASTM A653 and ASTM A36 steel.

4.3 Modes of Failure

In this experimental program, three types of failure modes are observed. The observed failure modes are as listed below:

(a) Tearing of plate at middle (TPM)

(b) Tearing of plate adjacent to the weld (TPAW)

(c) Weld throat failure (WTF)

Figure 4.12 displays the three failure modes observed in this study. Figure 4.12a shows the "Tearing of plate at middle (TPM) "failure mode and Figure 4.12b shows the "Tearing of plate adjacent to the weld (TPAW)" failure mode. Normally "Tearing of plate adjacent to weld" (TPAW) and" Tearing of plate at middle" (TPM) failure mode was observed in plate thickness less than 2.04mm. For below 2.04mm thick plate, the throat thickness will be almost same thickness to the plate as one leg is three to five times more than the other leg. As a result, the weld capacity is much more than the plate net section capacity. Figure 4.12c shows the "Weld throat failure (WTF)" failure mode. "Weld throat failure" mode is mainly observed in above 3.10mm thick plate specimen. For plates exceeding 3.10mm in thickness, the weld throat thickness is found to be smaller than that of the cover plate, with the failure mode identified as "Weld throat failure".

(a). Tearing of plate at middle (TPM)

(b). Tearing of plate adjacent to the weld (TPAW)

(c) . Weld throat failure (WTF)

Figure 4.12: Failure mode observed in the experimental program

4.3.1 Effect of Plate Thickness

Table 4.1 and Table 4.2 illustrates the changes in the failure mode with the plate thickness for ASTM A653 Gr.50 (F_y =345 MPa) and ASTM A36 (F_y =250 MPa) steel. It is observed that "Tearing of Plate adjacent to weld (TPAW)" and "Tearing of Plate at Middle (TPM)" failure mode mainly observed in 1.65 to 2.04 mm thick plate specimen. For plates below 2.04mm thickness, the weld throat thickness will almost match the thickness of the plate. This is due to one leg of the weld being three to five times longer than the other. As a result, the weld can withstand loads better than the plate net section capacity. On the other hand, "Weld Throat Failure (WTF)" failure mode is observed in 3.10 and 3.11mm thick plate specimen. Weld throat failure can become more likely with increasing plate thickness due to several factors such as increased stress concentration, reduced heat dissipation, and increased residual stress. As plate thickness increases, the stresses at the weld throat also rise due to the larger cross-sectional area of the material being welded. This elevation in stress concentrations makes the weld throat more vulnerable to failure. Additionally, welding thicker plates demands more heat input to achieve proper fusion, penetration, and weld throat formation. However, thicker plates dissipate heat more slowly than thinner ones. Consequently, the weld metal and surrounding base metal may cool at a slower rate, potentially leading to issues such as slower solidification rates, larger grain size, and heightened susceptibility to defects like lack of fusion or incomplete penetration. Moreover, welding thicker plates may introduce higher levels of residual stresses due to the larger volume of material involved. These residual stresses can induce distortion and warping of the plate, concentrating stresses at the weld throat and elevating the risk of failure. "Weld Throat Failure (WTF)" mode is consistent for plate thickness above 3.10mm except one specimen. But other two failure mode "Tearing of plate adjacent to the weld (TPAW)" and "Tearing of plate at middle (TPM)" do not exhibit a consistent correlation with the plate thickness.

Table 4.1: Variation in failure modes with plate thickness for ASTM A653 steel specimen.

ASTM A653 Gr.50 (F_y =345 MPa)		
Specimen ID	Plate Thickness, (mm)	Failure Mode
M34C3D1H2F	1.66	Tearing of Plate adjacent to weld
S41C3D1H2F	1.66	Tearing of Plate adjacent to weld
S48C3D1H2F	1.66	Tearing of Plate adjacent to weld
F48C3D1H2F	1.66	Tearing of Plate at Middle
M34C3D2H2F	2.04	Tearing of Plate adjacent to weld
S41C3D2H2F	2.04	Tearing of Plate adjacent to weld
S48C3D2H2F	2.04	Tearing of Plate adjacent to weld
F48C3D2H2F	2.04	Tearing of Plate adjacent to weld
M34C3D3H2F	3.11	Tearing of Plate adjacent to weld
S41C3D3H2F	3.11	Weld Throat Failure
S48C3D3H2F	3.11	Weld Throat Failure
F48C3D3H2F	3.11	Weld Throat Failure

Table 4.2: Variation in failure modes with plate thickness for ASTM A36 steel specimen.

ASTM A36(F_y =250 MPa)		
Specimen ID	Plate Thickness, (mm)	Failure Mode
M34C2D1H2F	1.65	Tearing of Plate adjacent to weld
S41C2D1H2F	1.65	Tearing of Plate adjacent to weld
S48C2D1H2F	1.65	Tearing of Plate at Middle
F48C2D1H2F	1.65	Tearing of Plate at Middle
M34C2D2H2F	2.03	Tearing of Plate at Middle
S41C2D2H2F	2.03	Tearing of Plate adjacent to weld
S48C2D2H2F	2.03	Tearing of Plate at Middle
F48C2D2H2F	2.03	Tearing of Plate adjacent to weld
M34C2D3H2F	3.10	Weld Throat Failure

S41C2D3H2F	3.10	Weld Throat Failure
S48C2D3H2F	3.10	Weld Throat Failure
F48C2D3H2F	3.10	Weld Throat Failure

4.3.2 Effect of Weld Grade

Table 4.3 explains the variations in failure modes corresponding to changes in weld grade. Notably, the failure mode appears independent of weld grade. All three types of failure patterns are observed consistently in MIG-34(F_u =345 MPa), SMA-48(F_u =483 MPa), and FCA-48(F_u =483 MPa) weld grades, with the exception of SMA-41(F_u =416 MPa).

Table 4.3: Variation in the failure mode with weld grade.

Weld Grade	Specimen ID	Plate Thickness, (mm)	Failure Mode
MIG-34	M34C3D1H2F	1.66	Tearing of plate adjacent to the weld (TPAW)
MIG-34	M34C2D1H2F	1.65	Tearing of plate adjacent to the weld (TPAW)
MIG-34	M34C3D2H2F	2.04	Tearing of plate adjacent to the weld (TPAW)
MIG-34	M34C2D2H2F	2.03	Tearing of plate at middle (TPM)
MIG-34	M34C3D3H2F	3.11	Tearing of plate adjacent to the weld (TPAW)
MIG-34	M34C2D3H2F	3.10	Weld throat failure (WTF)
SMA-41	S41C3D1H2F	1.66	Tearing of plate adjacent to the weld (TPAW)
SMA-41	S41C2D1H2F	1.65	Tearing of plate adjacent to the weld (TPAW)
SMA-41	S41C3D2H2F	2.04	Tearing of plate adjacent to the weld (TPAW)
SMA-41	S41C2D2H2F	2.03	Tearing of plate adjacent to the weld (TPAW)
SMA-41	S41C3D3H2F	3.11	Weld throat failure (WTF)
SMA-41	S41C2D3H2F	3.10	Weld throat failure (WTF)

SMA-48	S48C3D1H2F	1.66	Tearing of plate adjacent to the weld (TPAW)
SMA-48	S48C2D1H2F	1.65	Tearing of plate at middle (TPM)
SMA-48	S48C3D2H2F	2.04	Tearing of plate adjacent to the weld (TPAW)
SMA-48	S48C2D2H2F	2.03	Tearing of plate at middle (TPM)
SMA-48	S48C3D3H2F	3.11	Weld throat failure (WTF)
SMA-48	S48C2D3H2F	3.10	Weld throat failure (WTF)
FCA-48	F48C3D1H2F	1.66	Tearing of plate at middle (TPM)
FCA-48	F48C2D1H2F	1.65	Tearing of plate at middle (TPM)
FCA-48	F48C3D2H2F	2.04	Tearing of plate adjacent to the weld (TPAW)
FCA-48	F48C2D2H2F	2.03	Tearing of plate adjacent to the weld (TPAW)
FCA-48	F48C3D3H2F	3.11	Weld throat failure (WTF)
FCA-48	F48C2D3H2F	3.10	Weld throat failure (WTF)

4.4 Connection Strength

Connection strength refers to the ability of a joint or connection between structural elements to resist applied forces without failing or undergoing deformation beyond acceptable limits. It is a critical parameter in structural engineering and design, influencing the overall stability and performance of a structure. The strength of a connection is often evaluated in terms of its capacity to withstand various types of loads, such as tension, compression, shear, or a combination of these. Connection strength depends on factors like the weld strength, welding techniques, material properties, and the geometry of the joint. Structural analysis and testing are commonly employed to determine and verify connection strength. The appropriate consideration of connection strength is crucial in preventing structural failures, ensuring the integrity and reliability of the structures. Connection strength, P_{max}

means the highest load observed on the load-elongation curve. In this section, we examine the strength of the connection in relation to weld strength, plate thickness, and steel grade.

4.4.1 Effect of Weld Strength on Connection Strength

For plate thicknesses ranging from 1.65 mm to 2.04 mm, the trend lines for connection strength are nearly flat with the increases of weld strength. Additionally, the failure mode observed in these cases is “tearing of the plate”. In the “tearing of plate failure mode”, specifically plate net section failure, the connection strength is primarily dependent on the strength of the plate itself rather than the strength of the weld. “Plate net section” failure occurs when the applied loads exceed the capacity of the plate cross sectional area to withstand them, resulting in tearing or rupture of the plate material. As a result, the weld strength does not significantly impact the connection strength for these thinner plate specimens. The flat trend lines suggest that increasing weld strength within this range doesn't result in a significant increase in connection strength. However, for a plate thickness of 3.10mm and 3.11 mm, the trend line for connection strength increases with the increase of weld strength. In this case, the failure mode observed is “weld throat failure”. A stronger weld provides more effective load transfer between the connected components. As the weld strength increases, it can better distribute applied forces across the joint, reducing stress concentrations and enhancing the overall connection strength. This indicates that the connection strength is influenced by weld strength for the 3.10 mm and 3.11 mm thick plate specimen. The increasing trend line suggests that stronger welds result in a higher connection strength for this thicker plate. One connection strength (for 3.10mm) shows lower value with the higher weld strength. This is happened due to the less weld leg size. A smaller weld leg size might result in less material being fused together, leading to reduced load-bearing capacity of the connection. The relationship between the connection strength and the weld strength are shown in figure 4.13.

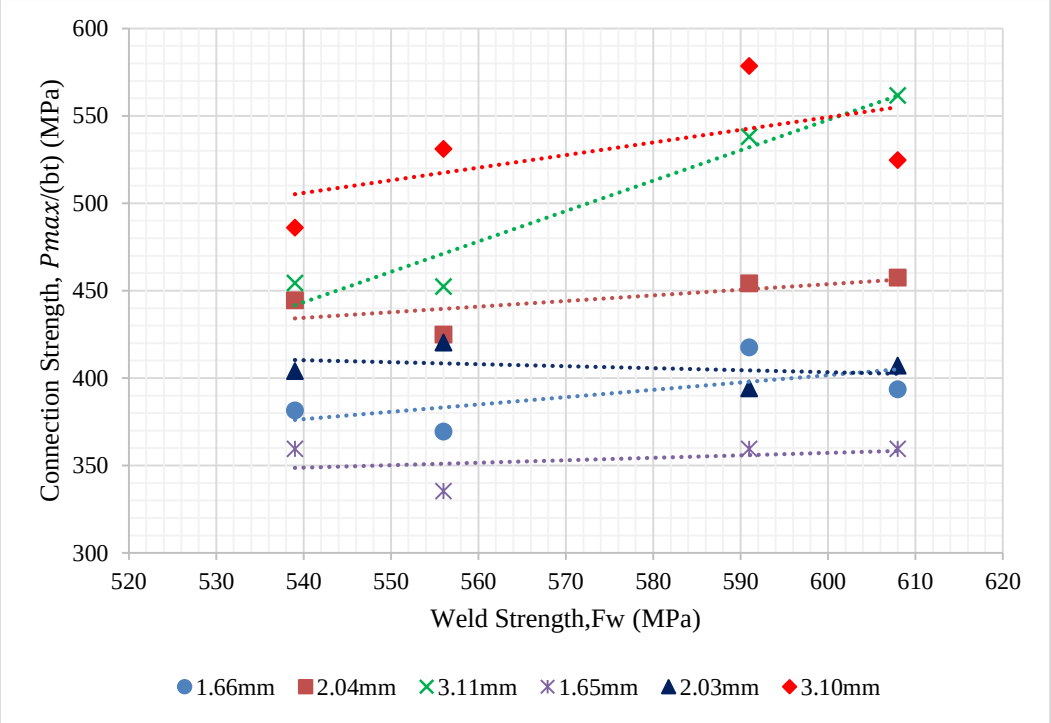

Figure 4.13: Effect of weld strength on connection Strength

4.4.2 Effect of Plate Thickness on Connection Strength

Effect of plate thickness on connection strength is studied for 24nos samples formed with ASTM A653 Gr.50 steel (F_y=345 MPa) and ASTM A36 steel (F_y=250 MPa). Figure 4.14 and Figure 4.15 reports the variation in connection strength with thickness for different welding electrode. The observations from Figures 4.14 and 4.15 indicate that as the thickness of the plate increases, the connection strength also increases. This correlation likely arises from the increased bearing area within the plate as thickness increases. Essentially, thicker plates provide a larger surface area for the connection, which enhances the load-bearing capacity of the connection. This observation aligns with the principle that thicker materials generally offer higher strength and stiffness characteristics, which can lead to stronger connections.

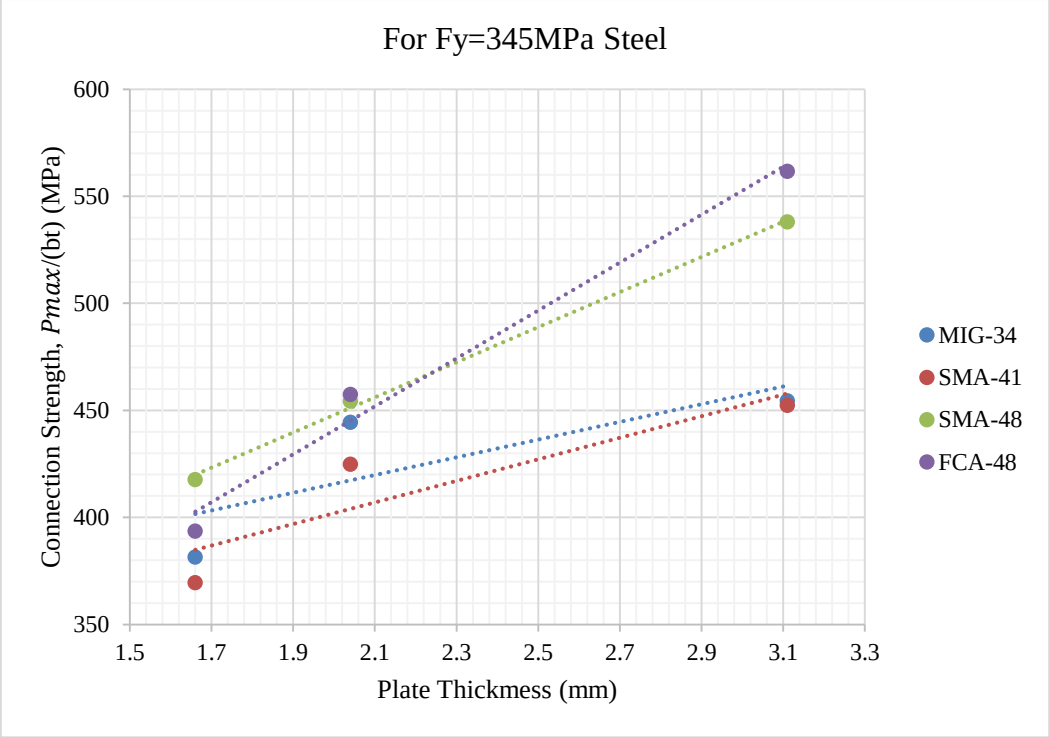

Figure 4.14: Effect of plate thickness on connection strength for ASTM A653 Gr.50 steel.

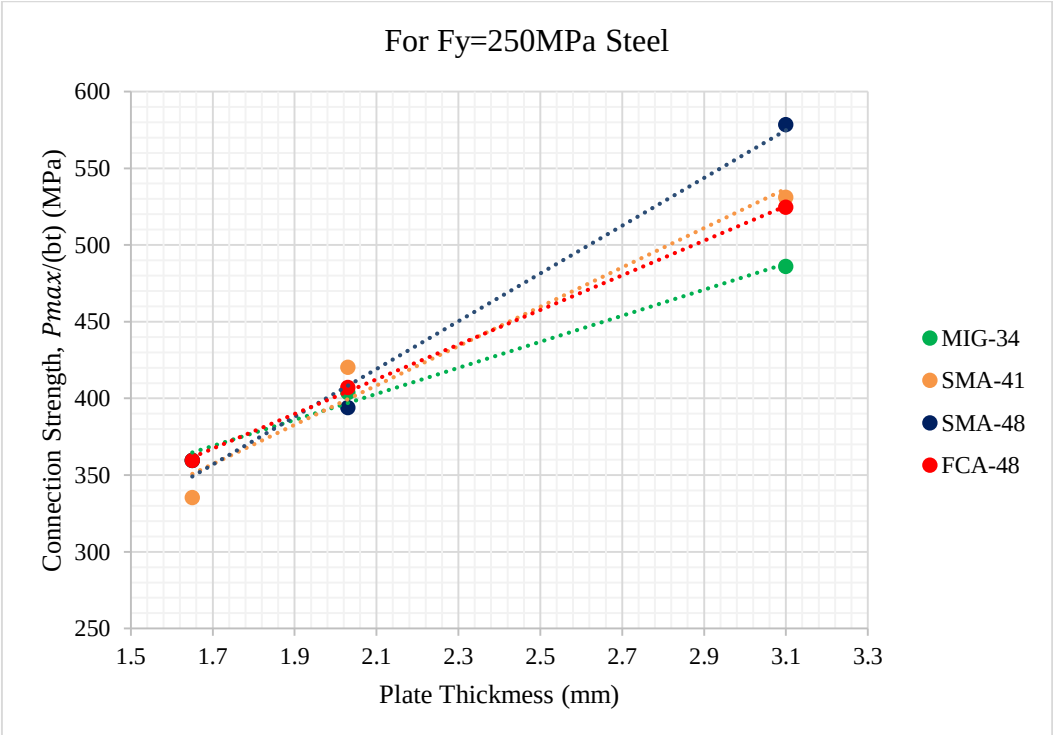

Figure 4.15: Effect of plate thickness on connection strength for ASTM A36 steel

4.4.3 Effect of Plate Ultimate Strength on Connection Strength

This study explores the relationship between plate ultimate strength and connection strength in cold-formed steel plates of different thicknesses. Connection strength tests were performed to evaluate the influence of plate ultimate strength on the structural performance of the connections. The findings indicate that connection strength increases with the ultimate strength of the plate for 1.65 mm to 2.04 mm thick plates specimen. This indicates a positive correlation between plate ultimate strength and connection strength for these thicknesses. However, plate ultimate strength has no significant impact on connection strength for 3.10mm and 3.11 mm thick plates specimen. Figure 4.16 shows the variation of connection strength with the plate ultimate strength. It is shows that, the trend line of connection strength increases with the increase of plate ultimate strength for plate thickness 1.65 mm to 2.04mm thick plate specimen and the failure pattern is observed “plate net section failure”. As the failure is “plate net section failure”, so the strength of connection is greatly depended on the plate ultimate strength. On the other hand, the trend line of connection strength is almost constant or decreasing with the increase of plate ultimate strength for 3.10 mm and 3.11 mm thick plate specimen and the failure mode is observed “weld throat failure”. As the trend line pattern for 3.10mm and 3.11mm thick plate specimen shows different behavior than those of 1.65mm to 2.04mm thick plate specimen. It means, plate ultimate strength has no significant impact on connection strength for 3.10mm and 3.11mm thick plate specimen. This research provides valuable insights into the structural behavior of cold-formed steel plates and their connections. In most cases, rupture rather than yielding is a more reliable criterion of failure. Hance the design formula is a function of the tensile strength of the plate material and not of the yield point.

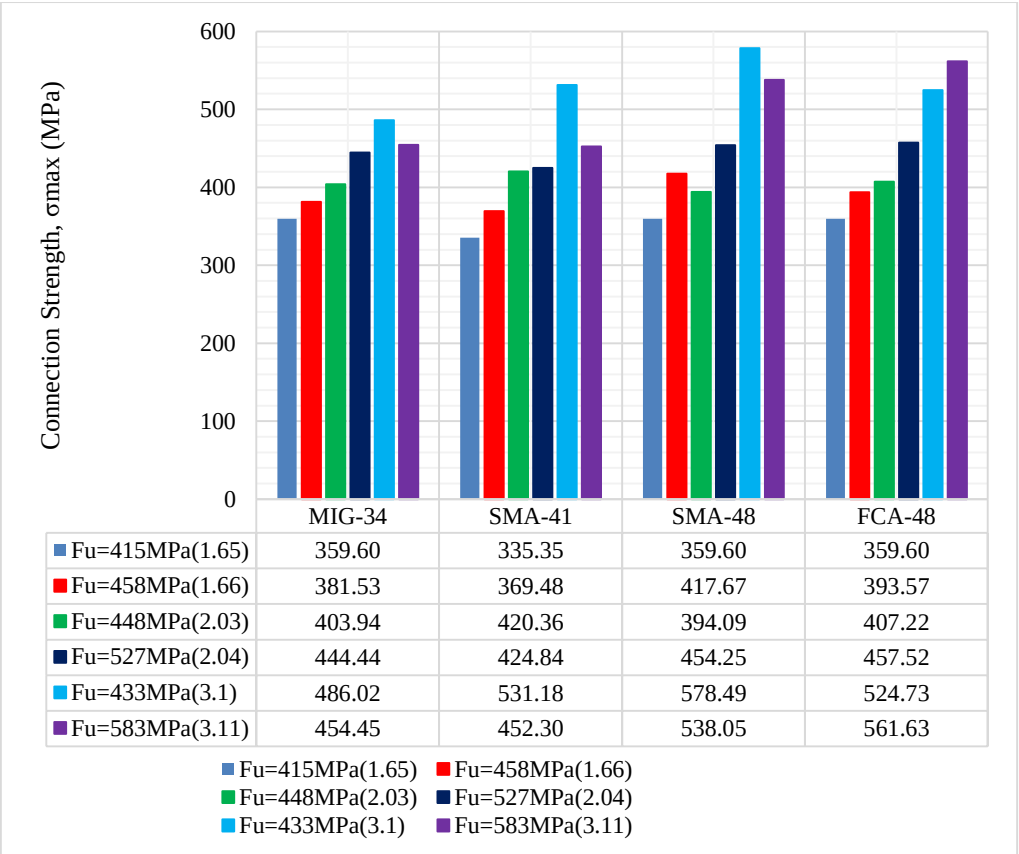

	MIG-34	SMA-41	SMA-48	FCA-48
Fu=415MPa(1.65)	359.60	335.35	359.60	359.60
Fu=458MPa(1.66)	381.53	369.48	417.67	393.57
Fu=448MPa(2.03)	403.94	420.36	394.09	407.22
Fu=527MPa(2.04)	444.44	424.84	454.25	457.52
Fu=433MPa(3.1)	486.02	531.18	578.49	524.73
Fu=583MPa(3.11)	454.45	452.30	538.05	561.63

Figure 4.16: Effect of plate ultimate strength on connection strength.

4.5 Connection Stiffness

Connection stiffness refers to the rigidity or resistance to deformation exhibited by a joint or connection between structural elements. The stiffness of a connection determines how much it deforms or displaces when subjected to external forces. A stiffer connection exhibits less deformation, providing greater stability and control over the structural response. On the other hand, a more flexible or less stiff connection allows for greater movement and deformation. Engineers consider connection stiffness when designing structures to ensure that the overall system behaves as intended, especially in terms of load distribution, deflection control, and response to dynamic forces. The stiffness of a connection is influenced by factors such as the type of fasteners used, welding techniques, material properties, and the geometry of the joint. The appropriate consideration of connection stiffness is essential in achieving the desired structural performance and ensuring that the structure can effectively resist loads and deformations while meeting safety and serviceability requirements. In this section, the influence of plate thickness will be investigated on the connection stiffness.

For the calculation of connection stiffness, Instron load deformation curve has been used. The stiffness found from the Instron load deformation curve is the stiffness of the whole sample which is denoted as K_{eq}. The connection stiffness needs to be calculated. As the connection is parallel with the hot rolled plate so series equation has been used to calculate axil stiffness of the connection. The sample was griped in the UTM machine at the black line in the sample. Total sample length is 340mm and the connection length is 150mm plus weld leg size. The axil stiffness of hot rolled steel outside the connection is K_1.The connection stiffness is defined as K_2 . Connection stiffness calculation procedure is shown in figure 4.17. The connection stiffness for ASTM A653 Gr.50 and ASTM A36 steel specimen are shown in table 4.4 and 4.5.

The stiffness of a double shear welded connection can be influenced by both hot rolled and cold rolled plates, which have distinct material properties due to their manufacturing processes. These differences can directly affect the overall stiffness of the connection. The load transfer mechanism between the hot rolled and cold rolled plates can affect the overall stiffness of the connection. Differences in material properties and welding quality can influence the loads transferred between the two materials, impacting the stiffness of the connection. Furthermore, geometric factors such as the dimensions of the connection and the welding leg size can also affect stiffness. Differences in these factors between hot rolled and cold rolled plates may result in variations in connection stiffness.

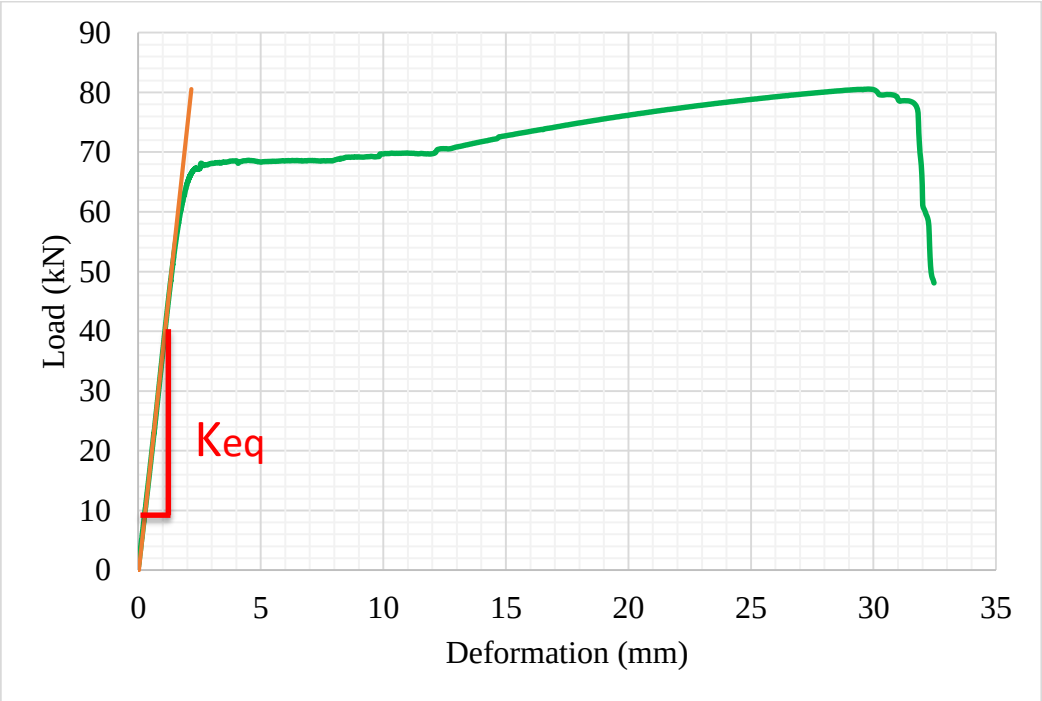

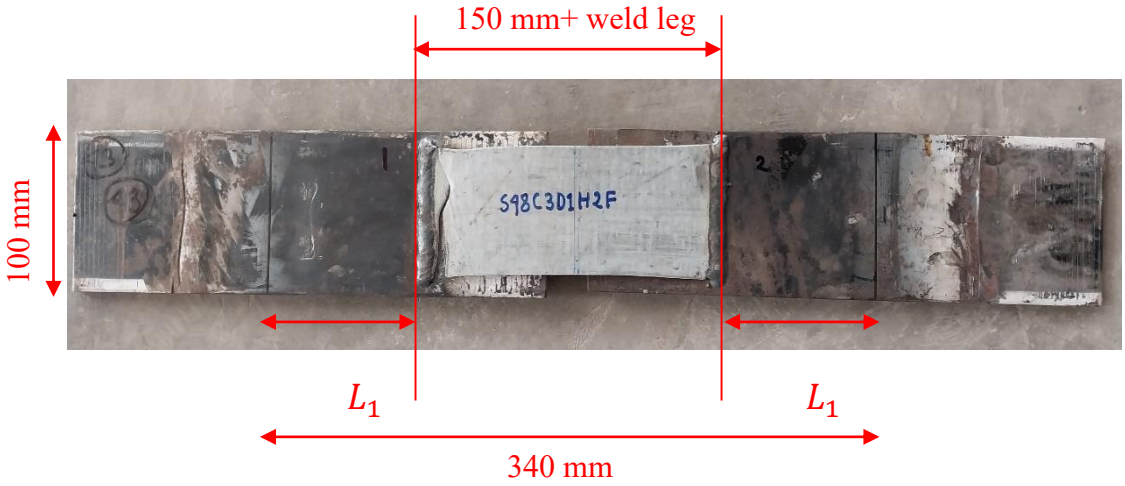

Figure 4.17: Connection stiffness calculation procedure

Axial Stiffness of hot rolled steel plate,

$$K_1 = \frac{AE}{L_1}$$

$$\frac{1}{K_{eqe}} = \frac{2}{K_1} + \frac{1}{K_2}$$

$$K_2 = \frac{K_{eqe}K_1}{K_1 - 2K_{eqe}}$$

Table 4.4: Stiffness for ASTM A653 Gr.50 (F_y =345 MPa) plate specimen.

ASTM A653 Gr.50 (F_y =345 MPa)		
Specimen ID	Cold Rolled Steel Thickness(mm)	Stiffness(kN/mm)
M34C3D1H2F	1.66	45.51
M34C3D2H2F	2.04	64.57
M34C3D3H2F	3.11	73.03
S41C3D1H2F	1.66	41.26
S41C3D2H2F	2.04	45.69
S41C3D3H2F	3.11	71.14
S48C3D1H2F	1.66	35.18
S48C3D2H2F	2.04	71.37
S48C3D3H2F	3.11	66.02
F48C3D1H2F	1.66	30.27
F48C3D2H2F	2.04	46.80
F48C3D3H2F	3.11	53.90

Table 4.5: Stiffness for ASTM A36 (F_y =250 MPa) plate specimen.

F_y=250 MPa Steel		
Specimen ID	Cold Rolled Steel Thickness(mm)	Stiffness(kN/mm)
M34C2D1H2F	1.65	43.78
M34C2D2H2F	2.03	51.24
M34C2D3H2F	3.10	53.00
S41C2D1H2F	1.65	39.64

S41C2D2H2F	2.03	35.52
S41C2D3H2F	3.10	60.40
S48C2D1H2F	1.65	50.69
S48C2D2H2F	2.03	28.04
S48C2D3H2F	3.10	69.64
F48C2D1H2F	1.65	41.59
F48C2D2H2F	2.03	58.36
F48C2D3H2F	3.10	49.43

4.5.1 Effect of Plate Thickness

Figure 4.18 presents variations in stiffness concerning plate thickness for samples fabricated with ASTM A653 Gr.50 (F_y =345 MPa) and ASTM A36 (F_y =250 MPa) using all four-grade electrodes. All 24nos samples from both ASTM A653 Gr.50 and ASTM A36 are encompassed. The connection stiffness generally rises with increasing plate thickness, with a few exceptions. Such an increase occurred due to the increase in bearing area with plate thickness.

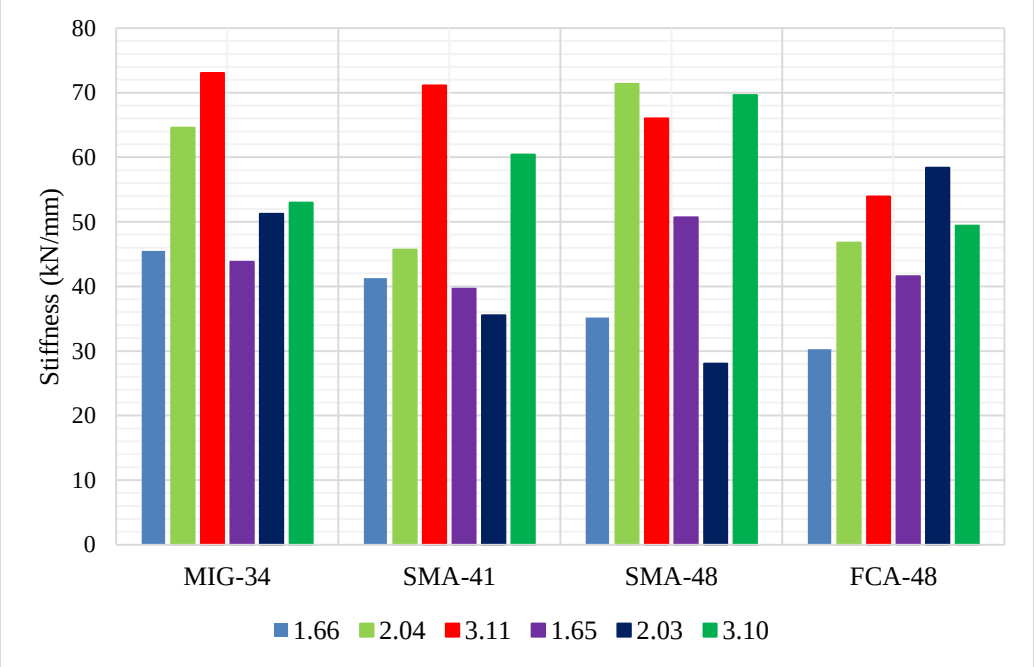

Figure 4.18: Effect of plate thickness on stiffness

4.6 Ductility of the Joint

The ductility of a joint refers to its ability to deform plastically before failure when subjected to tensile stress. In engineering, especially in fields like structural engineering and metallurgy, ductility is a crucial property. In structural joints, such as those found in buildings, bridges, or machinery, ductility ensures that the joint can absorb energy and undergo significant deformation before fracturing. This is important because it allows structures to withstand unexpected loads or stresses, such as those from seismic activity or heavy winds. Ductile joints are often preferred over brittle joints because they provide warning signs of impending failure through visible deformation, allowing for maintenance or repair before catastrophic failure occurs. Moreover, ductile joints can often undergo plastic deformation without losing their load-bearing capacity entirely. Various factors influence the ductility of a joint, including the materials used, the design of the joint, and the manufacturing process. Proper material selection, joint design, and fabrication techniques are essential to ensure adequate ductility in engineering applications.

In this study, ductility of joints is studied based on two displacement-based ductility namely initial ductility, r_i and final ductility, r_f . d_y, d_u and d_f is the displacement corresponding to yield, ultimate and failure point as illustrated in Figure 4.19. The failure point is the point in load-elongation curve where the load drops drastically with a change in elongation close to zero. Also, after the failure point negative slope of the curve increases drastically.

In this section ductility of double shear welded joint will be studied based on plate thickness, and failure mode. The failure mode is an important criterion in defining ductility. Therefore, some of the results of ductility may show deviation from the regular range.

Initial ductility, $r_i = \frac{d_u}{d_y}$

Final ductility, $r_f = \frac{d_f}{d_u}$

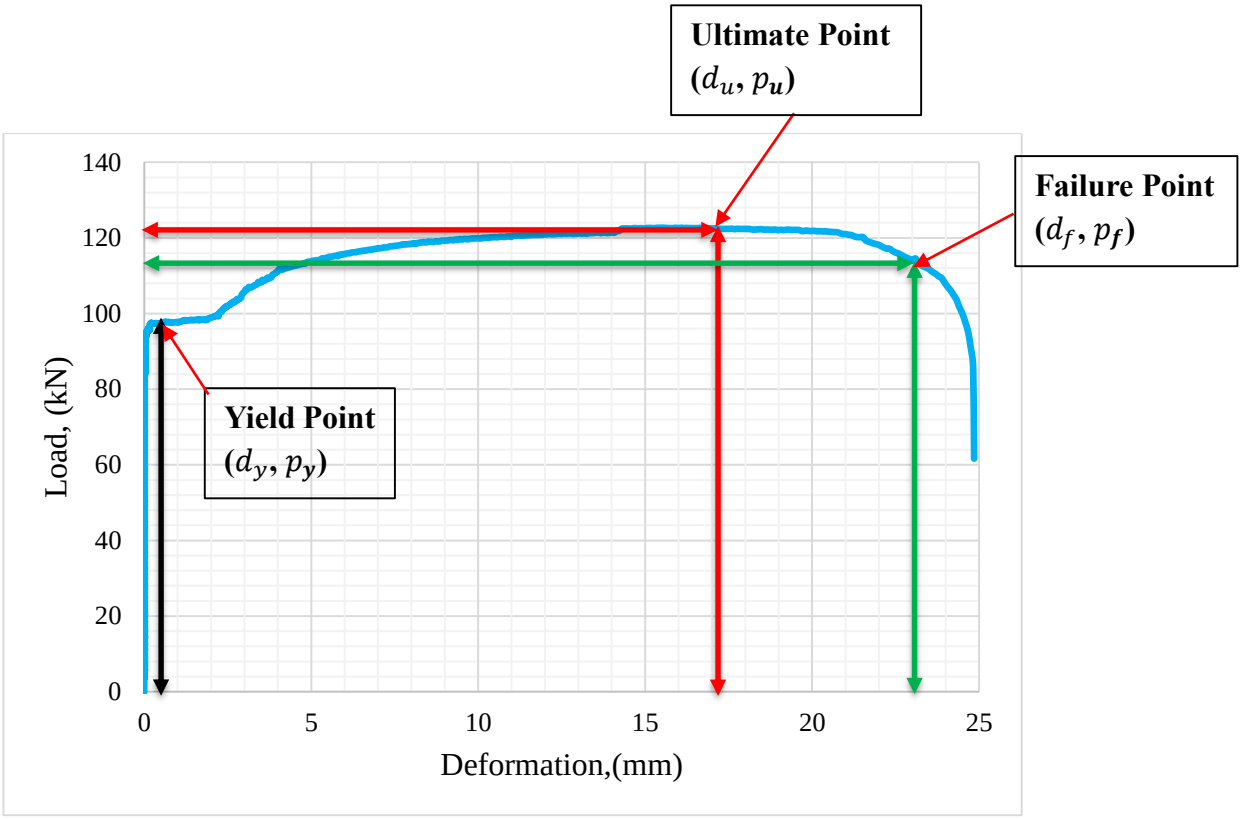

Figure 4.19: Definition of ductility

4.6.1 Effect of Plate Thickness

Figure 4.20 plots the initial and final ductility for varying plate thickness using 24nos samples formed with ASTM A653 Gr.50 (F_y =345 MPa) and ASTM A36 (F_y =250 MPa) steel for all four-grade electrode. Both Figure 4.20a and 4.20b shows significant variation in the plot with the variation in plate thickness. 1.65mm to 2.04 mm thick plate connection shows higher initial ductility but 3.10mm and 3.11 mm thick plate connection shows lower initial ductility. Thinner plates generally exhibit higher ductility compared to thicker plates due to factors such as reduced strain localization, less strain hardening, increased formability. Thicker plates are more susceptible to strain localization. Thicker plates tend to develop concentrated areas of deformation, which can cause to premature failure, reducing their overall ductility. Thinner plates are less susceptible to strain localization due to their smaller thickness, allowing for more uniform deformation and increased ductility. Thicker plates may experience more strain hardening during deformation, where the material becomes stronger but less ductile as it deforms. Thinner plates may exhibit less strain hardening due to lower volume of material being deformed, allowing for continued

ductile behavior at higher strains. Thinner plates are often more formable than thicker plates, meaning they can undergo greater deformation without fracturing. This increased formability is directly related to ductility since it allows the material to deform more before failure.

In Figure 4.20b, final ductility of the samples is in the range of 1 to 2.1. Ductility of welded joints cannot be described easily with a single parameter. It requires consideration of failure mode, more design variables, and advanced computational methods for proper identification.

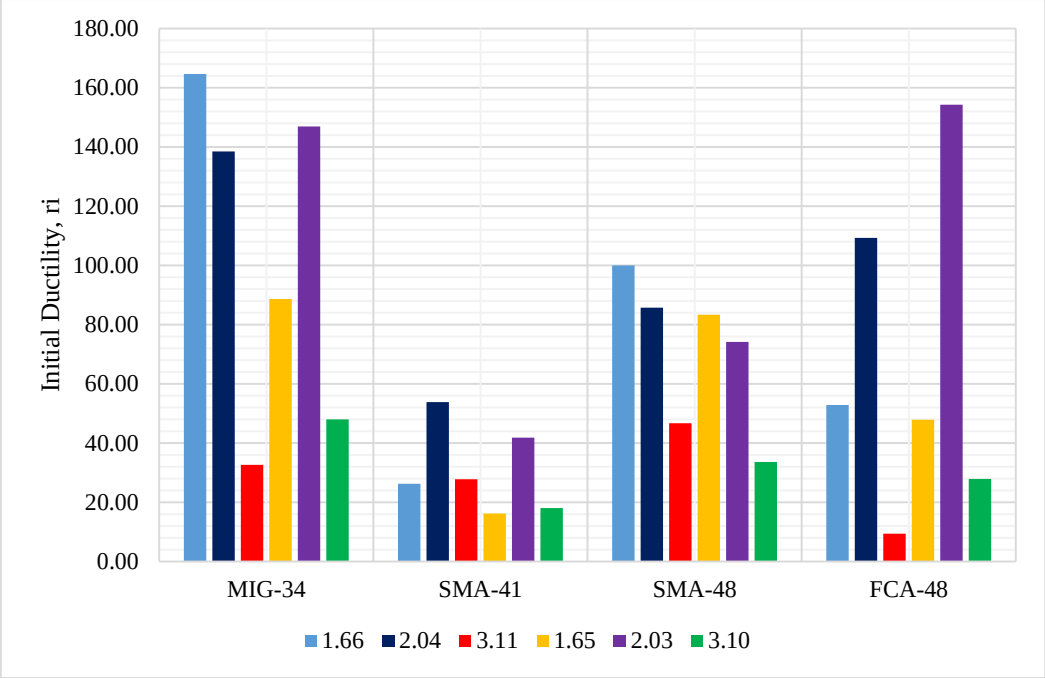

(a) Variation in initial ductility with plate thickness

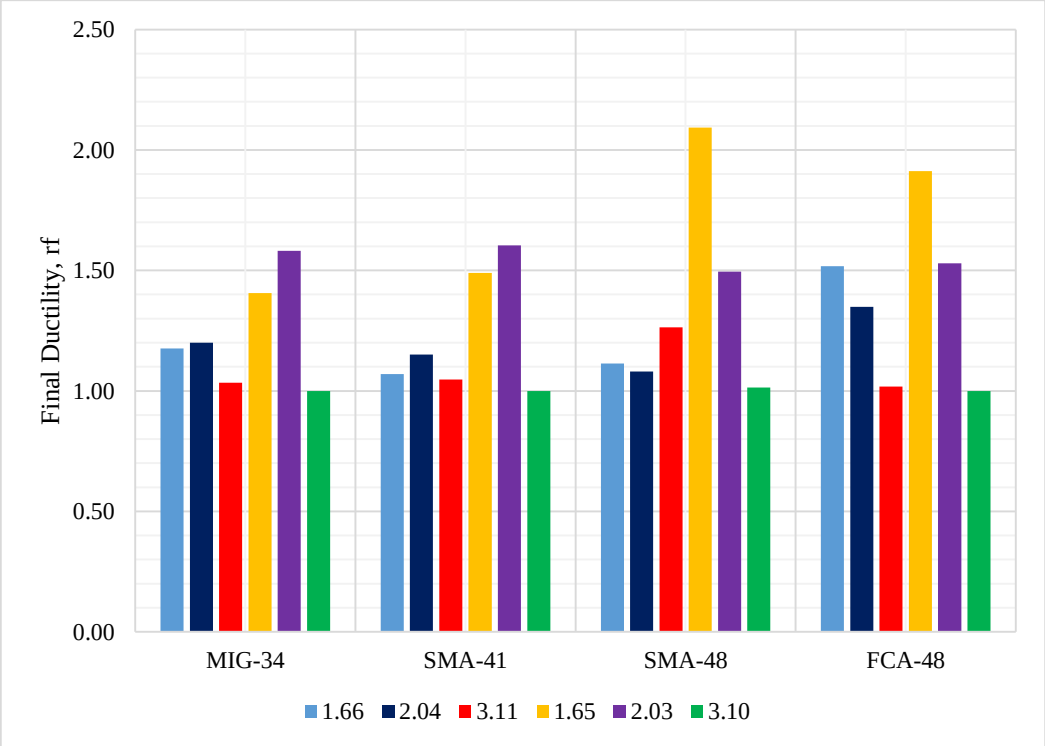

(b)Variation in final ductility with plate thickness

Figure 4.20: Relationship between ductility and plate thickness

4.6.2 Effect of Failure Mode

The failure mode in a welded joint significantly affects both initial and final ductility. Ductility, the material ability to deform plastically before fracturing, varies based on the failure mode. Plate net section failure typically indicates ductile behavior, while weld throat failure tends to be brittle.

Ductile failure modes involve substantial plastic deformation before fracture, providing warning signs such as necking or stretching before complete failure. Welded joints exhibiting ductile nature are generally preferred due to their higher overall ductility. Notably, specimens with thicknesses between 1.65 to 2.04 mm, experiencing net section failure, show higher initial ductility, although there are variations in results among few specimens.

Conversely, brittle failure involves minimal plastic deformation before fracture, leading to sudden failures without warning. Welded joints prone to brittle failure have limited ability to deform before fracture, resulting in a more abrupt failure. Specimens with thicknesses of 3.10 mm and 3.11 mm, showing weld throat failure, exhibit lower initial ductility, and this failure mode is characterized by its sudden nature.

When considering final ductility, net section failure specimens demonstrate a gradual failure after reaching the ultimate load, indicating higher final ductility. Despite variations in a few specimens, it suggests that net section failure specimens absorb more energy before failure. On the other hand, weld throat failure is sudden, occurring immediately after reaching the ultimate load. This lack of warning or signs before failure results in final ductility values close to one for weld throat failure specimens, except for one specimen that show different values.

The thickness of the specimen influences the failure mode, with thinner specimens exhibiting net section failure and thicker specimens displaying weld throat failure. Net section failure is associated with higher initial and final ductility due to its ductile nature and the ability to absorb more energy before failure. In contrast, weld throat failure, being a brittle mode, results in lower initial ductility and sudden final failure, with minimal warning or deformation before fracture. Figure 4.21 shows the Variation of ductility with failure mode.

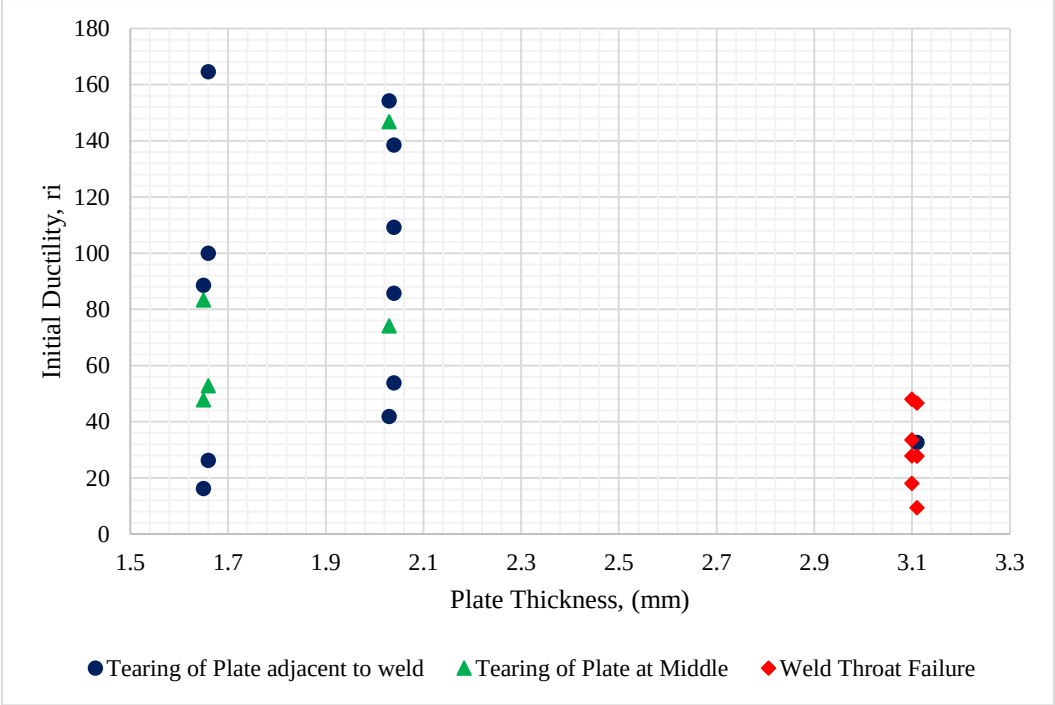

(a)Variation in initial ductility with failure mode

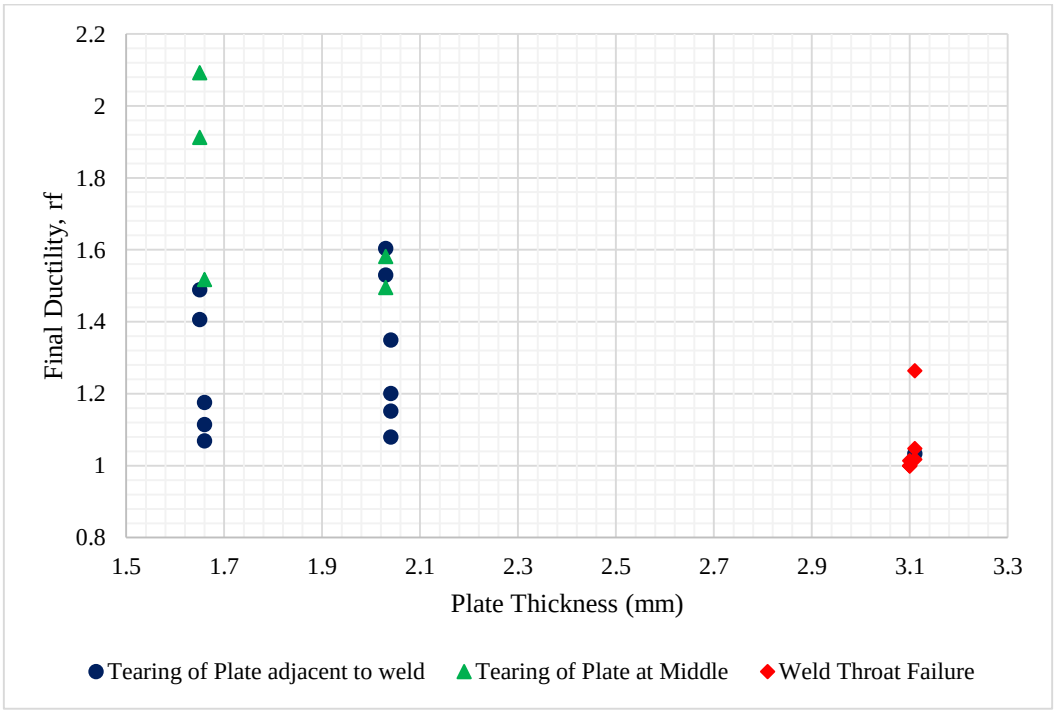

(b)Variation in final ductility with failure mode

Figure 4.21: Relationship between ductility and failure mode

4.7 Comparison with Design Standards

A total of 24nos specimens undertook testing in a universal testing machine to assess connection strength and failure modes. Theoretical capacities and failure modes, as per the AISI code equations, were also determined. Discrepancies were noted between the code predictions and actual test results.

For plate specimens with a thickness below 2.04mm, the AISI code equation consistently yielded overestimated results compared to the actual test results. The code equation determines the connection strength based on the plate ultimate strength for thicknesses below 2.54mm. The discrepancy between the predicted strength by code equation and the actual strength observed in tests may differ for several factors. Welding can create stress concentrations, especially at the weld joints, weakening the plate ultimate strength by accelerating crack formation. This can lead to a connection strength lower than predicted by the code equation. Additionally, residual stresses from welding can intensify this issue, increasing the risk of premature joint failure. The plate ultimate strength is further reduced due to these residual stresses, resulting in a decreased connection strength compared to the code equation expectations.

Conversely, above 3.10mm thick plates, the AISI code was notably conservative, providing significantly lower results than observed in the tests. There are several reason why the code equation are conservative then the test result. In the code equation, the throat thickness is typically assumed to be 0.7 times the plate thickness in calculating connection capacity, implying that failure will occur along the weld throat thickness. However, in reality, failure often occurs along the weld leg size instead of the throat thickness. This discrepancy results in the throat thickness being supposed as having more area for the transfer of loads without interruption, leading to conservative results of the connection strength compared to actual test result. Additionally, the code equation typically includes a multiplication factor, such as 0.75, which further contributes to conservative results. This factor is applied to account for uncertainties, variations in material properties, or other factors not explicitly considered in the equation. While this factor helps ensure a level of safety in design, it can lead to conservative estimates of connection capacity compared to actual test results.

According to the AISI code, failure modes were predicted to be "tearing of plate adjacent to weld" for plates up to 2.54mm thick and "weld throat failure mode" for plates exceeding

2.54mm. Interestingly, in the experimental findings, both "tearing of plate adjacent to weld" and "tearing of plate at middle" failure modes were observed for plates up to 2.04mm, aligning with the AISI code. For plate less than 2.54mm thick,the weld throat thickness typically aligns closely with the plate thickness because one leg of the weld is usually three to five times longer than the other leg. Consequently, the weld can withstand loads more effectively than the plate net section capacity. This often leads to failure occurring in the plate net section rather than the weld itself. Welding reduces the plate capacity compared to its virgin capacity, resulting in failure adjacent to the weld.

For the 3.10mm and 3.11mm plate thickness, the observed failure mode was consistent with the AISI code, primarily indicating weld throat failure, with a single specimen displaying a change. Weld throat failure can occur due to higher stress concentration, reduced heat dissipation, and increased residual stress. Thicker plates are particularly susceptible to weld throat failure because of their larger cross-sectional area, which results in greater stress at the weld throat. Welding thicker plates requires more heat input, but they dissipate heat slower. This slower dissipation can result in slower solidification rates, larger grain size, and possible weld defects. Moreover, thicker plates may experience increased residual stresses which can cause distortion and increase the risk of failure at the weld throat.

Table 4.6 and Table 4.7 represent a comprehensive comparison between the test results and the predictions from the AISI Code for ASTM A653 Gr.50 and ASTM A36 steel, highlighting the discrepancies and agreements between the experimental and theoretical assessments.

Table 4.6: Prediction using current AISI guidelines for ASTM A653 steel specimen

ASTM A653 Gr.50 steel (F_y=345 MPa)						
Specimen ID	Plate Thickness, (mm)	Maximum Strength, P_{max} (kN)	P_{AISI} (kN)	P_{max}/P_{AISI}	Failure Mode (Test)	Failure Mode (AISI)
M34C3D1H2F	1.66	95	114	0.83	Tearing of Plate adjacent to weld	Tearing of Plate adjacent to weld
S41C3D1H2F	1.66	92	114	0.81	Tearing of Plate adjacent to weld	Tearing of Plate adjacent to weld
S48C3D1H2F	1.66	104	114	0.91	Tearing of Plate adjacent to weld	Tearing of Plate adjacent to weld
F48C3D1H2F	1.66	98	114	0.86	Tearing of Plate at Middle	Tearing of Plate adjacent to weld
M34C3D2H2F	2.04	136	161	0.84	Tearing of Plate adjacent to weld	Tearing of Plate adjacent to weld
S41C3D2H2F	2.04	130	161	0.81	Tearing of Plate adjacent to weld	Tearing of Plate adjacent to weld
S48C3D2H2F	2.04	139	161	0.86	Tearing of Plate adjacent to weld	Tearing of Plate adjacent to weld
F48C3D2H2F	2.04	140	161	0.87	Tearing of Plate adjacent to weld	Tearing of Plate adjacent to weld
M34C3D3H2F	3.11	212	133	1.59	Tearing of Plate adjacent to weld	Weld Throat Failure
S41C3D3H2F	3.11	211	138	1.53	Weld Throat Failure	Weld Throat Failure
S48C3D3H2F	3.11	251	146	1.72	Weld Throat Failure	Weld Throat Failure
F48C3D3H2F	3.11	262	150	1.75	Weld Throat Failure	Weld Throat Failure

Table 4.7: Prediction using current AISI guidelines for ASTM A36 steel specimen

ASTM A36 steel (F_y=250 MPa)						
Specimen ID	Plate Thickness, (mm)	Maximum Strength, P_{max} (kN)	P_{AISI} (kN)	P_{max}/P_{AISI}	Failure Mode (Test)	Failure Mode (AISI)
M34C2D1H2F	1.65	89	103	0.86	Tearing of Plate adjacent to weld	Tearing of Plate adjacent to weld
S41C2D1H2F	1.65	83	103	0.81	Tearing of Plate adjacent to weld	Tearing of Plate adjacent to weld
S48C2D1H2F	1.65	89	103	0.86	Tearing of Plate at Middle	Tearing of Plate adjacent to weld
F48C2D1H2F	1.65	89	103	0.86	Tearing of Plate at Middle	Tearing of Plate adjacent to weld
M34C2D2H2F	2.03	123	136	0.90	Tearing of Plate at Middle	Tearing of Plate adjacent to weld
S41C2D2H2F	2.03	128	136	0.94	Tearing of Plate adjacent to weld	Tearing of Plate adjacent to weld
S48C2D2H2F	2.03	120	136	0.88	Tearing of Plate at Middle	Tearing of Plate adjacent to weld
F48C2D2H2F	2.03	124	136	0.91	Tearing of Plate adjacent to weld	Tearing of Plate adjacent to weld
M34C2D3H2F	3.10	226	133	1.70	Weld Throat Failure	Weld Throat Failure
S41C2D3H2F	3.10	247	137	1.80	Weld Throat Failure	Weld Throat Failure
S48C2D3H2F	3.10	269	146	1.84	Weld Throat Failure	Weld Throat Failure
F48C2D3H2F	3.10	244	150	1.63	Weld Throat Failure	Weld Throat Failure

4.8 Influence of Heat Affected Zone

The microstructure of metal will be changed in the heat affected zone due to exposed to high temperature. The welding temperature, and material properties are the important parameter which influence the HAZ area. Below 2.04mm plate specimen are failed in HAZ zone of the cover plate rather than the weld although few specimens show different result. The HAZ tensile strength F_{HAZ} will be found dividing the ultimate test load by the actual dimension of the cover plate. The actual dimension are the average plate width and the average plate thickness. Table 4.8 and Table 4.9 represents the HAZ effect for 1.66, 2.04mm and 1.65,2.03mm thick plate for ASTM A653 Gr.50 and ASTM A36 steel respectively. It is proven that the tensile strength in HAZ zone is lower than that the actual tensile strength of the corresponding coupons from the same plate for below 2.04mm thick plate. For plate thicknesses above 3.10 mm, the HAZ effect could not be reliably determined. This is attributed to the predominant failure mode being weld throat failure rather than plate net section failure within the HAZ area.

Table 4.8: Strength of HAZ for ASTM A653 steel specimen

ASTM A653 Gr.50 steel (F_y=345 MPa)						
Specimen ID	Plate Thickness, (mm)	Plate width (mm)	Plate Ultimate Strength,F_u, (MPa)	Maximum Strength, P_{max} (kN)	HAZ Strength, F_{HAZ} (MPa)	$\frac{F_{HAZ}}{F_u}$
M34C3D1H2F	1.66	75	458	95	382	0.83
S41C3D1H2F	1.66	75	458	92	369	0.81
S48C3D1H2F	1.66	75	458	104	418	0.91
F48C3D1H2F	1.66	75	458	98	394	0.86
M34C3D2H2F	2.04	75	527	136	444	0.84
S41C3D2H2F	2.04	75	527	130	425	0.81
S48C3D2H2F	2.04	75	527	139	454	0.86
F48C3D2H2F	2.04	75	527	140	458	0.87

Table 4.9: Strength of HAZ for ASTM A36 steel specimen

ASTM A36 steel (F_y=250 MPa)						
Specimen ID	Plate Thickness, (mm)	Plate width (mm)	Plate Ultimate Strength,F_u, (MPa)	Maximum Strength, P_{max} (kN)	HAZ Strength, F_{HAZ} (MPa)	$\frac{F_{HAZ}}{F_u}$
M34C2D1H2F	1.65	75	415	89	360	0.87
S41C2D1H2F	1.65	75	415	83	335	0.81
S48C2D1H2F	1.65	75	415	89	360	0.87
F48C2D1H2F	1.65	75	415	89	360	0.87
M34C2D2H2F	2.03	75	448	123	404	0.90
S41C2D2H2F	2.03	75	448	128	420	0.94
S48C2D2H2F	2.03	75	448	120	394	0.88
F48C2D2H2F	2.03	75	448	124	407	0.91

4.9 Prediction of Failure Mode

Figure 4.22 displays how many failure modes are correctly determined by the AISI of the studied samples. It is observed that “Weld throat failure” mode are match in 7nos sample out of 8nos sample with the code.” Tearing of plate adjacent to weld “failure mode are match in 12nos sample out of 16nos sample with the code. “Tearing of plate at middle” failure mode are not described in the code but in the experiment 5nos sample are found. Hence, it can be concluded that the AISI S100-16 guideline effectively predicts failure modes for plate specimens with thicknesses of 3.10mm and 3.11mm.

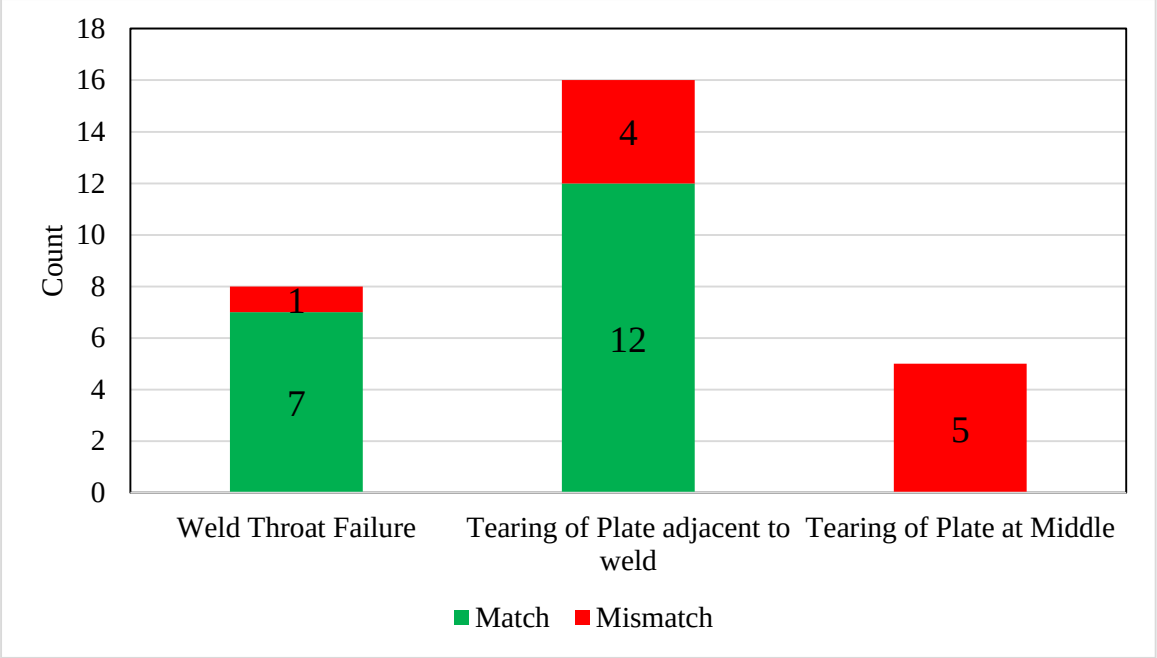

Figure 4.22: Evaluation of AISI guideline in failure mode prediction

4.10 Summary of the Experimental Outcome

The significant observations and discussion on load-elongation response, failure mode, connection strength, stiffness, and ductility and influence of heat affected zone are summarized as following:

a. The initial segment of the load-elongation curve indicates a high level of rigidity in the welded connection. Lower thickness specimens exhibit greater deformation, while higher thickness specimens display reduced deformation.

b. Three types of failure were observed in this study. Failure mode is “Tearing of plate adjacent to weld “, “Tearing of plate at middle” and “Weld throat failure”.

c. “Tearing of plate adjacent to weld “and “Tearing of plate at middle” failure mode is observed for plate thickness up to 2.04mm and “Weld throat failure” mode is observed for plate thickness above 3.10mm.

d. The strength of the weld significantly influences connection strength for plate thicknesses exceeding 3.10mm, while the ultimate strength of the plate affects connection strength for plates below 2.04mm in thickness.

e. Overall Increase in plate thickness shows increase of connection strength and stiffness.

f. Initial ductility depends on the failure mode. “Tearing of plate adjacent to weld “and “Tearing of plate at middle” failure mode shows higher initial ductility where “weld throat failure” mode shows lower initial ductility.

g. The final ductility indicates the energy absorption capacity before failure after reaching the ultimate load. The value close to 1.0 indicate immediate failure after the reaching the ultimate load and larger value indicate warning before failure.

h. The code equation for 3.10mm and 3.11mm plate are significantly over conservative for both grade of steel.

i. The code equation is overestimated with the test result for both grade of steel for up to 2.04mm plate.

j. The microstructure of metal will be changed in the heat affected zone due to welding. The tensile strength in HAZ zone is lower than that the actual tensile strength of the corresponding coupons from the same plate steel.

CHAPTER 5
CONCLUSIONS AND FUTURE RECOMMENDATIONS

5.1 Introduction

In this investigation, an experimental study was carried out to determine the connection strength, stiffness, and failure mode of double-shear welded connections. Two distinct grades of steel, namely ASTM A653 Gr.50 steel and ASTM A36 steel, were investigated. Each set of samples consisted of two overlapped plates with similar thicknesses. The study also aimed to assess the impact of plate thickness, steel grade, and weld strength on the behavior of the connections. Four different electrodes along with three welding processes were employed for the specimens. The welding was conducted along the transverse direction of the plate. Before specimen preparation, a total of four weld coupons were tested to understand the weld specifications. The plate thickness is 1.65mm, 1.66mm, 2.03mm, 2.04mm, 3.10mm, and 3.11mm. The connection behavior was analyzed concerning the load-elongation curve, failure mode, maximum connection capacity, joint stiffness, ductility, and influence of heat affected zone. In addition, the connection strength dependencies on the different failure modes are meticulously scrutinized. Finally, the strength and failure type obtained from the experimental program were compared with those calculated using the AISI S100-16 guideline to evaluate the applicability of this provision.

5.2 Conclusion

Based on this study, the key findings may be concluded as follows:

a. Plate thickness is found to be the most influencing parameter in defining failure mode and connection strength. For below 2.04mm plate, the failure mode is “tearing of plate” and the connection strength depends on plate ultimate strength. On the other hand, plates exceeding 3.10mm thickness experience "weld throat failure mode," with connection strength influenced by weld strength.
b. AISI S100-16 provides conservative design for the higher thick plate specimens of the tested samples for both grades of steel. However, for below 2.04mm plate, the code equation is overestimated than the test result for both grades of steel. This discrepancy is possibly observed because the thinner plates tend to experience more

significant strength reduction due to welding compared to thicker plates. Welding introduces various factors that can affect the strength and integrity of the material, such as heat-affected zones, residual stresses, and changes in material properties. Thinner plates are more susceptible to these effects because they have less mass to dissipate heat and are generally more sensitive to changes in temperature and stress distribution. When predicting failure modes, AISI S100-16 demonstrates effective performance, particularly when applied to samples with large thickness.

c. The tensile strength of heat affected zone (HAZ) in ASTM A653 Gr.50 (F_y=345 MPa) and ASTM A36 (F_y=250 MPa) steel is lower than that of the virgin steel for up to 2.04mm thick plate. This is because for thicker sections, the HAZ typically has more room to dissipate heat, allowing for better control of the welding process and potentially minimizing the decrease in tensile strength. However, for thinner plates (up to 2.04mm thick), the heat input during welding may be relatively higher compared to the thicker thickness of the material. This can lead to localized heating and rapid cooling, which may affect the microstructure and result in reduced tensile strength in the HAZ compared to the base material. The strength of the joint is found to be reduced by 6 to 19% due to the Heat Affected Zone (HAZ) effect.

5.3 Recommendation for Further Study

This study recommends some area related to welded connection to be investigated in the future.

a. As a future recommendation, the effect of welding can be studied for samples formed with further smaller thickness plate since there are even smaller thicknesses that are used/necessary in the construction industry.
b. In order to understand the surface stress and strain behavior, the digital image correlation can be used to analyze how the strain pattern varies for different weld arrangements.
c. This study has been limited to the experimental program and code comparison only. A further numerical model development with validation and thus parameter dependency check could lead to new development in optimizing cold form steel design.

d. The data for this work can be accumulated with some other data from literature and employed in modeling a more generalized strength and failure mode prediction system through using modern computational techniques such as artificial intelligence and machine learning.
e. The performance of other joints such as butt welding, T welding or seated beam of cold form steel can be experimentally tested to understand their response and connection strength.

REFERENCES

Afkhami, S., Björk, T. & Larkiola, J. (2019). Weldability of cold-formed high strength and ultra-high strength steels. Journal of Constructional Steel Research, 158**,** 86-98.

Ali, N., Hamza, J. K. & Sofyan, S. E.(2019). Effects of welding on the change of microstructure and mechanical properties of low carbon steel.2019. IOP Publishing, 012065.

ASTM E8/E8M (2013).Standard Test Methods for Tension Testing of Metallic Materials West Conshohocken (USA).

ASTM E2248-15 (2018). Standard Test Method for Impact Testing of Miniaturized Charpy V-Notch Specimens. West Conshohocken (USA).

AISI S100 (2016).North American Specification for the Design of Cold-Formed Steel Structural Members. Washington DC, U.S.A.

Allen, D. (2022). Tips for Creating Acoustically Isolated Walls with Cold-Formed Steel (CFS) Framing. Retrieved from https://www.buysuperstud.com/news/architects-and-engineers/tips-for-creating-acoustically-isolated-walls-with-cold-formed steel-cfs-framing .

Austalian Standard (2003). Methods for destructive testing of welds in metal. Method.

Amanie, J. (2011). Effect of submerged arc welding parameters on the microstructure of SA516 and A709 steel welds.

ASTM A653/A653M-23 (1997). Standard Specification for Steel Sheet, Zinc-Coated (Galvanized) or Zinc-Iron Alloy-Coated (Galvannealed) by the Hot-Dip Process.

ASTM A36/A36M (2019).Standard Specification for carbon structural steel.

AWS D1. 3 (2008).Structural Welding Code-Sheet Steel. Miami, FL.

Amraei, M., Afkhami, S., Javaheri, V., Larkiola, J., Skriko, T., Björk, T. & Zhao, X.-L. (2020). Mechanical properties and microstructural evaluation of the heat-affected zone in ultra-high strength steels. Thin-Walled Structures, 157**,** 107072.

Amraei, M., Ahola, A., Afkhami, S., Björk, T., Heidarpour, A. & Zhao, X.-L. (2019). Effects of heat input on the mechanical properties of butt-welded high and ultra-high strength steels. Engineering Structures, 198**,** 109460.

Bhadeshia, H. & Honeycombe, R. (2017). Steels: microstructure and properties, Butterworth-Heinemann.

Charles G.Salmon, J. E. J., Faris A.Malhas (2009). Welding. Steel Structures Design and Behavior. Fifth ed. New Jersey: Pearson Prentice Hall.

Chen, Y. W., Dunne, D., Norrish, J. & Szalla, J. (1999). Effect of GMA welding on microstructure and mechanical properties of G550 sheet steel. Research Rep., Dept. of Materials Engineering, Univ. of Wollongong, Wollongon, Australia.

Das, C. R., Albert, S. K., Bhaduri, A. K., Srinivasan, G. & Murty, B. S. (2008). Effect of prior microstructure on microstructure and mechanical properties of modified 9Cr–1Mo steel weld joints. Materials Science and Engineering: A, 477**,** 185-192.

Davies, J. M. (2000). Recent research advances in cold-formed steel structures. Journal of constructional steel research, 55**,** 267-288.

Dhalla, A. K. & Peköz, T. (1971). Tests on puddle and fillet weld connections.

García Rentería, M. A., López Morelos, V. H., García Hernández, R., Curiel López, F. & Lemus-Ruíz, J. (2013). Effect on the Microstructure and Mechanical Properties of the Electromagnetic Stirring during GMA Welding of 2205 DSS Plates. Materials Science Forum, 755**,** 61-68.

Guo, W., Crowther, D., Francis, J. A., Thompson, A., Liu, Z. & Li, L. (2015). Microstructure and mechanical properties of laser welded S960 high strength steel. Materials & Design, 85**,** 534-548.

Guo, W., Li, L., Dong, S., Crowther, D. & Thompson, A. (2017). Comparison of microstructure and mechanical properties of ultra-narrow gap laser and gas-metal-arc welded S960 high strength steel. Optics and Lasers in Engineering, 91**,** 1-15.

Hancock, G., Wilkinson, T. & Teh, L.(2000). Welded connections in high strength cold-formed steels. Proceedings of the 4 th International Conference on Connections in Steel Structures: Steel Connections in the New Millenium, 2000. 216-316.

Hancock, G. J., Murray, T. M. & Ellifritt, D. S. (2001). Connections. Cold-Formed Steel Structures to the AISI Specification. New York: Marcel Dekker, Inc.

Hancock, G. J. & Rogers, C. A. (1998). Design of cold-formed steel structures of high strength steel. Journal of Constructional Steel Research, 1**,** 167-168.

Jha, R. & Jha, A. K. (2014). Investigating the effect of welding current on the tensile properties of SMAW welded mild steel joints. Int. J. Eng. Res, 3.

Kuhlmann, U., Günther, H. P. & Rasche, C. (2008). High-strength steel fillet welded connections. Steel Construction: Design and Research, 1**,** 77-84.

Lee, Y. H., Tan, C. S., Mohammad, S., Md Tahir, M. & Shek, P. N. (2014). Review on Cold-Formed Steel Connections. The Scientific World Journal, 2014**,** 951216.

Lennon, R., Pedreschi, R. & Sinha, B. P. (1999). Comparative study of some mechanical connections in cold formed steel. Construction and Building Materials, 13**,** 109-116.

Liu, X., Chung, K.-F., Ho, H.-C., Xiao, M., Hou, Z.-X. & Nethercot, D. A. (2018). Mechanical behavior of high strength S690-QT steel welded sections with various heat input energy. Engineering Structures, 175**,** 245-256.

Maali, M., Sağıroğlu, M., Kılıç, M. & Aydın, A. C. J. C. (2022). Experimental study on the rotation capacity of bolted and welded beam-to-column connection using cold-formed steel sections. Challenge journal of structural mechanics, 8**,** 133-140.

Maali, M., Sagiroglu, M. & Semih Solak, M. (2018). Experimental behavior of screwed beam-to-column connections in cold-formed steel frames. Arabian Journal of Geosciences, 11**,** 205.

Mallepogu, N. & Madhavan, M. (2022). Experimental analysis of the cold-formed steel beam-to-column connection using the welded clip-angle. Thin-Walled Structures, 179**,** 109357.

Mallepogu, N. & Madhavan, M. (2023). Shear capacity of the cold-formed steel beam to column welded moment connection using clip-angle and flange-cleat. Thin-Walled Structures, 187**,** 110660.

Mcguire, W. & Peköz, T.(1980). Welding of Sheet Steel. 5th International Specialty Conference on Cold-Formed Steel Structures, 1980 St Louis,Missouri. University of Missouri--Rolla, 637-662.

Merchant Samir, Y. (2015). Investigation on effect of welding current on welding speed and hardness of HAZ and weld metal of mild steel. International Journal of Research in Engineering and Technology, 4**,** 44-48.

Nassar, A., Lefta, R. & Abdulsada, M. (2021). Experimental study of the effect of welding electrode types on tensile properties of low carbon steel AISI1010. Kufa Journal of Engineering, 9**,** 163-173.

"Nippon Steel Cold rolled steel sheets and coils manufacturing Process". Retrieved from https://www.nipponsteel.com/en/product/sheet/process/.

Ogbunnaoffor, C. K., Odo, J. U. & Nnuka, E. E. (2016). The effect of welding current and electrode types on tensile properties of mild steel. International Journal of Scientific & Engineering Research, 7**,** 1120-1123.

Ovat, F. A., Asuquo, L. O. & Anyandi, A. J. (2012). Microstructural effects of electrodes types on the mechanical behaviour of welded steel joints. Research journal in engineering and applied sciences, 1**,** 171-176.

Owolabi, O. B., Aduloju, S. C., Metu, C. S., Chukwunyelu, C. E. & Okwuego, E. C. (2016). Evaluation of the effects of welding current on mechanical properties of welded joints between mild steel and low carbon steel. Am. J. Mater. Sci. Appl, 4**,** 1.

Oyyaravelu, R., Kuppan, P. & Arivazhagan, N. (2016). Metallurgical and mechanical properties of laser welded high strength low alloy steel. Journal of advanced research, 7**,** 463-472.

Pathak, D., Singh, R. P., Gaur, S. & Balu, V. (2020). Experimental investigation of effects of welding current and electrode angle on tensile strength of shielded metal arc welded low carbon steel plates. Materials Today: Proceedings, 26**,** 929-931.

Porter, D.(2015). Weldable high-strength steels: Challenges and engineering applications. 68th IIW Annu. Assem. Int. Conf. High Strength Mater.-Challenges Appl, 2015 Finland, Helsinki.

Qin1a, Y. & Chen, Z. (2016). Research on cold-formed steel connections: A state-of-the-art review. Steel and Composite Structures, 20**,** 21-41.

Sild, S. (2022). Flux-Cored Arc Welding (FCAW) Explained. Retrieved 16 August,2022, from https://fractory.com/flux-cored-arc-welding-explained/.

Sild, S.(2022). MIG Welding Explained. Retrieved 19 April,2022, from https://fractory.com/mig-welding-explained/.

Sild, S. (2022). Shielded Metal Arc Welding (SMAW) Explained. Retrieved 4 August,2022, from https://fractory.com/shielded-metal-arc-welding/.

Steel, T. B. (2020). Light gauge steel framing [Online]. Retrieved from https://tatabluescopesteel.com/blogs/light-gauge-framing-system-lgfs-a-smart and-sustainable-steel-building-technology/ .

Talabi, S. I., Owolabi, O. B., Adebisi, J. A. & Yahaya, T. (2014). Effect of welding variables on mechanical properties of low carbon steel welded joint. Advances in Production Engineering & Management, 9**,** 181-186.

Teh, L. H. & Hancock, G. J. (2000). Strength of Fillet Welded Connections in G450 Sheet Steels (No. R802). School of Civil Engineering, The University of Sydney.

Teh, L. H. & Hancock, G. J.(2002). Strength and Behavior of Fillet Welded Connections in G450 Sheet Steel. 16th International Specialty Conference on Cold-Formed Steel Structures, 2002 Missouri. University of Missouri--Rolla.

Toma, A. W. & Stark, J. W. B.(1978). Connections in cold-formed sections and steel sheets. 4th International Specialty Conference on Cold-Formed Steel Structures, 1978 St Louis,Missouri. University of Missouri--Rolla.

Torabian, S., Xiao, F., Haws, R. B. & Schafer, B. W. (2018).. Design of transverse fillet welds in the lapped joints of thin steel plates. International Journal of Steel Structures, 18**,** 337-348.

Yu, W.-W. & Laboube, R. A. (2010). Introduction. Cold-formed steel design. Fourth ed. Hoboken: John Wiley & Sons.

Yu, W.-W., Laboube, R. A. & Chen, H. (2019). Introduction. Cold-formed steel design. Fifth ed. Hoboken: John Wiley & Sons.

Zhao, X.-L. & Hancock, G. (1996). Welded connections in thin cold-formed rectangular hollow sections. In: BJORHOVDE, R., COLSON, A. & ZANDONINI, R. (eds.) Connections in Steel Structures III. Oxford: Pergamon.

Zhao, X.-L. & Hancock Gregory, J. (1995). Butt Welds and Transverse Fillet Welds in Thin Cold-Formed RHS Members. Journal of Structural Engineering, 121**,** 1674-1682.